

# **A Design Model and Comparison of Fixed and Tracking Photovoltaic Systems for a Single-Family House in Erbil, Iraq**

**Parinaz Mohammed Abdulkarim**

Submitted to the  
Institute of Graduate Studies and Research  
in partial fulfillment of the requirements for the degree of

Master of Science  
in  
Electrical and Electronic Engineering

Eastern Mediterranean University  
February 2021  
Gazimağusa, North Cyprus

Approval of the Institute of Graduate Studies and Research

---

Prof. Dr. Ali Hakan Ulusoy  
Director

I certify that this thesis satisfies all the requirements as a thesis for the degree of Master of Science in Electrical and Electronic Engineering.

---

Assoc. Prof. Dr. Rasime Uygurođlu  
Chair, Department of Electrical and  
Electronic Engineering

We certify that we have read this thesis and that in our opinion it is fully adequate in scope and quality as a thesis for the degree of Master of Science in Electrical and Electronic Engineering.

---

Prof. Dr. Osman Kükre  
Supervisor

---

Examining Committee

1. Prof. Dr. Osman Kükre

2. Assoc. Prof. Dr. Reza Sirjani

3. Asst. Prof. Dr. Mehmet Őenol

## ABSTRACT

This thesis reviewed the photovoltaic (PV) technology. It also analyzed the potential of the PV plants to solve the problem of power shortages in Iraq. The use of PV power is the most advanced renewable energy application; however, it has not been commercialized in the study location. In this thesis, three separate PV plant systems were assessed in Erbil, Kurdistan region for installation. The study examined the feasibility of the plants proposed and compares the efficiency of both a fixed and dual-axis tracking systems for an off-grid PV system. This thesis presented a study on an off-grid photovoltaic system for electrification of a residential household in Erbil (36.18° N, 44.01 ° E, 392 m) using PVsyst software for household load estimation and solar energy requirements. According to meteorological data, Iraq is characterized by a solar irradiation ranging from 1800 kWh/m<sup>2</sup>/year to 2390 kWh/m<sup>2</sup>/year of direct normal solar irradiation (Al-Kayiem, 2019). Using the Meteonorm solar radiation map, a suitable location was selected for the plant, calculating PV arrays and arrangements to determine the appropriate number of panels, maximizing AC power generation, storage capacity of the battery, and charge controller size to fulfil the required load. To calculate the annual energy generation, the design data was used in a simulation. Three scenarios were simulated; fixed panels, East-West single, and dual-axis tracking systems based on the altitude of azimuth angle tracking. The study compared both the photovoltaic properties and the amount of energy generated by the installed systems: one with a fixed tilt angle, and the other fitted with solar trackers. The results showed that the dual-axis tracking system is 30% more efficient than the other systems, although the single-axis tracking system offers an economically better alternative.

**Keywords:** photovoltaic system (PV), fixed-tilt PV installation, single-axis tracking system, dual-axis tracking system, off-grid system design, PVsyst software.

## ÖZ

Bu tezde fotovoltaik teknolojisinin uygulanması üzerinde durulmuştur. PV teknolojisinin Irak'taki elektrik kesintilerinin yol açtığı sorunları çözme potansiyeli incelenmiştir. PV güç üretimi yenilenebilir enerjinin en ileri uygulamalarındandır; fakat, ele alınan bölgede yeterince ticarileşmemiştir. Bu tezde, Irak Kürdistan bölgesindeki Erbil için üç farklı PV sistemi değerlendirilmesi yapılmıştır. Önerilen tesislerin fizibilitesi, ayrıca sabit, tek ve çift eksenli takip sistemlerinin verimleri incelenmiştir. Erbil'deki bir eve (36.18 ° N, 44.01 ° E, 392 m) şebekeden bağımsız bir PV sistemi ile elektrik götürülmesi, evin yük kestirimi ve güneş enerjisi gereksinimi için PVsyst yazılımına dayalı çalışma yapılmıştır. Havadurumu verileri Irak'ın güneş enerjisi bakımından yeterli olduğunu göstermektedir. Güneş ışınım haritası kullanarak tesis için uygun bir konum seçilmiş, uygun panel sayısını belirlemek için PV dizinlerinin hesaplanması yapılmıştır. Yıllık enerji üretiminin benzetim yoluyla hesaplanması için tasarım verileri kullanıldı. Sabit panel, tek-eksenli takip ve çift-eksenli takipten oluşan üç senaryo benzetimi yapıldı. Bu üç sistemin fotovoltaik özellikleri ve bunlara dayalı oluşturulan sistemlerin ürettiği enerji miktarları karşılaştırılmıştır. Bu sonuçlar, çift-eksenli takip sisteminin veriminin diğerlerine göre daha yüksek olduğunu, fakat tek-eksenli takip sisteminin ekonomik olarak daha iyi bir seçenek sunduğunu göstermiştir.

**Anahtar Sözcükler:** Fotovoltaik sistem (PV), Sabit eğimli tesis, tek-eksenli takip sistemi, çift-eksenli takip sistemi, Şebekeden bağımsız sistem, PVsyst yazılımı.

# DEDICATION

*I dedicate this thesis to my father's soul (RIP), my family, my lovely husband and my*

*little daughter who helped me during this journey.*

*And everyone who has supported me and who's continuing to support me.*

## **ACKNOWLEDGMENT**

I take this opportunity to express my sincere appreciation to my supervisor Prof. Dr. Osman Kükreer for his guidance and encouragement throughout this thesis and also the staff of the Electrical Electronics Engineering Department at Eastern Mediterranean University, especially my adviser, Assoc. Prof. Dr. Reza Sirjani and the Head of Department Assoc. Prof. Dr. Rasime Uygurođlu.

A very special thanks and appreciation to my lovely family who always were the source of inspiration and motivation. I am eternally grateful to my parents for always believing in me and encouraging me to follow my dreams. I would like to thank my husband and my cute daughter and I thank everyone who supported me and encouraged me.

# TABLE OF CONTENTS

ABSTRACT .....	iii
ÖZ .....	v
DEDICATION .....	vi
ACKNOWLEDGMENT .....	vii
LIST OF TABLES .....	xiii
LIST OF FIGURES .....	xiv
LIST OF ABBREVIATIONS .....	xvii
1 INTRODUCTION .....	1
1.1 Background of the Study.....	1
1.2 Aim and Objectives.....	3
1.3 Scope of Research and Limitations.....	5
1.4 Structure of the Thesis .....	5
2 PHOTOVOLTAIC SYSTEMS.....	7
2.1 History of Solar Energy .....	7
2.2 The Time of the Invention of Solar Panels .....	8
2.3 PV Systems in General .....	8
2.3.1 On-grid PV System .....	9
2.3.2 Standalone/Off-grid PV System.....	10
2.3.3 Hybrid System.....	11
2.4 Solar Energy.....	12
2.4.1 Working Mechanism of Solar Energy.....	12
2.5 The Electrical Characteristics of a PV Cell, PV Module, PV String, and a PV Array .....	13



2.5.1 Solar Cell.....	13
2.5.2 Types of Solar Cells .....	14
2.5.2.1 Monocrystalline.....	14
2.5.2.2 Polycrystalline.....	15
2.5.2.3 Thin-film Silicon.....	16
2.5.3 Photovoltaic Module .....	17
2.5.4 Sub-Array (String) .....	18
2.5.5 Photovoltaic Array .....	19
2.6 Classification of Solar Trackers .....	21
2.6.1 Based on the Driving System Used.....	21
2.6.1.1 Passive Solar Tracking System .....	21
2.6.1.2 Active Solar Tracking Systems.....	23
2.6.2 Based on the Control System Used.....	24
2.6.2.1 Closed-loop Tracking System.....	24
2.6.2.2 Open-loop Tracking System .....	25
2.6.3 Based on the Degree of Freedom .....	26
2.6.3.1 Latitude .....	26
2.6.3.2 Longitude .....	27
2.6.3.3 Air Mass.....	28
2.6.3.4 Incidence Angle .....	29
2.6.3.5 Declination Angle .....	30
2.6.3.6 Elevation/ Altitude Angle .....	30
2.6.3.7 Zenith Angle.....	31
2.6.3.8 Tilt Angle .....	32
2.6.3.9 Solar Azimuth Angle.....	33

2.6.4 Based on Tracking Strategies .....	33
2.6.4.1 Date and Time .....	33
2.6.4.2 Microprocessors and Electro-optical Sensors .....	33
2.6.4.3 Sensors, Date, and Time.....	34
2.7 Fixed PV Systems .....	34
2.8 Tracking PV Systems.....	35
2.8.1 Single-Axis Tracking PV Systems.....	36
2.8.1.1 Horizontal Single-Axis Solar Tracker (HSAT).....	37
2.8.1.2 Horizontal Tilted Single-Axis Solar Tracker (HTSAT).....	38
2.8.1.3 Vertical Single-Axis Solar Tracker (VSAT).....	38
2.8.1.4 Vertical-Tilted Single-Axis Solar Tracker (VTSAT) .....	39
2.8.2 Advantages of Single-Axis Trackers .....	40
2.9 Dual-Axis Tracking PV Systems .....	40
<b>3 THE DESIGN METHOD AND APPLICATION .....</b>	<b>43</b>
3.1 The Proposed Design Model.....	43
3.2 Application of the Design Model.....	45
3.3 Steps of Design .....	45
3.3.1 Project Design and Type of PV Solar System .....	45
3.3.2 Define the Geographical Location and Meteorological Data .....	46
3.3.3 Orientation (Define Module Azimuth and Tilt) .....	47
3.3.4 User’s needs (Define a Daily Profile for the Full Year) .....	48
3.3.5 Selecting the System Components (Choose the System Modules, Battery Storage, Controller, and the Inverter) .....	51
3.3.5.1 PV Module Selection .....	51
3.3.5.2 Battery Storage.....	53

3.3.5.3 Charge Controller.....	54
3.3.5.4 Inverter .....	55
3.3.6 Detailed Losses –Mismatch .....	56
3.3.7 Horizon.....	56
3.3.8 Near Shading .....	57
4 RESULTS AND DISCUSSION .....	58
4.1 Results of Fixed Installation PV System.....	58
4.1.1 Balances and Main Simulation Results.....	58
4.1.2 Performance Ratio PR and Solar Fraction SF.....	59
4.1.3 Normalized Production .....	59
4.1.4 Shading Factor .....	60
4.1.5 Shading Diagram.....	61
4.1.6 Loss Diagram .....	63
4.2 Results of Single-Axis Tracking PV System .....	65
4.2.1 Balances and Main Simulation Results.....	65
4.2.2 Performance Ratio PR and Solar Fraction SF.....	66
4.2.3 Normalized Production .....	66
4.2.4 Shading Diagram.....	67
4.2.5 Loss Diagram .....	68
4.3 Results of Dual-Axis Tracking PV System.....	69
4.3.1 Balances and Main Simulation Results.....	69
4.3.2 Performance Ratio PR and Solar Fraction SF.....	70
4.3.3 Normalized Production .....	71
4.3.4 Shading Diagram.....	71
4.3.5 Loss Diagram .....	72

4.4 Discussion .....	73
5 CONCLUSION AND RECOMMENDATION .....	78
5.1 Conclusion of the Study .....	78
5.2 Recommendation for Future Studies.....	81
REFERENCES.....	82
APPENDICES .....	90
Appendix A: Results of Fixed Tilt Installation PV System.....	91
Appendix B: Results of Single Axis Tracking Installation PV System.....	97
Appendix C: Results of Dual Axis Tracking Installation PV System .....	103

## LIST OF TABLES

Table 1: Monocrystalline (Trina_TSM_205_D80.PAN with 32V) parameters. ....	52
Table 2: Battery specifications.....	54
Table 3: Outlines the recommended charge controller specifications. ....	55
Table 4: Discussion summary of the main study findings. ....	76

## LIST OF FIGURES

Figure 1: The research methodology workflow.....	4
Figure 2: The schematic presentation of the structure of the thesis.....	6
Figure 3: The schematic diagram of an on-grid system (Alfadhli, et al., 2019).....	9
Figure 4: The schematic diagram of an off-grid system (Alfadhli, et al., 2019). ....	10
Figure 5: The schematic diagram of a Hybrid system (Alfadhli, et al., 2019).....	11
Figure 6: Internal reaction of solar energy (Shaikh, 2017).....	12
Figure 7: The working mechanism of solar energy (Sobamowo, et al., 2020).....	13
Figure 8: Monocrystalline panel (Guda and Aliyu, 2015). ....	15
Figure 9: Polycrystalline panel (Guda and Aliyu 2015). ....	16
Figure 10: Thin-film silicon panel (Bagher et al., 2015). ....	17
Figure 11: Photovoltaic module with multiple cells (Kumar et al., 2020).....	18
Figure 12: Photovoltaic panel with modules in series (Kumar et al., 2020).....	19
Figure 13: Photovoltaic array with strings in parallel (Singh & Rajput, 2016). ....	20
Figure 14: Passive solar tracking system (Nadia, et al., 2018). ....	22
Figure 15: Active solar tracking system (Nadia, et al., 2018). ....	24
Figure 16: Scheme of a closed-loop tracker (Huynh, et al., 2013). ....	25
Figure 17: Scheme of an open-loop tracker (Huynh, D. C. et al., 2013). ....	26
Figure 18: latitude (Racharla, & Rajan, 2017).....	27
Figure 19: Longitude (Racharla & Rajan, 2017). ....	28
Figure 20: Air mass (Rida, et al., 2016).....	29
Figure 21: Incidence angle (Ismail, et al. 2016).....	29
Figure 22: Declination angle (Racharla & Rajan, 2017).....	30
Figure 23: Elevation/ altitude angle (PAL & SUBBRA DAS, 2015).....	31

Figure 24: Tilt angle (Fouad, et al., 2017). .....	32
Figure 25: Position of a fixed PV panel during a day (Bailek, et al., 2018). .....	35
Figure 26: Position of a solar tracker system during a day (Bailek, et al., 2018). .....	36
Figure 27: Single-axis tracking on a horizontal axis (Li, Tang, & Zhong, 2012). .....	37
Figure 28: Single-axis tracking on a vertical axis (Li, Tang, & Zhong, 2012). .....	39
Figure 29: Dual-axis tracking solar panel (Burnham, et al., 2019). .....	42
Figure 30: The main stages of the proposed model. ....	44
Figure 31: Selection of project design and type of PV solar system. ....	45
Figure 32: Defining the geographical location of the case study .....	46
Figure 33: Determining metrological data of the case study .....	47
Figure 34: Selection of orientation for fixed installation <b>(a)</b> , single-axis <b>(b)</b> , and dual-axis tracking system <b>(c)</b> . .....	48
Figure 35: Load calculation of daily energy consumptions for the household, all load are AC. ....	50
Figure 36: Hourly distribution of the loads. ....	50
Figure 37: Horizon (for shading) definition at Erbil. ....	57
Figure 38: Shading scene construction. ....	57
Figure 39: Balances and main result of the photovoltaic system for Fixed-tilt. ....	58
Figure 40: PR 59.9% and solar fraction 100%. .....	59
Figure 41: Normalized production for 280W Panel. ....	60
Figure 42: Shading factor. ....	61
Figure 43: Iso-shading curve for fixed tilt. ....	62
Figure 44: Losses diagram – fixed tilt. ....	64
Figure 45: Balances and main result of the photovoltaic system for Single-Axis Tracker .....	65

Figure 46: PR 56.5% and solar fraction 100% .....	66
Figure 47: Normalized production for 280W Panel.....	67
Figure 48: Iso-shading curve- single-axis tracker.....	68
Figure 49: Losses diagram- single-axis tracker .....	69
Figure 50: Balances and main result of the photovoltaic system for Dual-axis tracker. .....	70
Figure 51: PR 46.6% and solar fraction 100% .....	70
Figure 52: Normalized production for dual-axis tracker.....	71
Figure 53: Iso-shading curve for the dual-axis tracking system. ....	72
Figure 54: Losses diagram- dual-axis tracker. ....	73



## LIST OF ABBREVIATIONS

AC	Alternating current
Ah	ampere hour
AM	Air Mass
°C	degree Celsius
DC	Direct current
DoD	Depth of Discharge
EW	East to West
HSAT	Horizontal Single-Axis Solar Tracker
HTSAT	Horizontal Tilted Single-Axis Solar Tracker
I	Current
IAM	Incidence Angle Modifier
Imp	Maximum power point current
kg	kilogram
kWh	kiloWatt-hour
mΩ	Milliohm
MPPT	Maximum Power Point Tracking
Pmp	Maximum Power Point
PR	Performance Ratio
PV	Photovoltaic
PWM	Pulse Width Modulation
SF	Solar Fraction
SOW	State of Wear (Battery Cycle's)

STC	Standard Test Condition (1,000 watts/m <sup>2</sup> , solar irradiance, 1.5 Air Mass, and a 25 °C)
V	Voltage
V <sub>mp</sub>	Maximum Power Point Voltage
VSAT	Vertical Single Axis Tracker
VTSAT	Vertical-Tilted Single-Axis Solar Tracker
W <sub>p</sub>	Watt Peak

# Chapter 1

## INTRODUCTION

### 1.1 Background of the Study

There has been a continuous shortage in energy generation due to long-term political and economic crises in Iraq. Daily electricity shortages are a common problem all around Iraq, including Erbil (Abdullah, et al., 2017). Erbil is the capital and most populated city in the Kurdistan Region in the north of Iraq and is located between latitudes 36.18° N and 44.01° E with an altitude of 392m above sea level. The Erbil Governorate encompasses an area of 15,074 km<sup>2</sup>, with a population of approximately 2,200,000 people (The European Union, 2018).

The inability to meet electricity demand, as well as the existing instabilities, have resulted in the increased use of fossil fuels; such as the diesel-based generators that are frequently used as a source of supplementary electricity generation to the main grid.

There is an average outage rotation of about eight to twelve hours of blackout in Erbil. Due to this regular disconnection rotation, consumers have to pay two different bills each month; one for the consumption amount of the main grid and the other for their generators. Currently, the local government has not displayed any motivation to resolve the inadequacies in electricity production by employing diverse electricity generation sources since oil is an inexpensive and locally-available source of energy production. However, this phenomenon has elevated the level of greenhouse gas emissions, which negatively affects the health of citizens (Al-Douri & Abed, 2016).

Nevertheless, global warming's severity and the sustainable development goals have necessitated the use of green energy from renewable sources, such as solar, wind, hydropower, biomass, etc (Sobhani, Zakeri, & Taghizadeh, 2014). The climatic conditions of the city, namely year-round solar radiation, supports the idea of electricity generation from solar power. Advancements in technology have facilitated this goal using photovoltaic (PV) systems. A PV cell converts solar power to electricity within a systematic process, and this power generation is very sustainable and green (Qadir & Saeed, 2011).

Electricity is one of the most important drivers for the rapid economic development of countries. Accordingly, various energy sources, such as coal, natural gas, uranium, solar photovoltaics, geothermal energy, water flow, and wind, have been used to generate electricity. Traditional energy sources, such as fossil fuels, are only available in limited amounts, and are responsible for global warming, earthquakes, and human health issues. Renewable energy, or clean energy, is developed from natural sources (e.g. recyclable sources), such as solar and wind. Renewables are becoming important sources of energy production and there are currently several increasingly innovative and low-cost ways of utilizing them. Therefore, the use of these profitable sources can lead to economic development in almost every country. Solar energy generation activities do not harm our environment as no greenhouse gasses are emitted when generating electricity from solar power (Mundaca & Richter, 2015). Renewable energy is generally accessible everywhere and by everyone and offers many advantages, including: pollutant free energy sources, low or reasonable cost, sustainable source (unlimited power source), economic development, etc. Hence, renewable energy, particularly solar power, can be profitably used to provide

electricity for the heating and cooling of buildings, industrial processes, and transportation (The European Union, 2018).

## 1.2 Aim and Objectives

The aim of this thesis is to develop a design model of a Standalone/off-grid solar PV system for a single-family house in Erbil, Iraq. The proposed model will be applied to design different PV system installations, including fixed, single-axis tracking, and two (dual)-axis tracking system. The study attempts to determine which of the available system installation methods most suitable in terms of energy generation.

The objectives of this thesis are:

- To understand electricity generation from solar power using a photovoltaic system (*chapter 2 includes: literature review* )
- To develop a design model of an off-grid photovoltaic system (*chapter 3 involves: the design model development*)
- To apply the model on a case study; a typical single-family house in Erbil, Iraq ( *chapter 4 includes: the application of the study*)
- To compare different PV installation systems (i.e. fixed, single-axis tracking, and dual-axis tracking system) for the study location (*chapter 4 involves: results and descusions* )
- To offer guidelines for designers, stakeholders, and policy makers concerning PV system design and installation methods in Erbil (*chapter 5 includes: conclusion and recommendations*)

Figure 1 shows the methodology workflow including study methods , tasks and outputs.

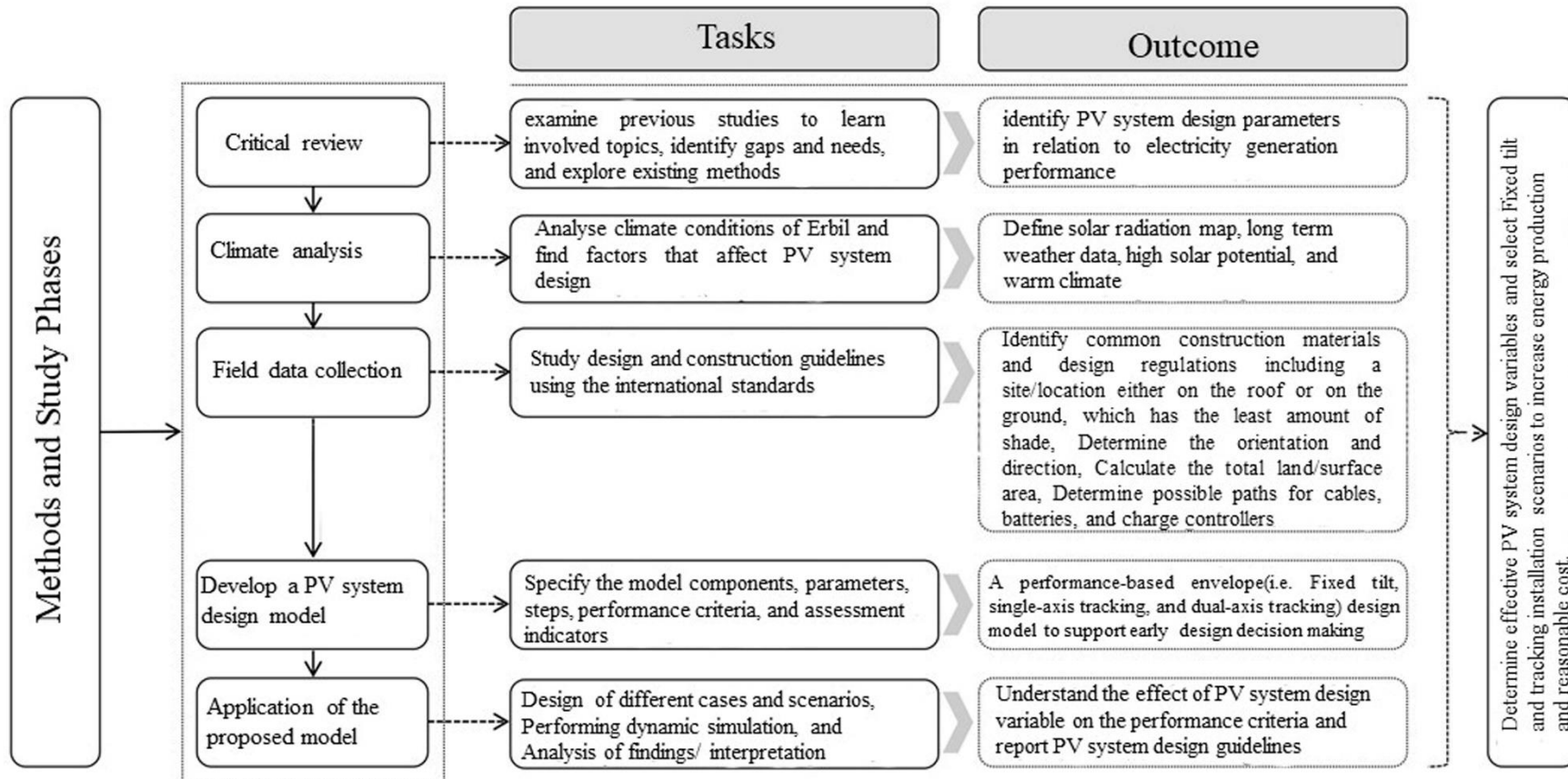


Figure 1: The research methodology workflow.

### **1.3 Scope of Research and Limitations**

The scope of this thesis demonstrated the optimal design for a utility size stand-alone solar PV system from the study location (Erbil). It focuses on a comparative analysis of three scenarios of stand-alone solar PV systems includes fixed-tilt, single-axis, and dual-axis tracking designs.

The Pvsyst simulation tool was used to assess the performances of the different methods. Besides, there were no restrictions to the area and shading.

### **1.4 Structure of the Thesis**

Chapter 1 introduces the background of the study, as well as discusses the problem statement, aim, and objective. It also includes the scope and limitations of the study, and an overview of the research methodology and tool. Chapter 2 introduces the literature review of PV system concerning PV systems in general, types of PV system working mechanism of solar energy, the electrical characteristics of a PV cell, PV module, PV string and a PV array, classification of solar trackers, fixed PV systems, and tracking PV systems . Chapter 3 is the methodological section and describes the research methods and approach used to develop a performance-based PV system design model and identifies the proposed design model, application of the design model, and steps of design . Chapter 4 is the methodological section and describes the research methods and development of the proposed model. Chapter 5 summarises the thesis and presents the main conclusions and recommendations. Figure 2 illustrates the schematic diagram of the structure of the study.

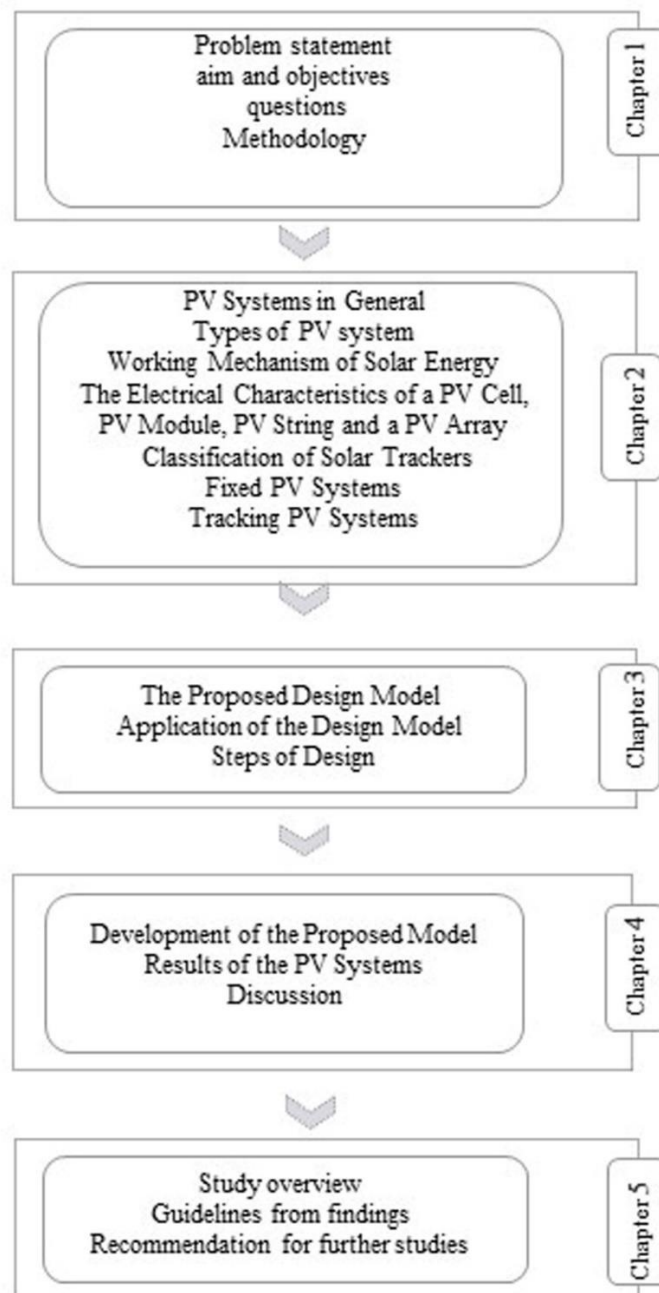


Figure 2: The schematic presentation of the structure of the thesis.



## Chapter 2

# PHOTOVOLTAIC SYSTEMS

### 2.1 History of Solar Energy

Humans have used solar energy since the early 7<sup>th</sup> century BC when humans used sunlight to light fires with a magnifier. Later, in the 3rd century BC, the Greeks and Romans were famous for curbing solar energy with mirrors to turn on torches for religious rites. These mirrors became commonplace, known as "burning mirrors." Later, Chinese civilization documented the use of mirrors for this purpose in the year 20 A.D.

Another early use for solar energy, which is still popular today, was the inclusion of "sunrooms" in buildings. These sunrooms used large windows to direct sunlight into a centralized area. Some of the prominent Roman baths, usually located on the south side of the buildings, were sunrooms.

In the late 1700s and 1800s, researchers and scientists succeeded in using sunlight to provide furnaces for long journeys. They also curbed the power of the sun to generate solar-powered steamships. Finally, even thousands of years before the age of solar panels, the idea of retouching the power of the sun was a popular notion (Jones, et al., (2012).

## **2.2 The Time of the Invention of Solar Panels**

The development of solar panel technology was due to the contribution of many scientists. Some people attribute the invention of the solar cell to the French scientist Edmund Becquerel, who said that when two metal electrodes were immersed in a conductive solution, light could increase power generation. This achievement, defined as the "photovoltaic effect", was influential in the subsequent evolution of PV with the element selenium.

In 1873, Willoughby Smith found that selenium had optical conductivity, leading to William Grylls Adam's and Richard Evans Day's discovery in 1876 that selenium generates electricity when exposed to sunlight. A few years later, in 1883, Charles Fritts produced the first solar cells made from selenium wafers. For this reason, some historians consider Charles Fritts to be the real inventor of solar cells. However, because solar cells are made of silicon and not selenium, some think that Daryl Chapin, Calvin Fuller, and Gerald Pearson at Bell Labs tie the true invention of the solar panel to the 1954 creation of a silicon photovoltaic cell (PV). Many argue that this event is a true sign of the invention of PV technology because it is the first sample of a solar technology that can power an electrical device for several hours a day. The first silicon solar cell could convert sunlight at four percent efficiency, less than a quarter the capacity of modern cells (The History of Solar Energy, 2020).

## **2.3 PV Systems in General**

In general, PV systems can be divided into three different systems: On-grid systems, stand-alone systems, and hybrid systems.

### 2.3.1 On-grid PV System

This is a basic solar setup having a standard on-grid inverter. The on-grid solar PV system does not have a battery bank for storage. On-grid system power can be generated and used only in the daytime. Such a system is simple to design, cost-effective, easily controllable and requires fewer repairs. A schematic diagram of the system is shown in Figure 3.



Figure 3: The schematic diagram of an on-grid system (Alfadhli, et al., 2019).

The main objective of the On-grid system is reducing the energy bill of its users. In this type of system, solar panels often generate more electricity than that requested by the loads. So instead of storing it in the batteries, this extra electricity can be given back to the grid. Also, by selling this surplus power back, money can be earned. The power generated by the PV panels is in DC form and converted into AC using an inverter. The On-grid system suffers from the significant disadvantage that it can't store the power for future use, such that the power can be used only during the day like

during power outages. However, this disadvantage can be overcome by using a battery bank to store power during the day.

### 2.3.2 Standalone/Off-grid PV System

This system is useful for customers who cannot easily connect to the grid. In off-grid solar PV systems, batteries are used for the storage of the generated electricity during the daytime, which can be used at any time at night or in cloudy days. While designing this system, site and climatic conditions are important points that have to be considered. During snowy, rainy and cloudy days for which the solar power cannot be sufficiently harvested, or when dust and snow restrict electricity generation of the PV panels, back-up generators need to be in operation. Additionally, to run the generator, gasoline, diesel, petroleum or propane can be used. In this system, converting the DC electrical current coming from the batteries into AC (alternating current) is done by a solar inverter. A schematic diagram of the system is shown in Figure 4.

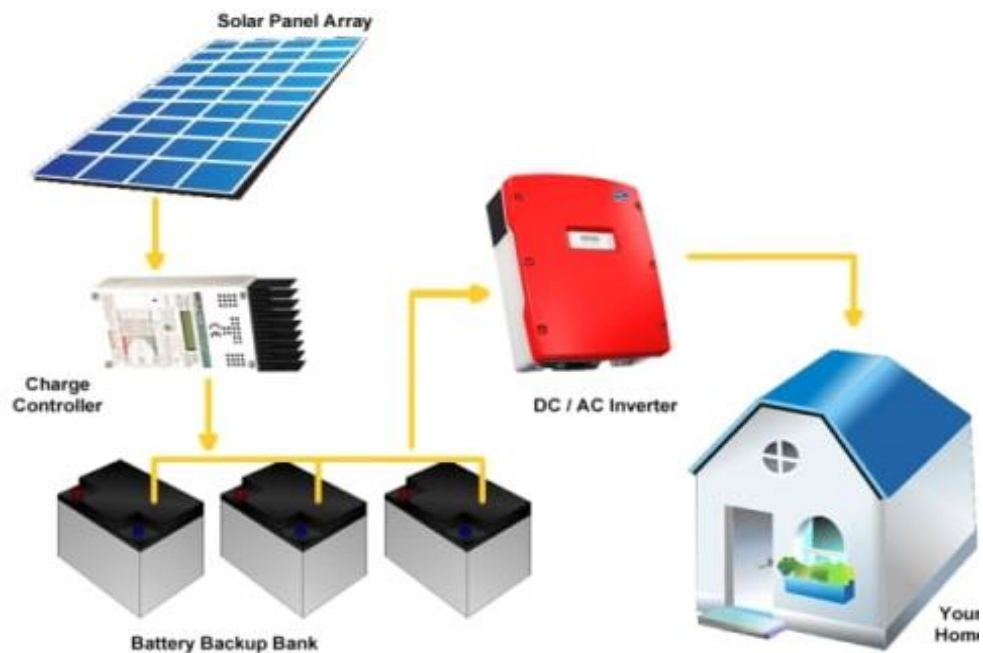


Figure 4: The schematic diagram of an off-grid system (Alfadhli, et al., 2019).

AC is the standard form of electricity for anything that "plugs in" to utility power and is the advisable current for usual household facilities. The main advantage of this system is that it provides enough energy for the household and is feasible for places far away from the grid. Off-grid systems have more elements and are comparatively more expensive than On-grid systems.

### 2.3.3 Hybrid System

This system is perfect for customers who are connected to the grid system and request a battery bank. This system provides the advantages of both On-grid and Off-grid systems. It also helps to reduce the users' bills. Furthermore, if there happens to be any power outage, emergency, or even during peak hours, the energy from the battery bank can be employed. In this study, an off-grid PV system is to be dimensioned. As the dimensioning methods for these three systems differ, only the off-grid PV system will be discussed from this point on. A schematic diagram of the system is shown in Fig. 5.

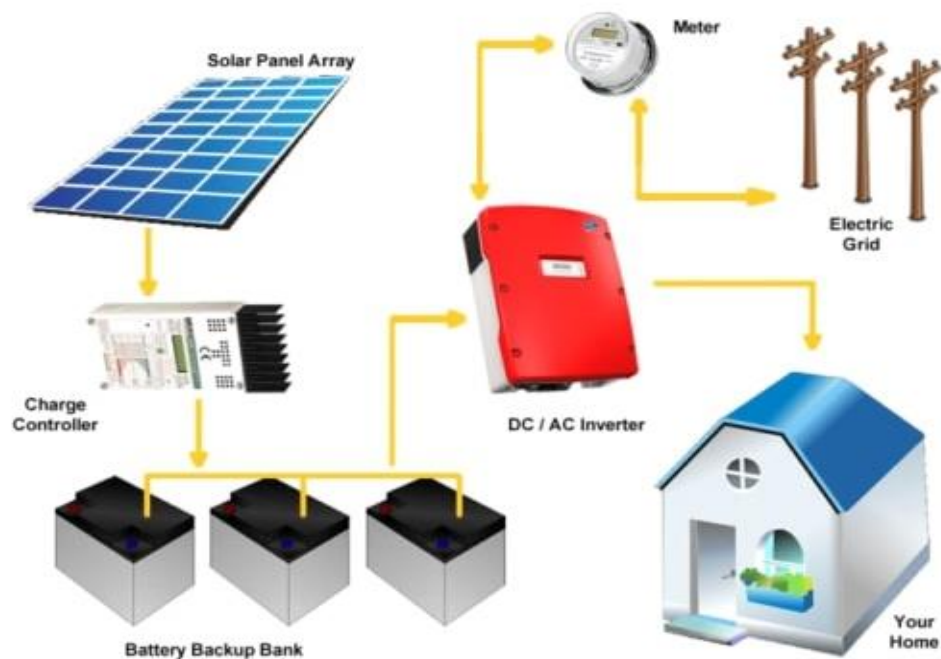


Figure 5: The schematic diagram of a Hybrid system (Alfadhli, et al., 2019).

## 2.4 Solar Energy

Energy in the form of heat and radiation is called solar energy. Radiant light and heat of the sun are shown in the figure below. It is a natural source of solar energy and is being developed using a wide range of technologies such as solar thermal energy, solar architecture, solar heating, and artificial photosynthesis. Approximately 30% of the sun's radiation returns to space while the ocean and clouds absorb the rest (Shaikh, 2017). This high solar power creates a very attractive source of electricity.

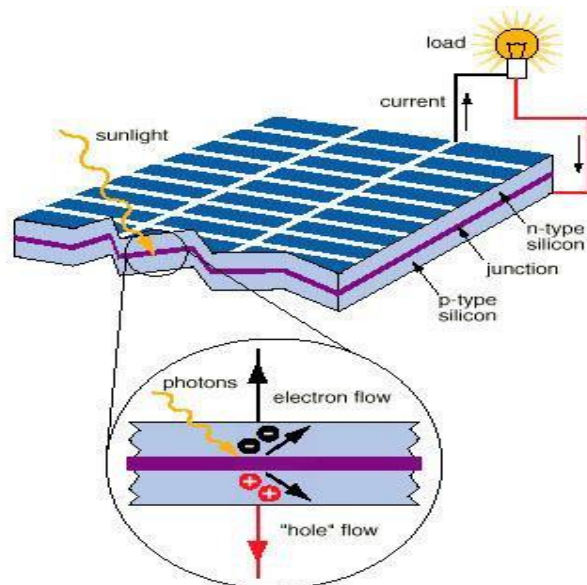


Figure 6: Internal reaction of solar energy (Shaikh, 2017).

### 2.4.1 Working Mechanism of Solar Energy

Solar power works by converting sunlight into direct current (DC) electricity. This is done by solar panels. Solar panels are made of silicon (PV) photovoltaic cells. Sunlight hits the solar panels and is absorbed by the solar PV cells. Electricity is generated through the photovoltaic effect. The electricity created is called direct current (DC) and it is not suitable for use by household appliances. Instead, the DC power is directed to a central inverter or micro-inverter and subsequently fed into a solar inverter that

can convert the DC electricity into Alternating Current (AC) electricity, which can be used by household appliances.

The Charge Controller acts as an energy controller for the solar panel. The basic actions of a controller are to block reverse current and a solar charge controller protects batteries from both overcharging and undercharging. It also shows the battery status and flow of power. Finally, batteries store energy generated by solar panels for later use. Therefore, the higher the battery's capacity, the more solar energy it can store (Shaikh, 2017). Figure 7 illustrates the working mechanism of solar energy.

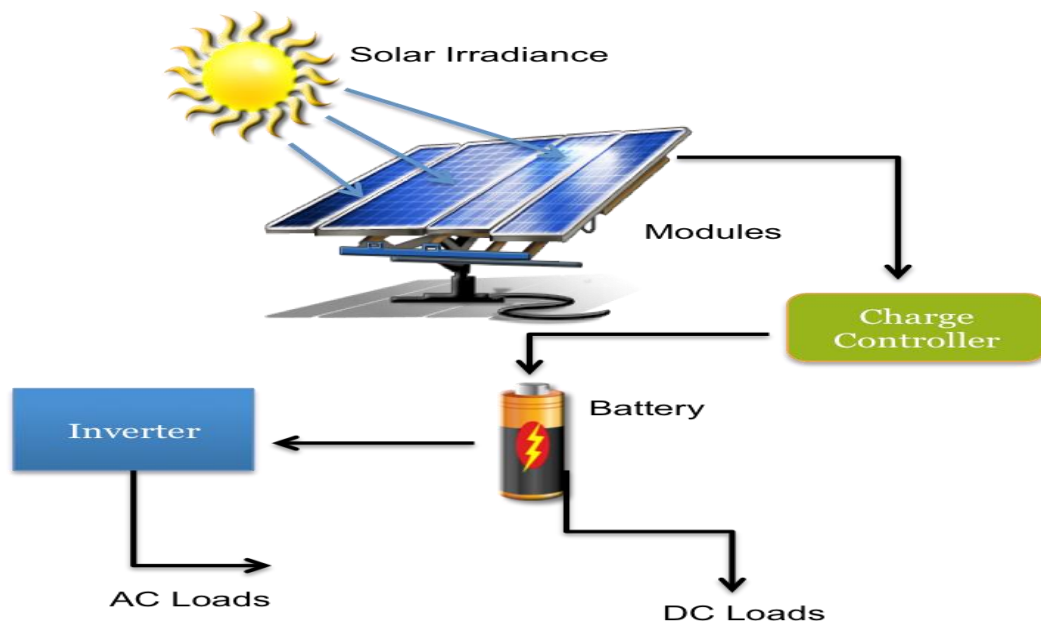


Figure 7: The working mechanism of solar energy (Sobamowo, et al., 2020).

## 2.5 The Electrical Characteristics of a PV Cell, PV Module, PV String, and a PV Array

### 2.5.1 Solar Cell

Each solar (photovoltaic) cell produces energy by converting sunlight directly into electricity. When light is attracted by a semiconductor, light photons can transfer their

energy to the electron, allowing the electron to pass through matter as an electric current. These steps are the basic way that energy from the sun is converted into electricity by solar cells. There are many photovoltaic cells in a solar panel, and the current generated by all the cells together provide enough electricity. A standard panel used in a rooftop residential system has 60 cells linked together. Larger panels with 72 or modern solar panels have one of these layouts: 60 full cells, 72 full cells, 120 half cells, 132 half cells, and 144 half cells and Silicon is the basic material used to make PV cells.

## **2.5.2 Types of Solar Cells**

### **2.5.2.1 Monocrystalline**

A Monocrystalline solar cell has a higher purity because each cell is made of a crystal of silicon. Therefore, monocrystalline panels are more efficient than poly panels. They also act better in an environment with high heat and low light. They cost more to produce, meaning it is more expensive compared to the poly cell with the same wattage.

The manufacturing process for mono panels is more wasteful than the other types of panels. Solar cells for Monocrystalline panels are produced with silicon wafers; the square silicon wafers are cut with the corners are shaved off at the end.

Lastly, as the cell is comprised of single-crystal silicon, it has a uniform black look and provides the electrons with more space to move for better current flow through the photovoltaic effect. In terms of efficiency, Monocrystalline solar cells have a commonly higher efficiency than their polycrystalline counterparts (Goodrich et al., 2012). Figure 8 shows the Monocrystalline panel with a close-up view of a single PV cell.



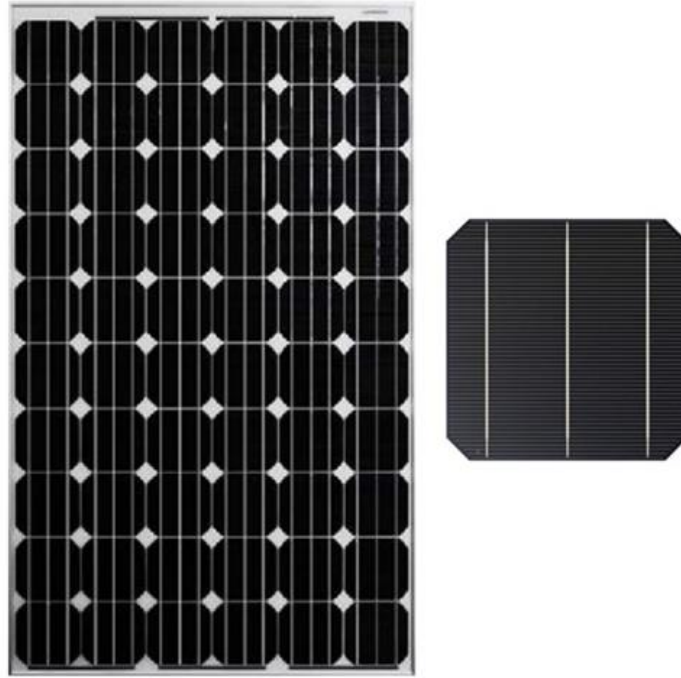


Figure 8: Monocrystalline panel (Guda and Aliyu, 2015).

### **2.5.2.2 Polycrystalline**

Polycrystalline panels are sometimes called Multi-crystalline panels. These types of solar cells are mixed from several pieces of silicon. They will not have the corners cut off and the way they are produced causes the panels to have a blue color. Polycrystalline panels will also include either 60 full cells, 120 half cells, 72 full cells, and 144 half cells. Polycrystalline cells have silicon particles that are placed in different directions, thus there is less freedom for the electrons, which makes it harder for electrons to flow. Therefore, the current flow is more difficult.

In terms of efficiency, polycrystalline solar cells generally have lower efficiencies than their Monocrystalline counterparts do. Polycrystalline panel efficiency ratings will usually range from 15% to 17%. Regardless, their advantage is that they come at a lower price and are cheaper to construct, which means they cost less for the user (Guda

and Aliyu, 2015). Figure 9 shows the Polycrystalline panel with a close-up view of a single PV cell.

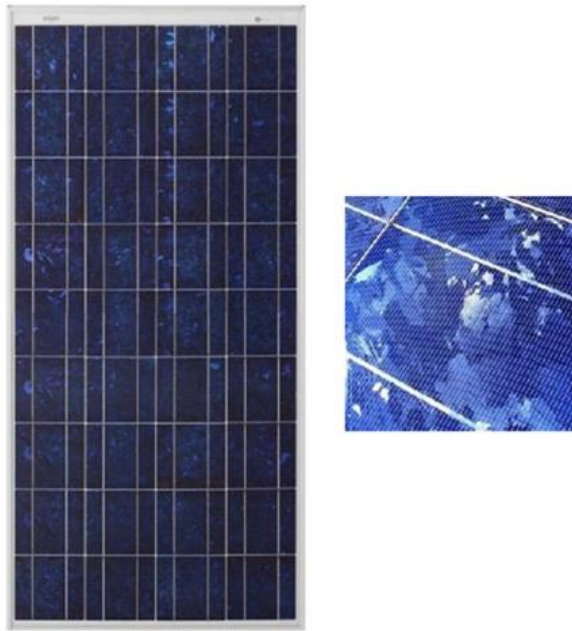


Figure 9: Polycrystalline panel (Guda and Aliyu 2015).

### **2.5.2.3 Thin-film Silicon**

Thin-film solar panels are completely different from Monocrystalline and polycrystalline solar panels. They are solid black and do not have the silicon cell margins you see on a crystal solar panel. Solar panels with a thin layer are usually lightweight, flexible, and easy to install. It has a shorter lifespan than other types of solar panels. For this reason, they are destroyed faster and need to be replaced more frequently.

Thin film technology has a reputation for being the worst of the solar panel technologies because they have the lowest efficiency. Thin-film solar panels also have the lowest cost among the three types of solar panels due to their low performance.

For this reason, they are used in operations on large-scale installations, such as industrial or utility solar projects and large-scale commercial projects. They are not suitable for residential installations (Bagher et al., 2015). Figure 10 shows the thin-film silicon panel with a close-up view of a single PV cell.



Figure 10: Thin-film silicon panel (Bagher et al., 2015).

### **2.5.3 Photovoltaic Module**

A PV module consists of solar cell circuits that are wired in series and/or in parallel to deliver voltage and current to a specific system, which is sealed in an environmentally friendly sheet and are the main structure blocks of the PV system. Thus, interconnected cells and their electrical connections are placed between an upper layer of clear plastic or glass and the lower layer of plastic and metal. An external frame is attached to gain mechanical strength and create a way to install the unit. This parcel is named a "module" or "panel" (see Figure 9).

Typically, a module is the main part of photovoltaic systems. The number of interconnected cells and their size determine the power output of a solar module. Generally, module efficiency is rated using Standard Test Conditions (STC): which is a radiation of  $1000 \text{ W/m}^2$  with an air mass 1.5 (1.5 AM) spectrum, a module temperature at  $25^\circ\text{C}$ , and no wind. Standard test conditions reflect normal working situations because the temperature of a full sun cell is above  $25^\circ\text{C}$ . However, STC-based performance calculations are applied in the flash tests of many manufacturers. PV modules are rated in peak watts [Wp], matching their output under STC. Thus, a 50 Wp module can be expected to supply 50 W of power under standard test conditions, although this efficiency is decreased by high temperatures (Kumar et al., 2020).



Figure 11: Photovoltaic module with multiple cells (Kumar et al., 2020).

#### **2.5.4 Sub-Array (String)**

A collection of PV modules is called a PV Panel, as shown in Figure 10. PV panels, also known as solar panels, can be connected in a string configuration to achieve the intended current and voltage at the inverter input. It can grab solar energy and change it into electricity. The electricity generated by PV panels is often used to power home appliances and equipment. The term solar panel is used conversationally for a

photovoltaic module and the PV module is a set of photovoltaic cells mounted in a frame for installation. Photovoltaic cells use sunlight as their energy source and generate direct current electricity (Kumar et al., 2020).

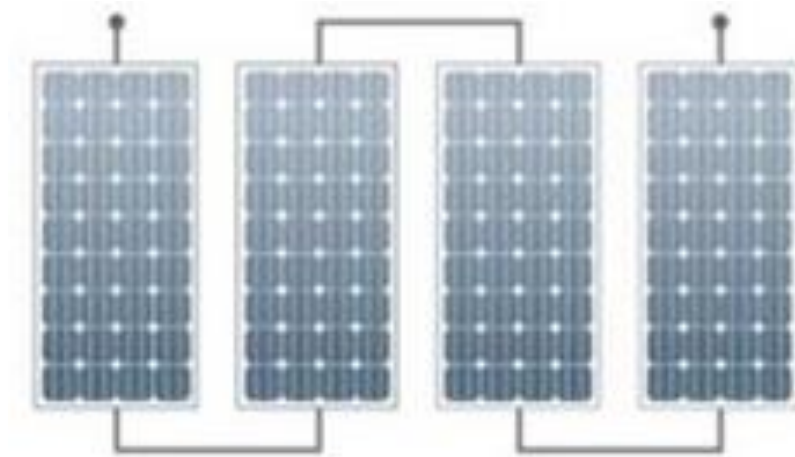


Figure 12: Photovoltaic panel with modules in series (Kumar et al., 2020).

### **2.5.5 Photovoltaic Array**

The Solar Photovoltaic array, also known simply as a solar array, is a system made up of several connected photovoltaic panels (see Figure 12). The higher the total array surface, the more solar power it will generate. In general, arrays are a way to enhance the potential of the solar power system to generate more electricity.

Hundreds of PV panels can only power a small or medium commercial business, or it can be made up of several separate PV modules or panels that are interconnected in an urban setting and installed on a rooftop.

Photovoltaic panels or modules from different producers must not be blended in an array, even if their voltage or current outputs are similar.

Differences in the characteristic I-V curves of solar panels and their spectral response are likely to result in additional loss of mismatch within the array, thus decreasing its total performance.

The panels in an array can be connected in series, in parallel, or a mixture of the two. For example, when two solar panels are wired in series, their voltage doubles while the current is constant.

In general, series connections are responsible for enhancing the module voltage, while the parallel connection is responsible for increasing the current in the array. The weather data is a compulsory need for the solar PV array model. Irradiance and temperature are input variables and the output can be current, voltage, power, or others. If slight changes in the input variables occur, this directly changes the output variables (Singh & Rajput, 2016).

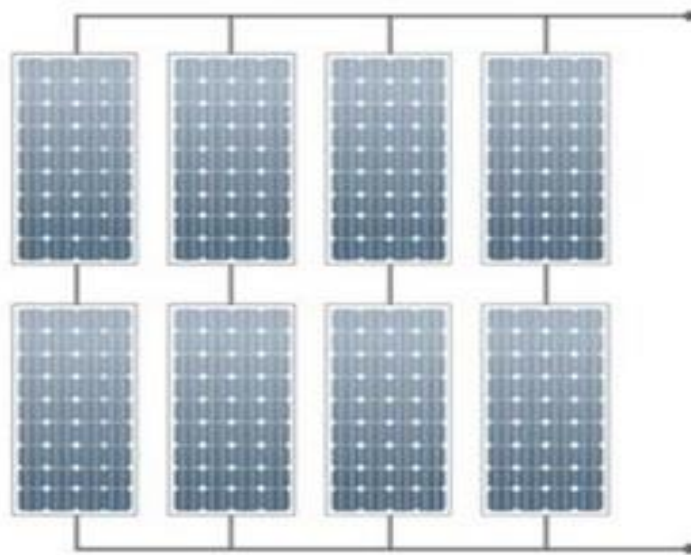


Figure 13: Photovoltaic array with strings in parallel (Singh & Rajput, 2016).

## **2.6 Classification of Solar Trackers**

The solar tracking system has an important role to play in various solar-energy applications. A solar tracker is a type of device with photovoltaic (PV) panels that accurately track the direction of the sun during the day and adjust the face of the solar panel or reflective area to track the sun's motion. The movement of solar trackers compared to standard panels increases the amount of solar energy by up to 40% (Banerjee, 2015).

While its advantages are not only limited to increasing efficiency and power compared to fixed systems, but it is also important in the economic analysis of solar energy applications. They are aligned to the equator with the ideal inclination angle to ensure the extreme impact of sunlight-based radiation on the collectors and solar panels. Site latitude and weather conditions determine the tracking angle.

Solar tracking systems have many classification bases; they are classified based on the type of drivers used, the control system used, the tracking strategy used, or the degree of freedom of movement indicated by the system. In other words, solar tracking systems are classified based on the mode of their motion (Banerjee, 2015).

### **2.6.1 Based on the Driving System Used**

#### **2.6.1.1 Passive Solar Tracking System**

Passive trackers use a pressurized gas liquid with a low boiling point, which is directed to one side or the other by creating gas pressure through solar heat. The resulting unbalance determines the motion of the tracker. That means during the time one side of the liquid-gas receives more thermal energy than the other side, the expanded gas moves to the other side of the tracker. Because this is not a precise orientation, it is not

suitable for some types of concentrated PV collectors, except for photovoltaic panels. These have sticky dampers to stop them from ample movement in response to the wind. An awning/reflector is applied to "arouse" the panel and tilt it towards the sun to reflect the morning sunshine, which takes about an hour.

The time to perform this can be decreased by adding a self-releasing knot that positions the panel a little past the climax so that liquids do not have to dominate gravity. For the use of passive solar tracking systems, the best geographical positions are close to the equator because there is minimal change in azimuth angles and altitudes, and solar radiation is high. In addition, this is useful for high power generation and separate applications. However, it has some drawbacks, namely: low efficiency, inaccuracy, and that the system depends on the thermic expansion process. Additionally, the tracking system is ineffective in the case of bad and unfavorable weather conditions (Hafez, et al., 2018). Figure 14 explains the working mechanism of the passive solar tracking system.

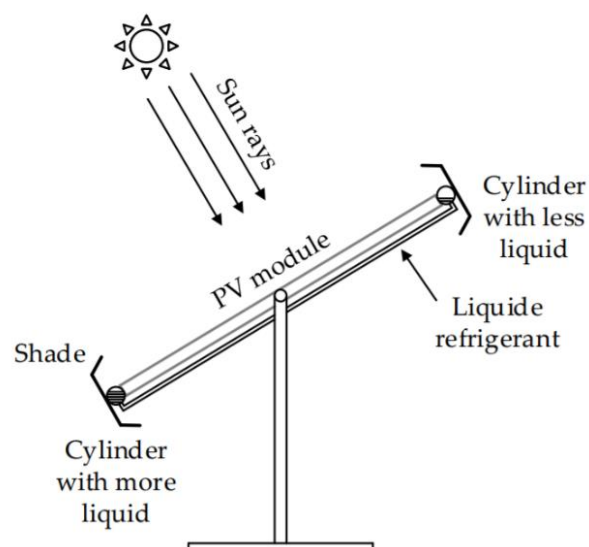


Figure 14: Passive solar tracking system (Nadia, et al., 2018).



### **2.6.1.2 Active Solar Tracking Systems**

Active solar tracking systems are those that use electrical drives and mechanical assemblies like motors, gear trains, and other controllers to direct the PV panels towards the sun. Active trackers are systems where during the day; the sensors determine the position of the sun's path in the sky.

These sensors stimulate the motor or actuator to move the actuator system towards the sun during the day. If the solar radiation rays are not perpendicular to the solar tracking system, this causes a difference in light intensity in one sensor compared to the other. It works so that the tracking system is perpendicular to the rays of sunlight. The active tracking system is arranged with a variety of controls such as microprocessors-based, electro-optical sensors-based, date and time methods, and auxiliary PV cells. For the purpose of controlling and managing the motion of these huge structures, special washing drives are designed and carefully tested.

The technologies used to guide the tracker are constantly developing and because machines consume energy, they are often only used when necessary. The heliostat moves in discrete stages instead of continuous motion. Also, if the light is below a predetermined threshold, not enough power will be provided to re-supply the direction. Therefore, cloudy cycles should be considered to prevent tracker energy loss (Nadia, et al., 2018). Figure 15 presents the active solar tracking system.

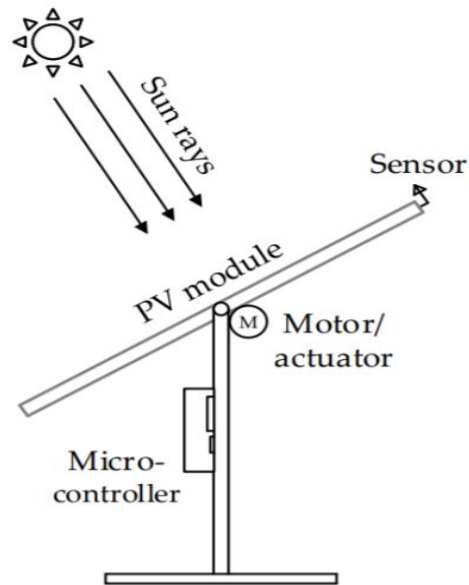


Figure 15: Active solar tracking system (Nadia, et al., 2018).

## 2.6.2 Based on the Control System Used

### 2.6.2.1 Closed-loop Tracking System

The closed-loop tracker is based on the principles of feedback control. In a closed-loop tracking control strategy, the position of the sun is searched at any time of the day. Light sensors are used and placed on a solar PV panel and after detecting the position of the sun by the sensor, it moves the axes of the PV tracking system. If the sun is not directly facing the solar PV screen, this results in a difference in light intensity between two different light sensors. This difference can be used to determine which direction the tracker should bend to be exposed to the sun. To determine the position of the sun, two similar light sensors are installed on the solar PV panel. They are placed in east and west or south and north to sense the intensity of the light source. A matte object is placed between the two sensors that separates the light from the other directions to search for a wide-angle and define the position of the sun faster. The sensed position is used to perform several calculations in mathematical equations. The results of these calculations can be used to determine the direction of the next tracker in the event of a

weather change. Closed-loop systems can consume more energy than the energy generated by the PV system. However, a closed-loop tracker can produce better tracking efficiency.

Feedback signals and tracking the position of the sun are eliminated by shading the LDRs or blocking the sun from the clouds. Besides, closed-loop trackers are more costly due to the presence of additional sensors and are more complex than open-loop trackers because they require LDRs mounted on the solar PV panel. In addition, a closed-loop controller is better compared to an open-loop controller, due to the reason that it can eliminate errors due to a variation in insolation (Huynh, et al., 2013). Figure 16 shows the schematic diagram of a closed-loop tracker.

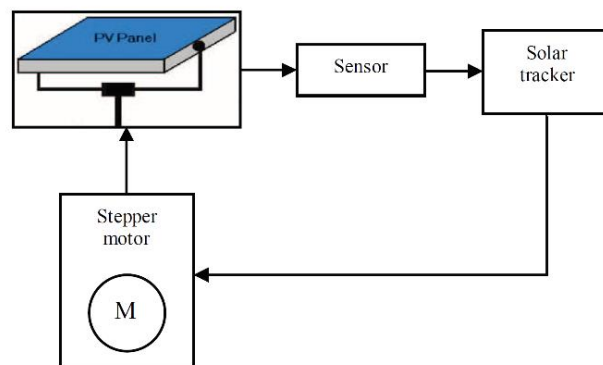


Figure 16: Scheme of a closed-loop tracker (Huynh, et al., 2013).

### 2.6.2.2 Open-loop Tracking System

An Open-loop Solar Tracker can track the sun without using a sensor. In this type of tracking control strategy, the tracker does not find the position of the sun; instead, the position of the sun for a special location is obtained by specification. The tracker receives the current time, day, month, and year and subsequently, without using any feedback, calculates the position of the sun and appraises the results of the actions of the trackers. Open-loop systems use control motors or actuators to track the position

of the sun based on mathematical equations. Moreover, the open-loop system is commonly simpler and inexpensive than the closed-loop system. This system does not control the results of the control process and cannot rectify errors or compensate for system malfunctions (Huynh, et al., 2013).

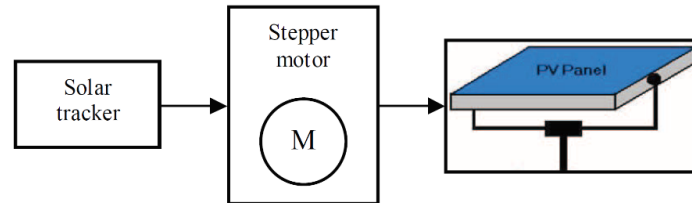


Figure 17: Scheme of an open-loop tracker (Huynh, D. C. et al., 2013).

### 2.6.3 Based on the Degree of Freedom

Anything that indicates the number of directions in which independent movement can happen is called the degree of freedom. Accordingly, tracking systems are classified into single-axis and dual-axis solar tracking systems. Before entering this classification, we examined the various types of axes and angles that play a significant role in determining the suitable locations and directions in these tracking systems, which play an essential role.

#### 2.6.3.1 Latitude

In geography, the distance on the surface of the earth, north or south of the equator, which is in angular measurements from 0 degrees in the equator to 90 degrees (north or south), is called the latitude (see Figure 18). This point or place is the angle created by the radial line that connects the place to the center of the earth by predicting the line on the equator.

The axis of rotation of the earth intersects the earth's surface at a latitude of 90 degrees (North Pole) and a latitude of 90 degrees (South Pole). Any place on the surface of the

earth can be defined by the junction of an angle of longitude and an angle of latitude (Racharla, & Rajan, 2017).

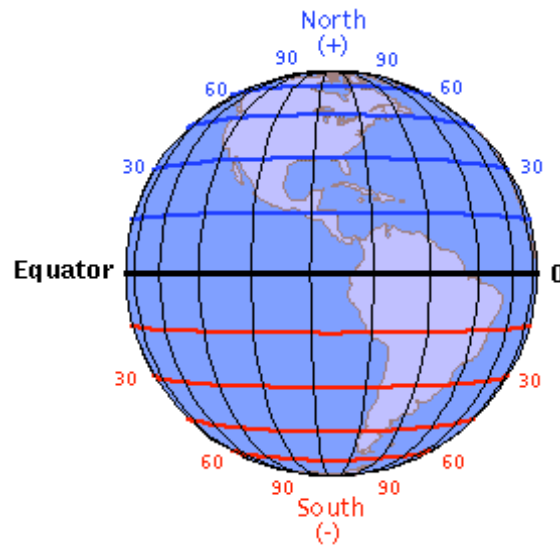


Figure 18: latitude (Racharla, & Rajan, 2017).

### 2.6.3.2 Longitude

The longitude lines, also called the meridian, cross the north and south, and come together at each pole. Each longitudinal line is a special numeric value starting at 0 degrees in the Prime Meridian – the main longitudinal line that passes through Greenwich, England – and increases up to 180 degrees to the east and 180 degrees to the west.

As a result, it covers the whole 360 degrees of the Earth. Like latitudinal degrees, longitudinal degrees are divided into 60 minutes. One minute is divided into 60 seconds. The longitudes, unlike latitude lines, which are parallel to each other, are not related to any definite distance from each other due to their convergent nature. For example, at the equator, one degree of longitude equals 60 nautical miles.

However, this distance gets smaller the farther away from the equator and the convergent path of all the longitude lines causes them to get closer to each other (Racharla & Rajan, 2017). Figure 19 shows longitude.

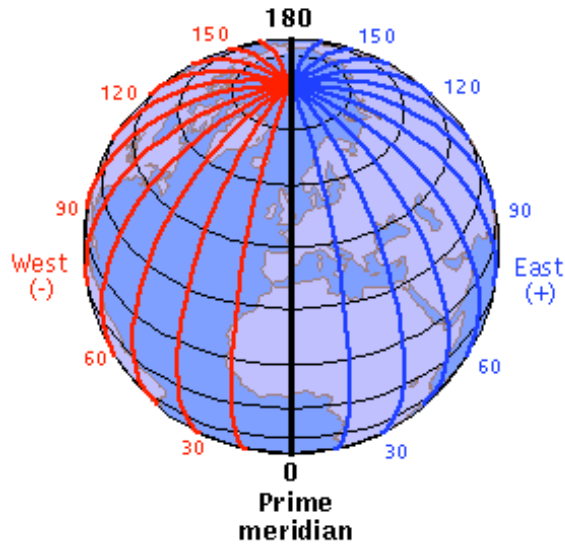


Figure 19: Longitude (Racharla & Rajan, 2017).

### 2.6.3.3 Air Mass

The path that light travels through the normalized atmosphere with the shortest possible length is called the Air Mass (i.e., when the sun is directly overhead). The Air Mass quantifies the reduction of the power of light as it passes through the atmosphere and is absorbed by air and dust. In the standard AM atmosphere, after attraction to calculate ordinary radiation, it is generally decreased from extraterrestrial solar radiation to  $1000 \text{ W/m}^2$ , which is the amount used for standard testing of PV devices (Rida, et al., 2016). Figure 20 demonstrates the air mass.

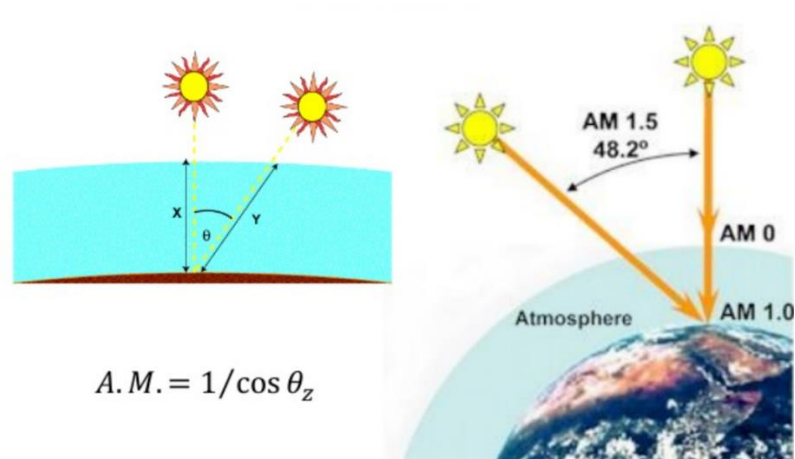


Figure 20: Air mass (Rida, et al., 2016).

### 2.6.3.4 Incidence Angle

The angle at which the sun's rays make a line perpendicular to the surface is called the incidence angle. For instance, the incidence angle of a direct surface facing the sun is zero, and the incidence angle of a surface parallel to the sun (such as sunrise with a horizontal roof) is 90° degrees. Sunlight tends to absorb at a 90° angle of incidence, while lower angles are reflected (Ismail, et al. 2016; Thomas et al. 1999). Figure 21 shows the incident angle of the sun.

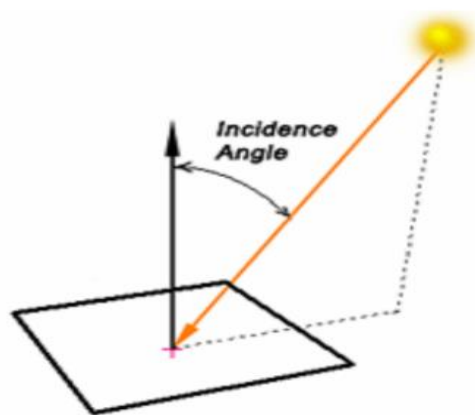


Figure 21: Incidence angle (Ismail, et al. 2016).

### 2.6.3.5 Declination Angle

The angle between the sun's rays and the equatorial plane is called the angle of declination. This angle is the declination of the sun, as illustrates in Figure 22. The declination is an ongoing variable function of time. This means that each day is considered a constant that changes the next day. The solar declination changes due to the rotation of the earth around an axis. The maximum value is  $23.45^\circ$  north on 21 December (Winter solstice) and the minimum is  $-23.45^\circ$  south on 21 June (Summer solstice) (Racharla & Rajan, 2017).

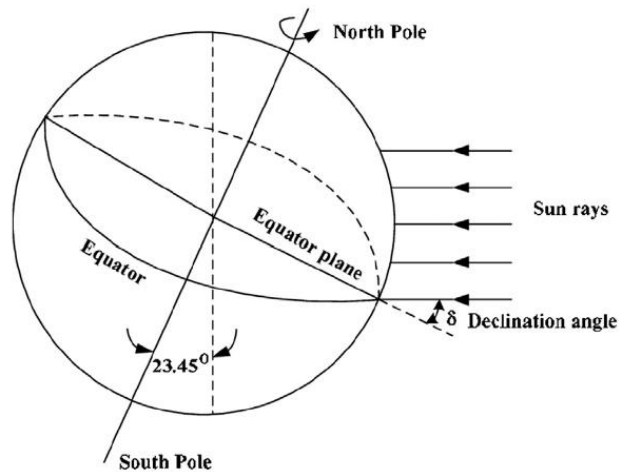


Figure 22: Declination angle (Racharla & Rajan, 2017).

### 2.6.3.6 Elevation/ Altitude Angle

The elevation angle (or altitude angle) is the angle between the sun's rays and a horizontal plane at a place on Earth. The elevation is  $0^\circ$  at sunrise and sunset, and  $90^\circ$  when the sun is straight overhead (i.e., at the equator in the spring and autumn equinoxes). If you are on the equator, one day of the equinox, at 12 solar hours, is  $90^\circ$ . Also during the night, the elevation is between  $-90^\circ$  and  $0^\circ$  (midnight). Furthermore, these two (the elevation and altitude angles) are used to explain the height in meters



above sea level. Elevation angles vary throughout the day and are dependent on the latitude of a specific place and the day of the year.

This is an important parameter in the design of PV solar systems as the maximum altitude angle is the maximum height of the sun in the sky at a specific time of year. This maximum altitude angle happens at sunny noon and is dependent on the declination and latitude angles (PAL & SUBBRA DAS, 2015).

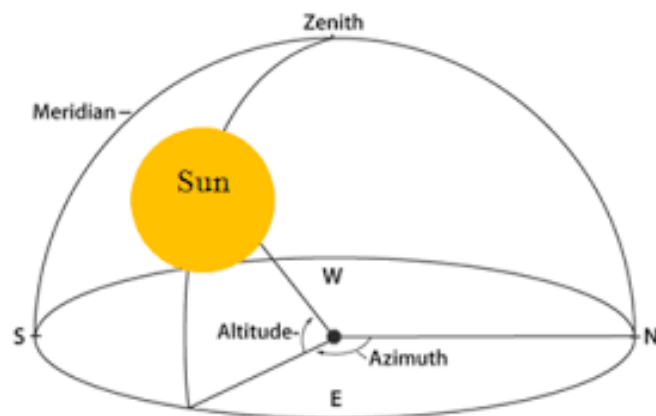


Figure 23: Elevation/ altitude angle (PAL & SUBBRA DAS, 2015).

### 2.6.3.7 Zenith Angle

The zenith angle is the angle between the sun's rays and the vertical line at a point on the Earth's surface. The zenith angle is the same as the altitude angle but is measured out vertically rather than horizontally, so the zenith angle equals  $90^\circ$  elevation. This is nearly related to the angle of elevation of the sun, which is the angle between the rays of the sun and the horizontal plane. Due to these two angles are supplementary, the cosine of each is equal to the sine of the other. The zenith angle is lowest at solar noon and equals latitude minus the angle of solar declination. The key parameters that specify the best position and path for solar tracking systems are the zenith angle. For

maximum illumination, the tilt angle of a PV module should be equal to the zenith angle (Nadia, et al., 2018) as shown in Figure 23.

### 2.6.3.8 Tilt Angle

The tilt angle is the angle between the solar panel and the horizontal ground and describes the solar panels' vertical angle. PV panels directly absorb solar radiation from the sun, the sky, and sunlight reflected from the PV panel's surrounding ground or area.

The selection effectiveness will be optimized by directing the photovoltaic panel in a direction and tilt to maximize its exposure to direct sunlight. The panel can most easily absorb solar radiation when the rays of the sun are perpendicular to the surface of the panel. The sun's angle differs throughout the year. Hence, in the winter, the optimal tilt angle for a PV panel would vary from the summer's optimal tilt angle. This angle can also differ by latitude. To obtain the best performance from solar panels,  $60^\circ$  is the best angle of inclination. The best angle during spring is  $45^\circ$ , and in the summer when the sun is high, it is better to have a low tilt at  $20^\circ$  (Yadav & Chandel, 2013).

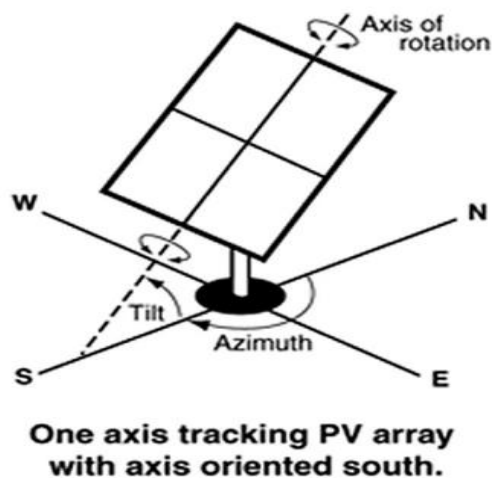


Figure 24: Tilt angle (Fouad, et al., 2017).

### **2.6.3.9 Solar Azimuth Angle**

The solar azimuth is an angle measurement that indicates the direction in which the tilted solar module or a solar array is facing. This angle is the direction of the compass from which sunlight comes. At solar noon, in the northern hemisphere, the sun is directly south, and in the southern hemisphere, directly north. The azimuth angle varies during the day. At the equinoxes, the sun rises straight to the east and sets straight to the west, regardless of latitude, thus determining the direction of the sun. For instance, the sun has an azimuth of  $0^\circ$  in the north,  $90^\circ$  east,  $180^\circ$  south, and  $270^\circ$  west (Awasthi, et al., 2020). The azimuth angle is shown in Figure 24.

## **2.6.4 Based on Tracking Strategies**

### **2.6.4.1 Date and Time**

This tracking system only uses predefined algorithms that stem from mathematical formulae and calculates the sun's position at a particular time to suitably orientate the PV panels. Accordingly, the panels do not involve any feedback loops or sensors.

Hence, the algorithm is only responsible for the efficiency of the system (Racharla, et al. 2017).

### **2.6.4.2 Microprocessors and Electro-optical Sensors**

This requires the detection of the location of the sun by sensors. The signals from the sensors are supplied to the microprocessor, which is programmed with instructions to provide control signals to the actuators. In 1996, Kalogirou has designed the solar tracking system with a perfectly accurate single-axis using 3 light-based resistors as sensors, an electronic circuit, and a DC motor with reduction gears. Here, sensors send the input to the electronic circuit that further stimulates the motor (Racharla, et al. 2017).

### **2.6.4.3 Sensors, Date, and Time**

In this tracking system, based on the date/time and sensor, electronic devices like a computer or microprocessor, from predefined algorithms based on geographical information or basic formulae, calculate the sun's position at a particular time to determine the orientation of the PV panels and subsequently send the signals to the electromotor. Hence, the algorithm and sensors are responsible for the efficiency of the system (Racharla, et al. 2017).

## **2.7 Fixed PV Systems**

The less complicated and cheapest solar panel stand is the fixed-tilt. This type of installation is fixed in position and does not track the sun through the sky during the day. The latitude of the panel site is typically equal to the faces in the direction of the southern sky at an angle. The quantity of electricity produced by the fixed-tilt photovoltaic solar system depends on the direction of the panels relative to the sun. When the rays of the sun are perpendicular to the panels, they absorb solar radiation efficiently (Perraki & Megas, 2014).

Two different angles that specify their orientation related to the sun are used by fixed-tilt photovoltaic systems: the azimuth and the tilt. Latitude is also the primary factor deciding the tilt of the panels, as tilting the panel at an angle equal to its latitude towards the south maximizes the annual exposure of the panel to direct sunlight (Karafil, et al., 2015).

Therefore, in the case of not changing the angle of the fixed mount solar plane and keeping it constant, an angle equal to latitude is an efficient angle. However, the angle of the fixed mount can be changed in winter and summer. In summer, it can be changed

up to 15 degrees to calculate higher sun angles. Besides, in the winter months, when the sun is lower in the sky and close to the Southern horizon, it can be set up to 15 degrees lower (Abdullah, et al., 2018).

Ideally, for better productivity, the tilt will be equivalent to 15 degrees less than your latitude during the summer months and 15 degrees higher than your latitude during the winter months. For more performance, you can manually adjust the tilt as often as you need, but a fixed tilt mount is not changed. In the ground-mount market share, many would say that the less advanced fixed-tilt technology is the second-best option (Bailek, et al., 2018). Figure 25 shows the fixed PV panel and the sun's incident angles during a day.

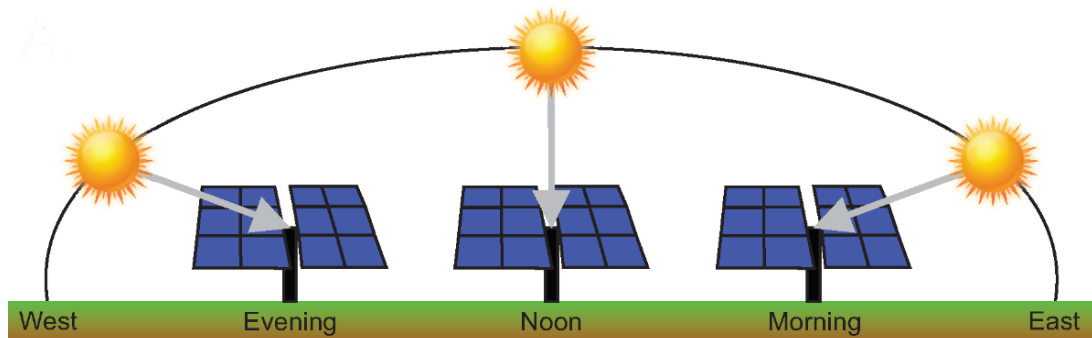


Figure 25: Position of a fixed PV panel during a day (Bailek, et al., 2018).

## 2.8 Tracking PV Systems

The solar panel is aligned towards the sun by a Solar Tracking system. During the day, the trackers alter the position of the panels to collect the maximum amount of solar energy. So these are known as sun tracking solar panels. The trackers operate towards getting the least angle of incidence; likewise, the incoming rays are nearly perpendicular to the panels. The angle reduction increases the output of energy through the panels (Banerjee, 2015). When adopting solar trackers, a few aspects must be

considered, namely the type of solar technology that needs to be applied, the expected amount of direct solar irradiation, feed-in tariffs in the project location, and the capital and regular maintenance cost of the system (Quesada, et al., 2015).

Power provided by the decentralized applications system can be increased using a tracker. Photovoltaic systems can be very efficient by using high-efficiency panels with trackers. Therefore, it is distinguished as a Single-axis tracking PV system and a Dual-axis tracking PV system. Solar tracking systems are more expensive compared to fixed angle systems because of having moving parts (Hafez, et al. 2018). Figure 26 shows the position of a solar tracker system during a day.

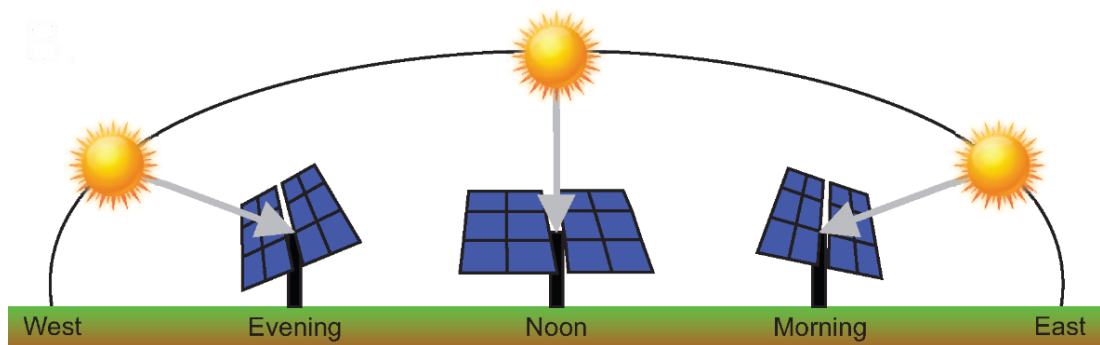


Figure 26: Position of a solar tracker system during a day (Bailek, et al., 2018).

### 2.8.1 Single-Axis Tracking PV Systems

One of the sun-tracking techniques is the single-axis solar tracking system, which rotates on one axis and moves in one direction, requiring the use of a pivotal point to rotate from one side to the other side. The single-axis solar tracker usually has a manual adjustment (tilt axis) on the second axis that is adjusted at regular periods throughout the year. Also, although the axis of rotation is aligned along the northern meridian, using the advanced tracking algorithm it can be aligned in any major direction. There

are several types of this system, including horizontal, vertical, tilted, and polar single-axis tracking (Seme, et al., 2020).

### 2.8.1.1 Horizontal Single-Axis Solar Tracker (HSAT)

In the horizontal single-axis tracking system, the rotation axis is configured parallel to the ground and commonly used in tropical regions. It rotates from East to West during the day and is used in many applications as the most cost-effective tracker geometry (Li, Tang, 2012).

At several points along the rotating axis, an HSAT structure can be assisted and thus requires less complexity and materials for manufacture than other tracking geometries. A horizontal tracking geometry is preferred because by holding the modules in a relatively low to the base and at a minimal overhung time load relative to the rotating axis without the need for special connections to rotate the system in its center of gravity, the structural needs of the material decrease (Li, Tang, & Zhong, 2012). Figure 27 illustrates the rotation of single-axis tracking using horizontal tilt.

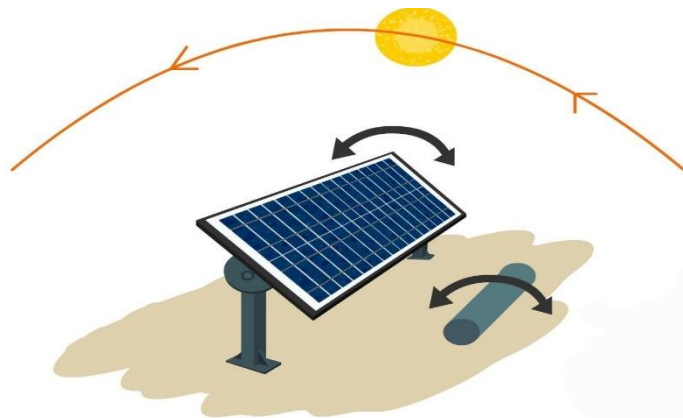


Figure 27: Single-axis tracking on a horizontal axis (Li, Tang, & Zhong, 2012).

### **2.8.1.2 Horizontal Tilted Single-Axis Solar Tracker (HTSAT)**

This type is similar to the HTSAT except that the system is installed on a certain tilt. In general, tilted-axis tracking systems are more complicated than horizontal one-axis trackers and require a concrete base. They tilt up and South (in the Northern hemisphere), rotating the panels East/West during the day to track the sun. Because of their complexity, HTSAT's are relatively expensive. They are also not able to be scaled or changed. This means that mechanical parts are not shared between units, therefore, in larger arrays, each panel may not cost less (Li, et al. 2012).

### **2.8.1.3 Vertical Single-Axis Solar Tracker (VSAT)**

In the vertical single-axis tracking system, the axis of rotation is configured vertically to the ground, and this type is commonly used in areas of high latitudes and mountains. Since their profiles are not parallel to the floor, these trackers have an easier time keeping a consistent solar incidence angle when the sun goes down in the sky. This is a specific advantage especially in Northern latitudes, for instance between 40° and 55°. However, to keep away from self-shading and unnecessary energy loss, they must expand the units and vertical field plan layouts must have higher vertical tracker specifications. As a result, they have relatively low-power densities per acre (Koussa, et al., 2011). Figure 28 shows a single-axis tracking system using a vertical axis to rotate the panel.



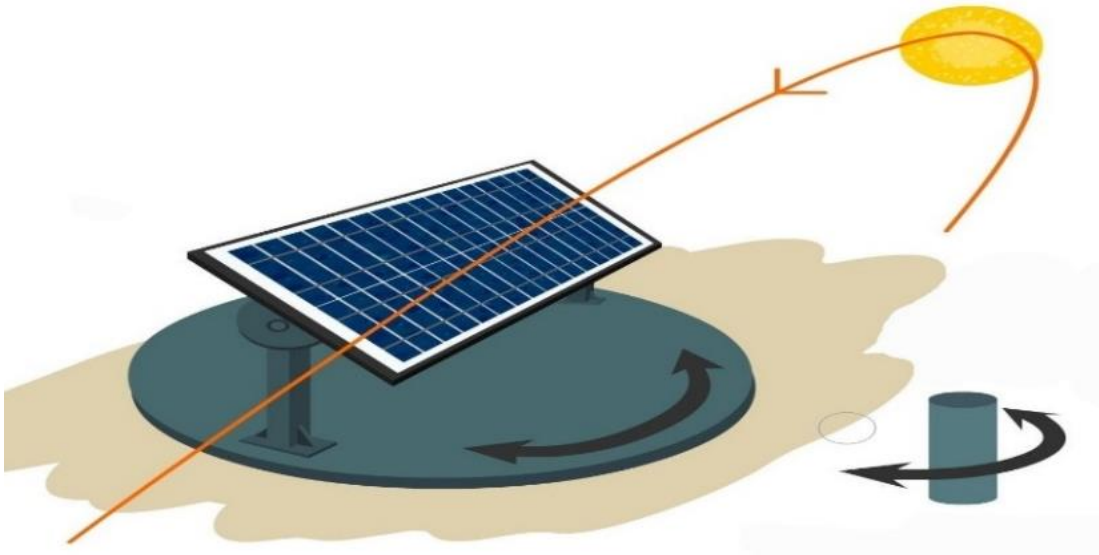


Figure 28: Single-axis tracking on a vertical axis (Li, Tang, & Zhong, 2012).

#### **2.8.1.4 Vertical-Tilted Single-Axis Solar Tracker (VTSAT)**

Except for the fact that the tilt is parallel to a horizontal plane and spins on a vertical axis, this is like the Horizontal Tilted Single-axis trackers. TSAT provides some of the benefits of horizontal designs, such as the advantage of dense packaging in each land unit. Compared to horizontal trackers, these trackers can significantly improve energy efficiency. However, compared to horizontal units, the tilted single-axis trackers and the optimal tilt angle are more prone to an increased wind load. As a consequence, the structural requirements are more, resulting in more steel and concrete being used compared to the horizontal array. In the tilted single-axis tracking system, the axis of rotation is between the horizontal and vertical axes, where the system collector is orientated parallel to the rotation of the axis. Single-axis detectors have only a single degree of inflection, which acts as a rotating axis. They are usually aligned from the north-south path, although they can be aligned in any main direction (Koussa, et al. 2011).

### **2.8.2 Advantages of Single-Axis Trackers**

1. Single-axis trackers are simple, inexpensive, and work at a low-cost (Banerjee, 2015).
2. They are more reliable.
3. They have a longer lifespan.
4. They are better for companies with a lower budget or zones with frequent clouds.
5. They have a better performance related to a PV panel in fixed form.
6. The effectuality of the single-axis solar tracker over the fixed solar tracking mount panel is 21% (as the thesis results).

The great disadvantage of this type of system is that it cannot track the sun during the annual motion, which means that it only tracks the sun during daily movement, and on cloudy days, due to rotation, the efficiency of the tracking system is greatly reduced. Besides, the incident light will not always be perpendicular to the aperture of the collector, thus solar energy collection is not adequate to sustain the maximum efficiency (Banerjee, 2015).

### **2.9 Dual-Axis Tracking PV Systems**

A dual-axis tracking system was implemented to overcome the limitations of the single-axis tracking system. In this type of tracking system, the rays of the sun are fully captured by tracking the sun's movement in four different directions (Sidek, et al., 2017). In addition to observing the East-West or North to South movement of the sun in the sky, it tracks the angular position of the sun. The dual-axis acts in the same manner as the single axis but takes the measurements of both the horizontal and the vertical axes (Abdullah, et al., 2017).

Dual-axis trackers are more popular among small residential and trading solar projects that have small spaces so they can produce enough power to meet up the energy they need. Two-axis tracking enables the solar system to be more precisely focused, provides a 40% energy absorption increase, and is more complicated and expensive. Ideally, the incidence angle is always zero in the case of dual-axis tracking, i.e., the surface is held perpendicular to the solar radiation (Sumathi, et al., 2017). To follow the sun, various manufacturers use various methods for tracking. For example, GPS signals are used by the AllEarth Renewables dual-axis trackers to determine the latitude and longitude of the tracker, as well as the date and time.

Using this information, the tracker determines the position of the sun for each time and directs its orientation towards the sun using a hydraulic actuator system. Even during cloudy times, the tracker will face the sun, so when the clouds split, the tracker is already in a position to generate maximum power generation immediately. Since the panels are directly interfacing with the sun, AllEarth approximations are such that its dual-axis trackers generate 45% more than a fixed-roof system and over 30% than a fixed-ground-mount system (Burnham, et al., 2019). Figure 29 illustrates the working mechanism of dual-axis tracking solar panels.

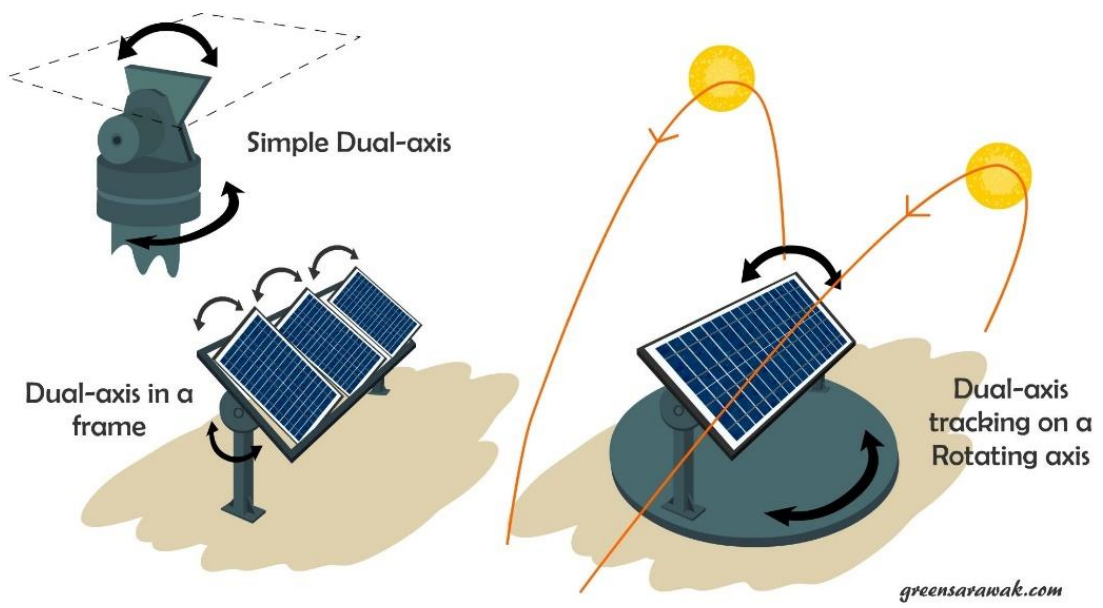


Figure 29: Dual-axis tracking solar panel (Burnham, et al., 2019).

## Chapter 3

### THE DESIGN METHOD AND APPLICATION

#### 3.1 The Proposed Design Model

This part of the chapter shows the methodology of designing a model of a standalone solar PV system with batteries for a single-family house having an energy consumption of 7.6 kWh/Day. The model is designed in multiple steps and each one, the required tasks are explained.

In the planning of a stand-alone solar PV System, the following site selection steps should be used in assessing and surveying the potential site (Mohanty,2016):

1. Select a site/location either on the roof or on the ground, which has the least amount of shade.
2. Determine the orientation and direction of the chosen site/location.
3. Calculate the total land/surface area of the chosen area available in the site/location.
4. In the case of the roof installation, the roof form and structure need to be considered.
5. Determine possible paths for cables, batteries, and charge controllers from selected site/location.

Figure 30 illustrates the workflow of the main stages and methods of the proposed model.

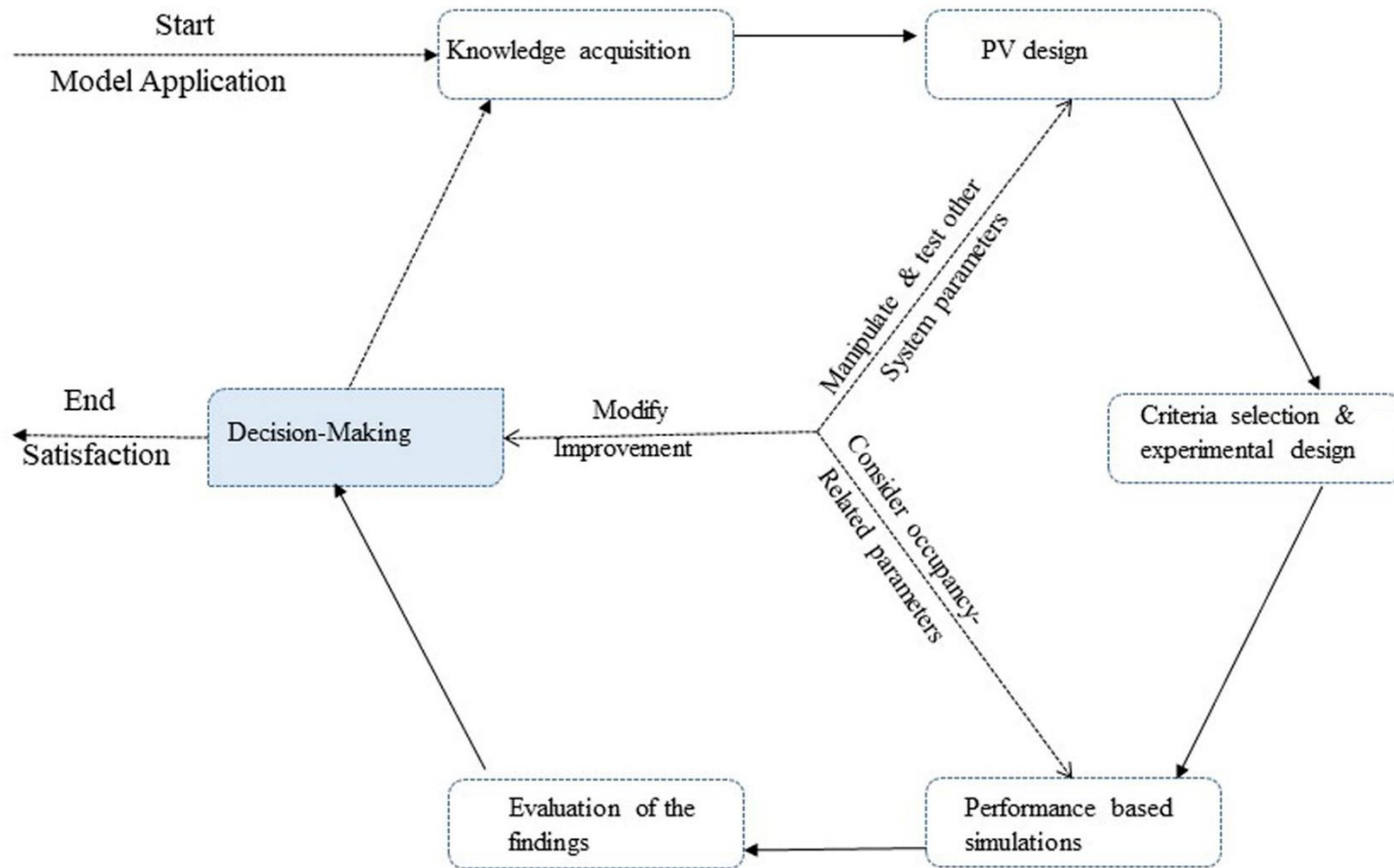


Figure 30: The main stages of the proposed model.

## 3.2 Application of the Design Model

The proposed model will be applied to design different PV system installations, including fixed-tilt, single-axis tracking, and two (dual)-axis tracking systems. The different PV installation systems will be compared based on the results obtained with PVsyst.

## 3.3 Steps of Design

Before designing the complete system in PVsyst, the pre-design step is performed to determine the magnitude of the design values. The steps followed are the following:

### 3.3.1 Project Design and Type of PV Solar System

Select Project Design and then Standalone on the PVsyst home screen, as presented in Figure 31.

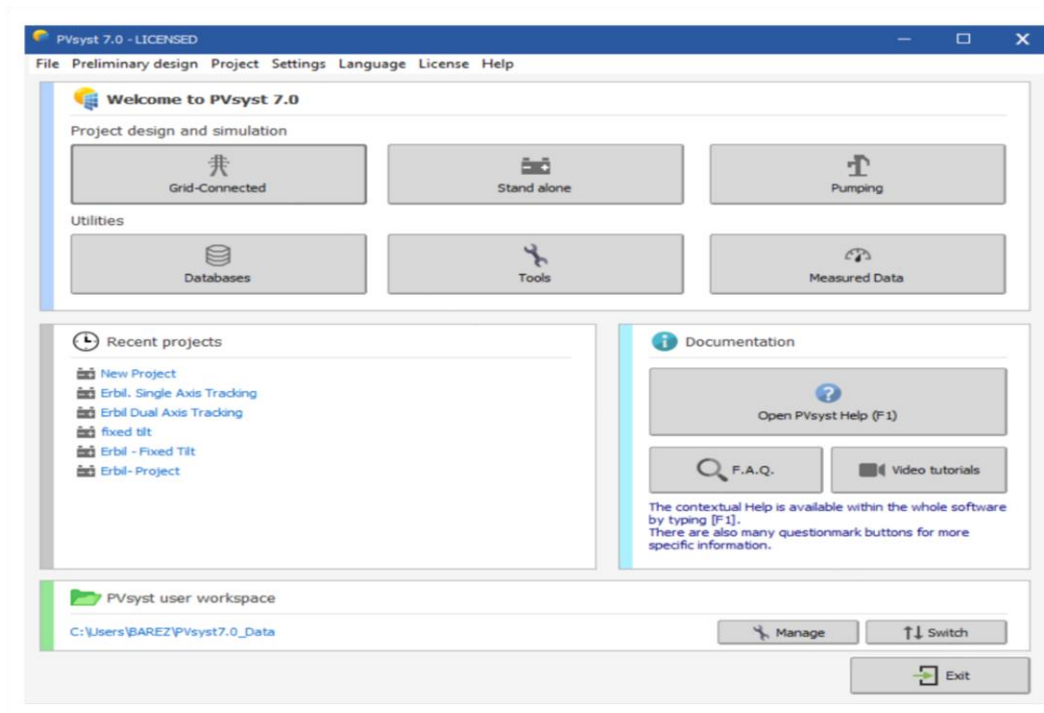


Figure 31: Selection of project design and type of PV solar system.

### 3.3.2 Define the Geographical Location and Meteorological Data

The appropriate site is selected based on solar radiation, which depends on the time of day and the geographical location. The building case selected for this study is located in Erbil, Iraq. Figure 32 shows the building's location on the map; its latitude is 36.1833, its longitude is 44.0119 and its altitude is 392 m. The detailed data is taken from Metronome 7.3 (1985-2000), Sat=100%, as a part of the PVsyst tool.

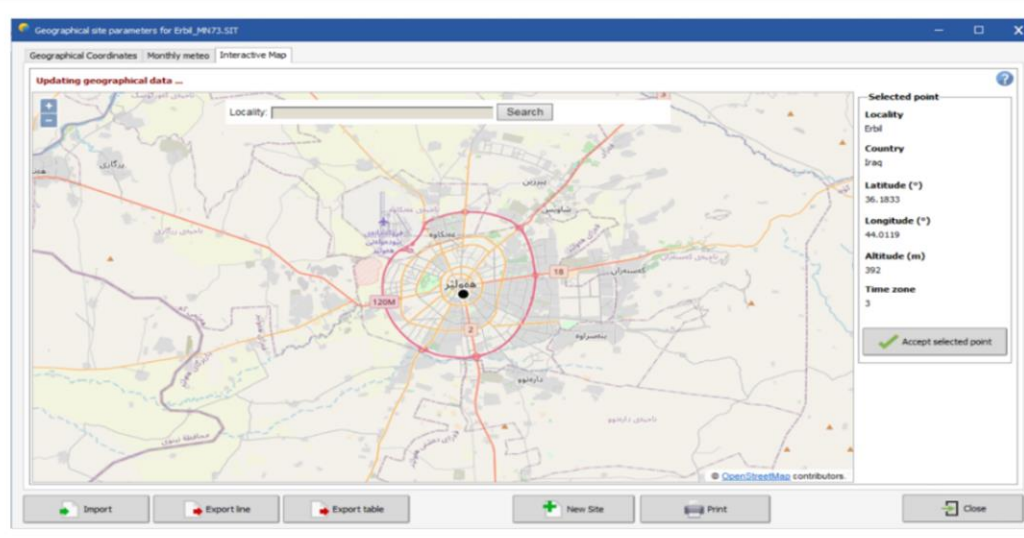


Figure 32: Defining the geographical location of the case study.

The building location has monthly meteorological data that is associated with each geographic site and is used to build hourly data. Monthly weather records contain the site name, country, and global area. Figure 33 below outlines the monthly global horizontal irradiation, averages of the ambient temperature, horizontal diffuse irradiation, and wind velocity.



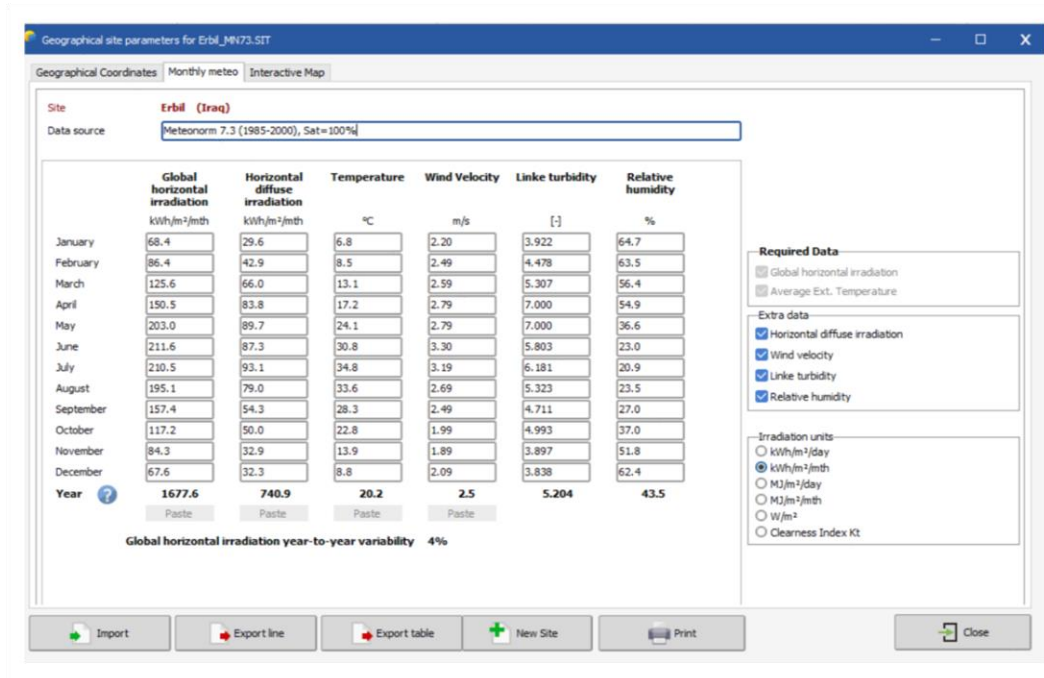


Figure 33: Determining metrological data of the case study

### 3.3.3 Orientation (Define Module Azimuth and Tilt)

The tilt angle can be adjusted depending on the position of installation and to optimize the yield of solar energy. To achieve optimum efficiency (i.e., zero losses), considering the weather and location of Erbil, the tilt angle is held around 30°, while the Azimuth angle is zero. In light of the aim of this research, three installation methods are applied, namely: fixed-tilt, single-axis tracking, and dual axes tracking, as illustrated in Figure 34.

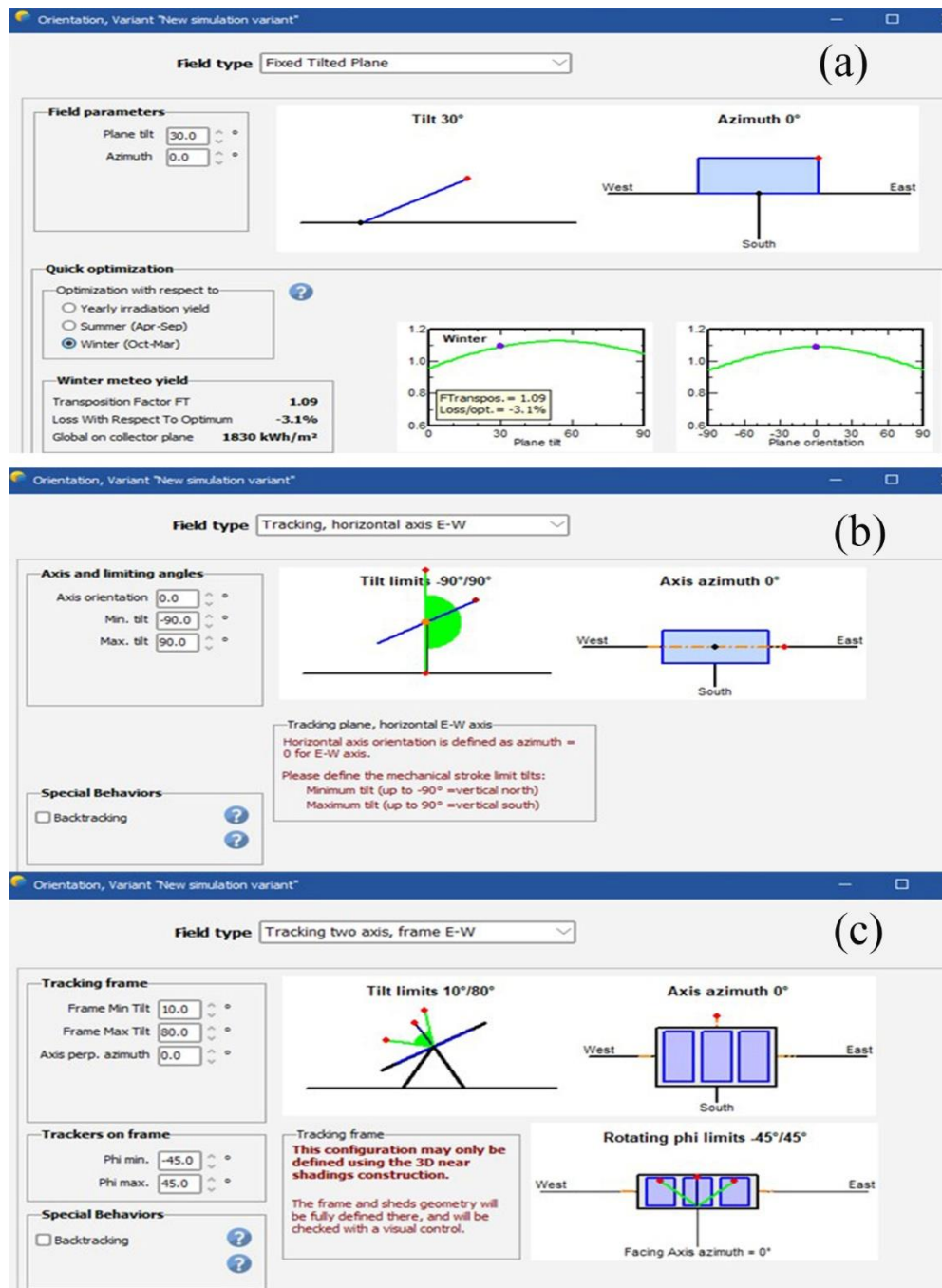


Figure 34: Selection of orientation for fixed installation (a), single-axis (b), and dual-axis tracking system (c).

### 3.3.4 User's needs (Define a Daily Profile for the Full Year)

This section of the pre-design phase focuses on the household load profile, particularly on important electrical equipment and the actions of users. The resulting estimates were applied to a comprehensive hourly load data profile for a single year as an input for the simulation. Site details, such as a load profile for regular household consumers

and the time of use of electrical appliances, are the key requirements for the design of the PV system. Figure 35 shows the standard house annual load profile that is constant over the year and the average energy consumption at 7.6 kWh/Day and Figure 36 illustrates the distribution schedule of the loads.

This is the fundamental step in designing a stand-alone solar PV system for a home or office or any other building is to calculate the total energy demand on a daily basis. For this purpose, the load of each lamp or appliance is measured in watts and the time of use or operation of that appliance is considered in hours. Load and the running time vary from appliance to appliance. Therefore, be careful in measuring and considering the load of appliances or any other devices along with their time of use as the size of stand-alone PV system dependent on this step (AlShemmary, 2013). The energy consumption demand of individual load in Wh (watt-hours) is calculated by multiplying the appliance's load power with its time of use as expressed in Equation 1:

$$E_i = P_i \times T_u \quad (1)$$

where:

- $E_i$  represents the energy demand per day of individual load in watt-hours.
- $P_i$  represents the rating of individual load in watts.
- $T_u$  represents the time of use of that load per day in hours.

Thus, the total energy demand in Wh on daily basis is calculated by adding the individual load demand of each appliance per day, mathematically expressed as:

$$E_t = \sum E_i = \sum (P_i \times T_u) \quad (2)$$

where:

- $E_t$  represents the total energy demand per day of all the load in watt-hours.

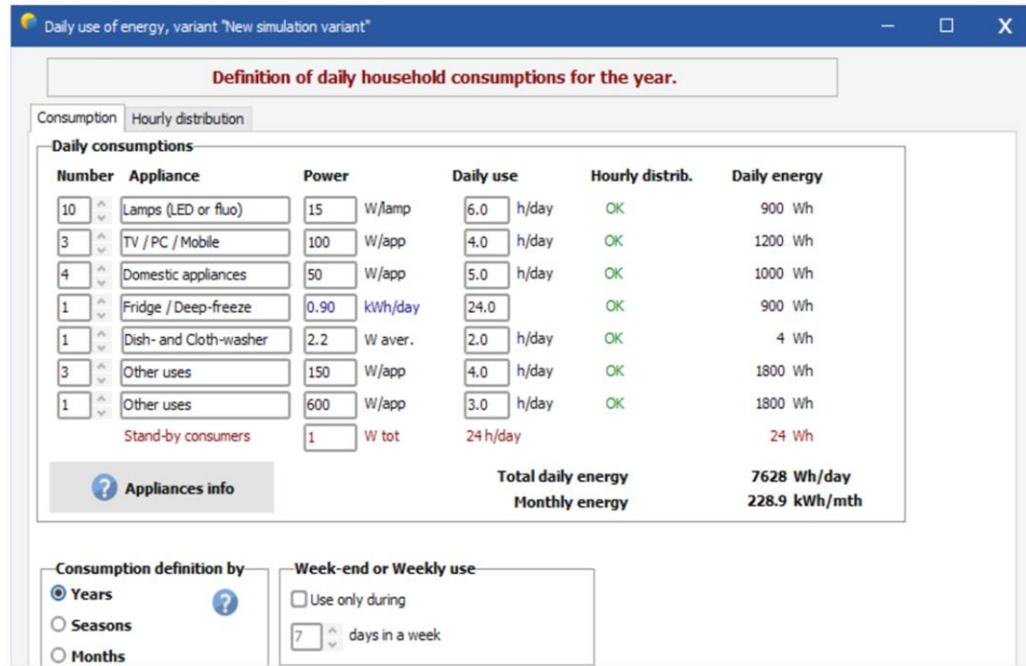


Figure 35: Load calculation of daily energy consumptions for the household, all load are AC.

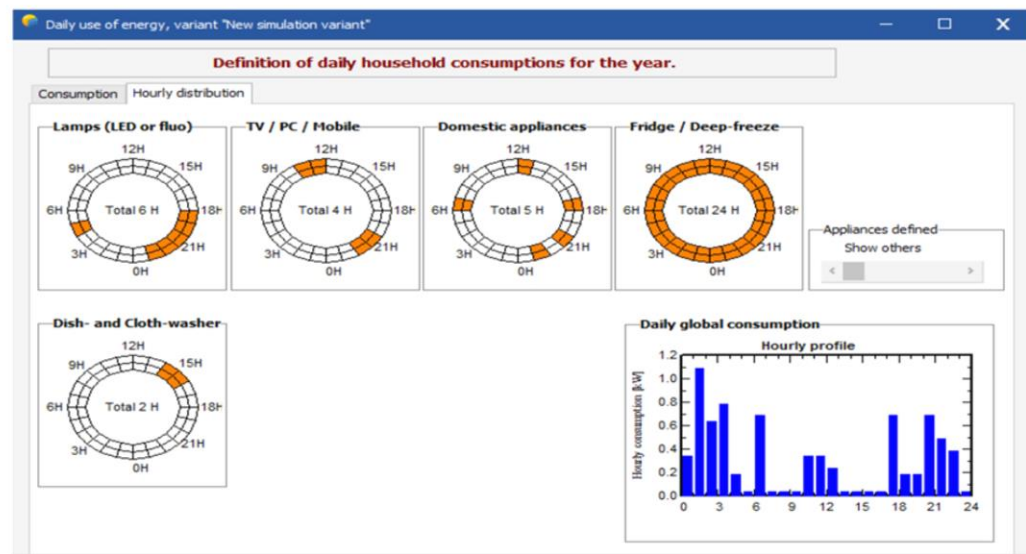


Figure 36: Hourly distribution of the loads.

### 3.3.5 Selecting the System Components (Choose the System Modules, Battery Storage, Controller, and the Inverter)

To fulfill the system design, parameter selection is very important for system configuration. All selected components are chosen based on the energy demand as determined by the load and potential meteorological information.

#### 3.3.5.1 PV Module Selection

There are different producers and technologies eligible to be chosen. PV array sizes depend on the available solar radiation. To build arrays, a large number of solar modules are connected. To provide adequate energy for the loads and to charge the battery, the PV array must be measured correctly. To balance the system's DC voltage, which is determined by the battery, the solar panels must be calibrated. Depending on the amount of the required load, the PV size may be increased or decreased as needed. The PV array must be at a certain angle to obtain the maximum amount of irradiance. The maximum performance of the PV array can be achieved using a tilt angle nearly equal to the site's latitude. The total number of panels required for a PV array design is 12 panels.

Therefore, to calculate the size and number of PV modules needed for specific loads, the rated peak-watts produced by the chosen panel is required. Thus, the total size of solar panels or PV array against specific load demand is calculated as (Ali, 2018):

$$P_{t-pv} = \frac{E_t}{PGF} \times 1.3 \quad (3)$$

$$P_{t-pv} = \frac{E_t}{T_{peak-hours}} \times 1.2 \quad (4)$$

where:

- $P_{t-pv}$  represents the complete size of the PV array in watts.

- PGF represents the power generation factor.
- $T_{peak-hours}$  represents the lowest daily average peak-sun hours of a month in a year.
- The value 1.3 represents the scaling factor.
- The value 1.2 represents the scaling factor same as in (3).

Hence, the number of PV modules or panels required against the total size of PV array in (3) or (4) is computed using the peak-watts of the chosen panel size on market availability as (Ali, 2018):

$$N_{modules} = \frac{P_{t-pv}}{Wp_i} \quad (5)$$

where:

- $N_{modules}$  represents the total number of modules.
- $Wp_i$  represents the rating in peak-watts of selected panel or module in watts.

Table 1 outlines the characteristics of the selected PV module.

Table 1: Monocrystalline (Trina\_TSM\_205\_D80.PAN with 32V) parameters.

<b>Parameters</b>	<b>Values</b>
Length	1581 mm
Width	809 mm
Weight	14.90 kg
Cells in Series	72
Cells in Parallel	1
Imp	5.42 A
Vmp	38 V
Voc	46.2 V
Isc	5.73 A
Power	205 W
Efficiency	16.10 %
No. of PV panels	12
No. of PV panels in series	4 modules
No. of PV panels in parallel	3 strings
Area needed	15.3 m <sup>2</sup>

### 3.3.5.2 Battery Storage

When the system is in operation, the battery charges and discharges when energy is exchanged. Various types of batteries can be included in the solar PV system, such as lead-acid batteries, lithium-ion batteries, alkaline batteries, etc. (Mahmoud, 2012; Pal, 2015 ).

The number of batteries selected depends on the loads and autonomous days, which indicates the number of days that a fully charged battery can handle system loads without any recharging from the PV array (Dunlop, 2015). Solar battery Depth of Discharge (DoD) is a very important factor to consider when selecting a battery and is expressed as a percentage of full capacity. If the battery is frequently discharged there will be fewer battery cycles to recharge it, in other words, a deeper level of discharge reduces the battery life. It is recommended that a battery is not discharged below 50% of its capacity. Important specifics to look for regarding the battery are size, Ah efficiency, capacity, cycle life, performance, auto-discharge rate, and space required, etc. The battery's voltage is dependent on the solar module configuration, which is between 12 and 48 volts, and the total number of amps.

According to AlShemmary (2013), the simplest relationship used to determine the size of batteries or battery bank for a certain load demand is expressed in Equation 6:

$$(Ah)_{bank} = \frac{E_t}{V_{dc-sys}} \times T_{backup} \times 0.05 \quad (6)$$

where:

- $T_{backup}$  represents the total time required for backup in hours.
- The value of 0.05 represents the derating factor.

Thus, the number of batteries required to construct the size of the battery bank in (6), is calculated using Equation 7:

$$N_{batteries} = \frac{(Ah)_{bank}}{(Ah)_{battery}} \quad (7)$$

where:

- $N_{batteries}$  represents the total number of batteries required against the size of  $(Ah)_{bank}$ .
- $(Ah)_{battery}$  represents the capacity of a single battery in an ampere-hour.

Table 2 shows the recommended battery specifications.

Table 2: Battery specifications.

<b>Battery characteristics</b>	
Battery type	MK_Battery_8G8D_Gel.BTR
Technology	Lead-acid, sealed, AGM
Autonomy	2 days
No. of batteries in series	4
No. of batteries in parallel	7
Battery pack voltage	48 V
Global capacity	1309 Ah
Stored energy	80 % DoD
Reference temperature	20 °C
Internal resistance	12.83 mΩ
Specific weight	36 kg

### 3.3.5.3 Charge Controller

In a stand-alone PV system, the main duty of the charge controller is to protect the battery from overcharging and over-discharging. Otherwise, the battery life will be shortened. It also regulates the voltage and current of PV panels and batteries and prevents the current from flowing back towards the modules.



There are two different types of charge controllers: PWM and MPPT. Both technologies are great for the standalone solar industry and are good options for efficient battery charging, although MPPT controllers have a higher rate of energy harvesting. Table 3 outlines the attributes of the selected charge controller. Thus, the ampere size or current rating of the solar charge controller is calculated mathematically by Equation 8:

$$I_{sec} = I_{sc} \times 1.3 \quad (8)$$

where:

- $I_{scc}$  represents the size of the solar charge controller in amperes.
- $I_{sc}$  represents the short circuit current rating of the selected PV unit.
- The value 1.3 represents the safety factor.

Table 3: Outlines the recommended charge controller specifications.

<b>Controller</b>	
Model	Universal controller with MPPT convertor
Technology	MPPT converter
Manufacture	Victron
No. of controllers	1
Max. charging current	56.6 A
Max. discharging current	22.7 A
Converter nom. power	1968 W
Nominal output voltage	48 V
Reference temperature	20 °C
Max. efficiency	97 %

### 3.3.5.4 Inverter

An inverter converts the DC electricity from the photovoltaic array into an alternating current (AC) that can connect seamlessly to the electricity grid. Most facilities are wired for AC, so the inverter plays a critical role. The efficiency of the modern inverter can be as high as 98%. The inverter also senses the utility power

frequency and synchronizes the photovoltaic-produced power to that frequency (Mohanty, 2016).

Thus, the size of the inverter is calculated by Equation 9:

$$(VA)_{inv} = (VA)_{t-load} \times CF. \quad (9)$$

where:

- $(VA)_{inv}$  represents the rating of the inverter in volt-ampere.
- CF represents the correction factor for safety whose value is 3 for motor loads and 1.25 for simple loads without a motor.
- $(VA)_{t-load}$  represents the total electrical load in voltampere and calculated by summation of the VA rating  $(VA)_i$  of all the individual loads as:

$$(VA)_{t-load} = \sum (VA)_i = \sum \frac{P_i}{pf} \quad (10)$$

- $pf$  is the power factor of each load.

### 3.3.6 Detailed Losses –Mismatch

This section is used in reporting the system status, useful for analyzing design options, and accurately calculating all losses (PV array losses, system losses, PV loss due to irradiance level, PV loss due to temperature, converter losses, and battery efficiency loss).

### 3.3.7 Horizon

The horizon shows the amount of useful sunlight available. The red line indicates the surrounding obstacles and the blue line is the auto-shading of the PV modules, while the solar field represents the distant trees.

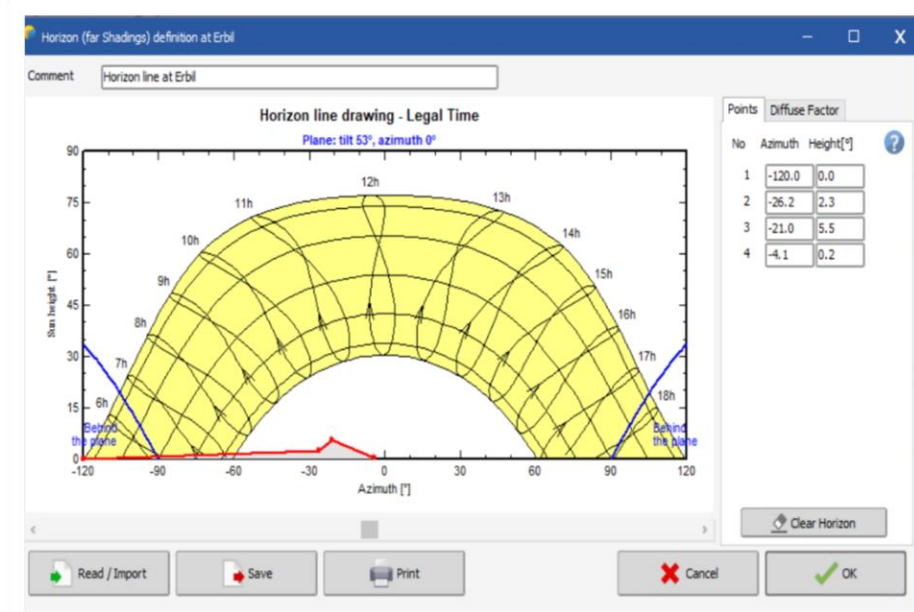


Figure 37: Horizon (for shading) definition at Erbil.

### 3.3.8 Near Shading

This section simulates the shadow impact of objects that are less than 50 m from the system. The 3D simulation can be performed using a house or tree with PV panels. It requires the architect to build 3D plans, which requires a prior understanding of the exact sizes, arrays' heights, surrounding barriers, and positions.

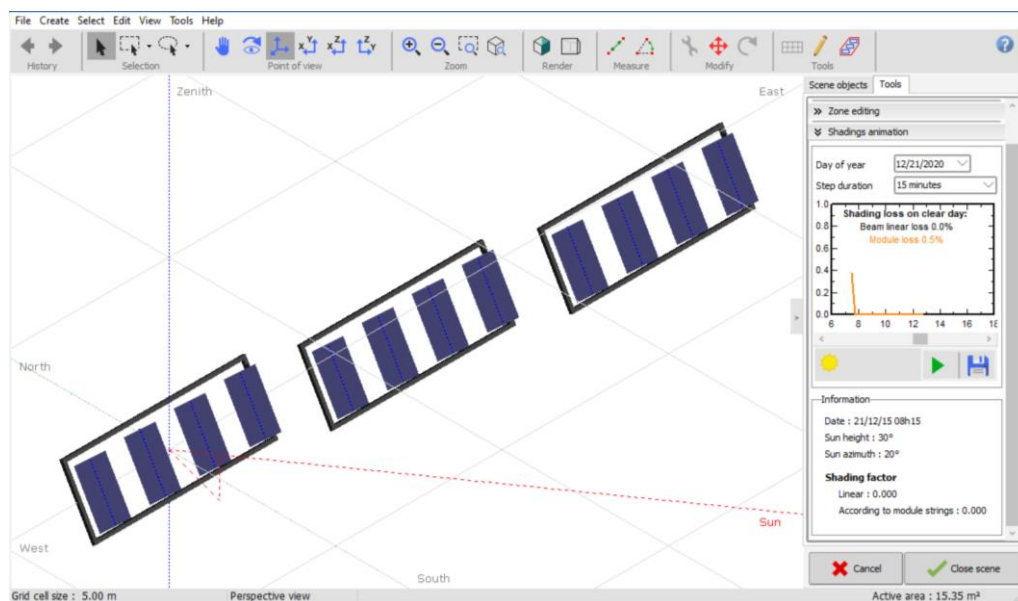


Figure 38: Shading scene construction.

## Chapter 4

### RESULTS AND DISCUSSION

#### 4.1 Results of Fixed Installation PV System

##### 4.1.1 Balances and Main Simulation Results

Figure 39 shows the balances and main results of the system for the 205W PV panels, where annual global horizontal irradiation is 1677.7 kWh/m<sup>2</sup>/year. The global effectiveness of IAM and shadings is 1838.8 kWh/m<sup>2</sup> per year. The available solar energy (E\_Avail) per year is 3731.4 kWh, the unused energy (full battery) is 774.1kWh, the missing energy (E\_Miss) is 0 kWh, the energy supplied to the user (E\_User) is 2784.4 kWh, the energy needed for load (ELoad) is 2784.4kWh, and solar fraction (SolFrac) is 1.000 For 205W PV panel.

	<b>GlobHor</b> kWh/m <sup>2</sup>	<b>GlobEff</b> kWh/m <sup>2</sup>	<b>E_Avail</b> kWh	<b>EUnused</b> kWh	<b>E_Miss</b> kWh	<b>E_User</b> kWh	<b>E_Load</b> kWh	<b>SolFrac</b> ratio
<b>January</b>	68.4	101.1	222.9	0.0	0.000	236.5	236.5	1.000
<b>February</b>	86.4	111.8	244.6	0.0	0.000	213.6	213.6	1.000
<b>March</b>	125.6	142.3	303.2	30.7	0.000	236.5	236.5	1.000
<b>April</b>	150.5	154.9	326.3	79.2	0.000	228.9	228.9	1.000
<b>May</b>	203.0	192.8	388.5	132.9	0.000	236.5	236.5	1.000
<b>June</b>	211.6	192.3	372.1	123.8	0.000	228.9	228.9	1.000
<b>July</b>	210.5	195.4	370.4	114.7	0.000	236.5	236.5	1.000
<b>August</b>	195.1	196.3	370.9	115.2	0.000	236.5	236.5	1.000
<b>September</b>	157.4	179.2	346.4	99.5	0.000	228.9	228.9	1.000
<b>October</b>	117.2	147.6	298.1	46.5	0.000	236.5	236.5	1.000
<b>November</b>	84.3	123.5	263.9	29.9	0.000	228.9	228.9	1.000
<b>December</b>	67.6	101.5	224.1	1.7	0.000	236.5	236.5	1.000
<b>Year</b>	1677.7	1838.8	3731.4	774.1	0.000	2784.4	2784.4	1.000

Legends:	GlobHor	Global horizontal irradiation	E_Miss	Missing energy
	GlobEff	Effective Global, corr. for IAM and shadings	E_User	Energy supplied to the user
	E_Avail	Available Solar Energy	E_Load	Energy need of the user (Load)
	EUnused	Unused energy (battery full)	SolFrac	Solar fraction (EUsed / ELoad)

Figure 39: Balances and main result of the photovoltaic system for Fixed-tilt.

### 4.1.2 Performance Ratio PR and Solar Fraction SF

Performance Ratio (PR) is the efficiency of the system throughout the year, which provides information about the effect of total losses of the system on the rated output. Losses include the modules, shade, dust, tilt angle, and temperature losses of the module. It describes the relationship between the PV plants theoretical and real energy outputs. There are fluctuations in system output throughout the year; although, the solar fraction shows a constant during the year.

By looking at Figure 40, the annual solar fraction and performance ratios are 100% and 59.9%, respectively. It is worth mentioning that the solar fraction (ESol / Eload) refers to the energy produced by the module to the energy fed to the load.

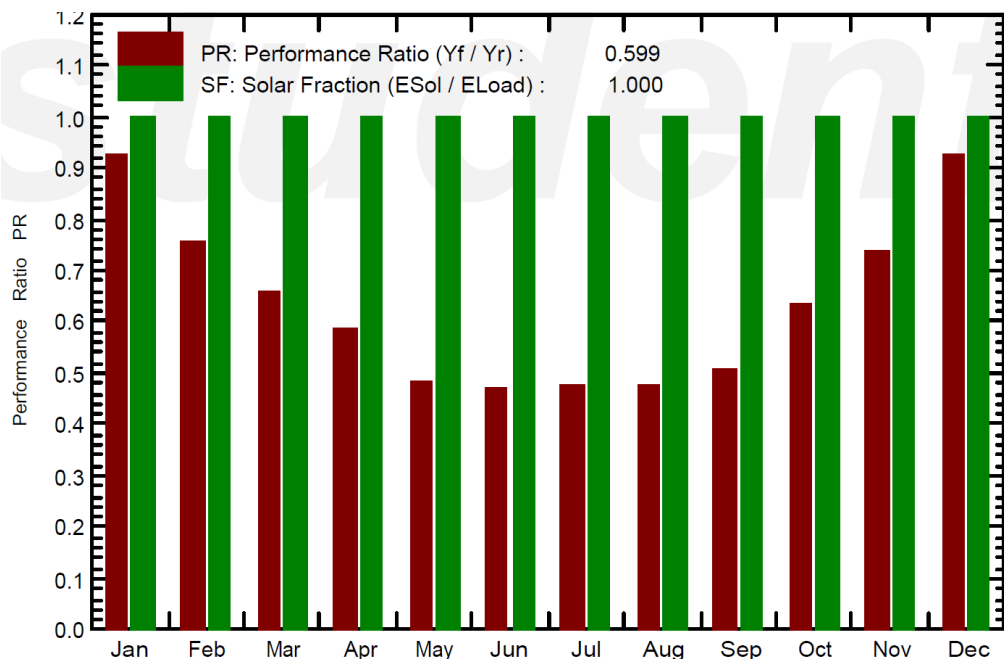


Figure 40: PR 59.9% and solar fraction 100%.

### 4.1.3 Normalized Production

Figure 38, shows the PV power plant's normalized production. It describes the unused energy, PV array collection losses, energy supplied to the user, system losses, and

battery charge. It also presents the monthly output and losses per kWh. Normalized productions (per installed kWp) are evaluated from the research on simulation as shown in Figure 41. For a 205W PV panel, the unused energy (battery full) is 0.86 kWh/kWp/day, collection loss (PV-array losses) is 0.88 kWh/kWp/day, system losses and battery charging is 0.34 kWh/kWp/day, and energy supplied to the user is 3.1 kWh/kWp/day.

The highest PV module losses occur in July, August, and September. In addition, the highest amount of unused energy is recorded in September and October, while September also has the most system losses.

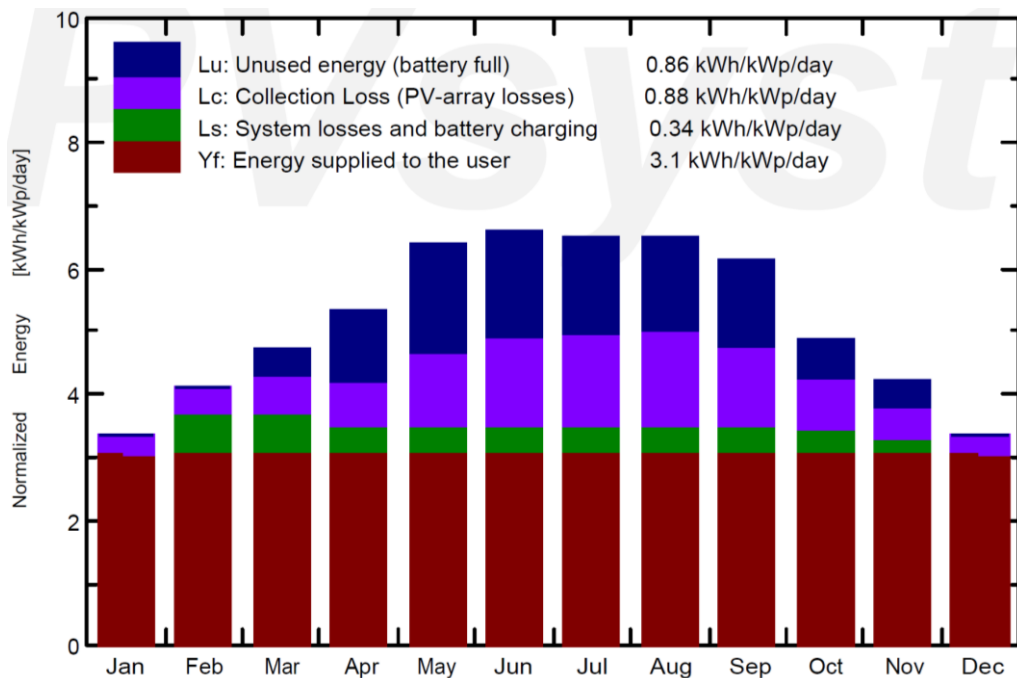


Figure 41: Normalized production for 280W Panel.

#### 4.1.4 Shading Factor

Figure 42 is used to calculate the shading factor integral for the diffuse and albedo sections, and to create the ISO-shadings diagrams. It is a table with pre-calculated values at the height of the sun (Tilt = 30° step) and azimuth (0° step), which is suitable

for obtaining the shading factor for any sun's direction. Shading Factor: The shaded part of the PV field is quite sensitive to the direction of the sun (values = 0 without shadow, 1 = fully shaded). Also, the blue color indicates the points (positions of the sun) located behind the area of the photovoltaic field.

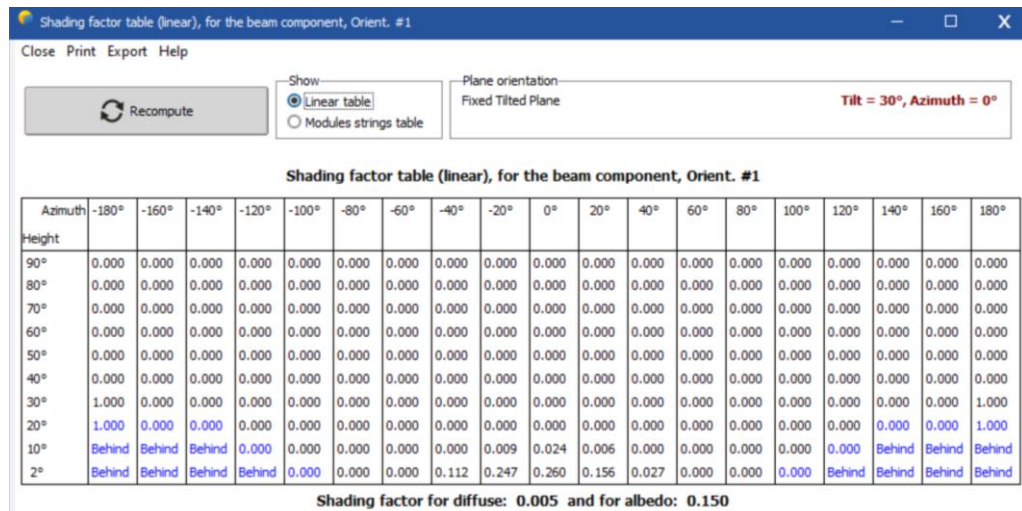


Figure 42: Shading factor.

#### 4.1.5 Shading Diagram

The PVsyst software determines the path of the sun in the sky, which comes up with details on losses that occur during the year because solar modules are unable to produce continuous electricity. The analysis of the shading factor gives an idea of how much energy is lost from the PV panels due to both near and far shading. Near shading is a partial shading affecting a portion of the panel. The shaded part changes day by day as well as during a season. For a near-shading scene, the shadow drop depends on the sun's height and the azimuth. The iso-lines (1, 5, 10, 20, and 40%) denote shading losses according to the time and date generated by PVsyst. This means that the losses due to shading are the last shading impacts that disappear every hour of the morning and the first shading effects that appear in the afternoon. The sun's motion throughout the year changes with a minimum altitude and maximum shading losses (40%) on 22nd

December to a maximum altitude and minimum shading losses (1%) on 22nd June. For these calculations, the damping for diffused light is 0.005 and the albedo is 0.15. All actual dates in the panels for which the shading losses have been depicted are related to the second half of each month. From Figure (43), it is clear that the notion of "behind the plane" applies just to fixed arrays. The iso-shading lines are increased upward because the azimuth angle increased in the (+80°, -80°) and (+118°/-118°) band, and especially in summer, it is close to behind the plane barrier. The fixed-tilt array experiences very small or no straight beam shading during the period from 7.00 am to 5.00 pm.

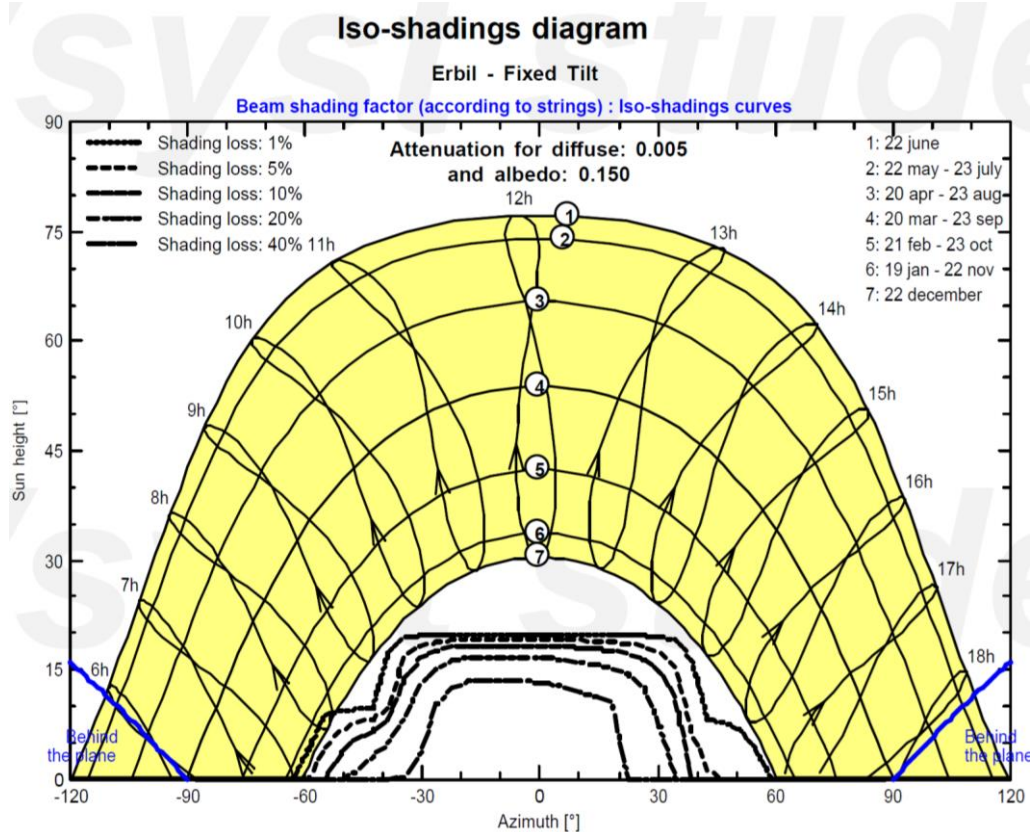


Figure 43: Iso-shading curve for fixed tilt.



#### **4.1.6 Loss Diagram**

This reports the system's performance with all details of losses. This diagram is useful for analyzing design choices and is used in comparing systems. The detailed over the whole year loss diagram is shown in Figure 44. The global horizontal irradiation is 1678 kWh/m<sup>2</sup>, the effective irradiation on collectors is 1839 kWh/m<sup>2</sup> \* 15 m<sup>2</sup> coll. Following the PV conversion, the array nominal energy at Standard Test Condition (STC) (1,000 watts/m<sup>2</sup>, solar irradiance, 1.5 Air Mass, and a 25 °C) is 4545 kWh, and efficiency at STC is 16.10%.

Effective energy at the output of the array is 3088 kWh. After the battery storage, the energy supplied to the user is 2784 kWh, and the energy requirement of the user is 2784 kWh. According to this, the missing energy is 0%. The diagram below shows that about 29.77% of the losses are accounted for as module losses, 4.24% as converter losses, and 8.7% as battery losses. In addition, the direct use of battery storage is 14.7% while stored energy accounts for 85.3%. It is observed that the highest loss occurs on the Unused energy(battery full) at 20.04%.

Loss diagram over the whole year

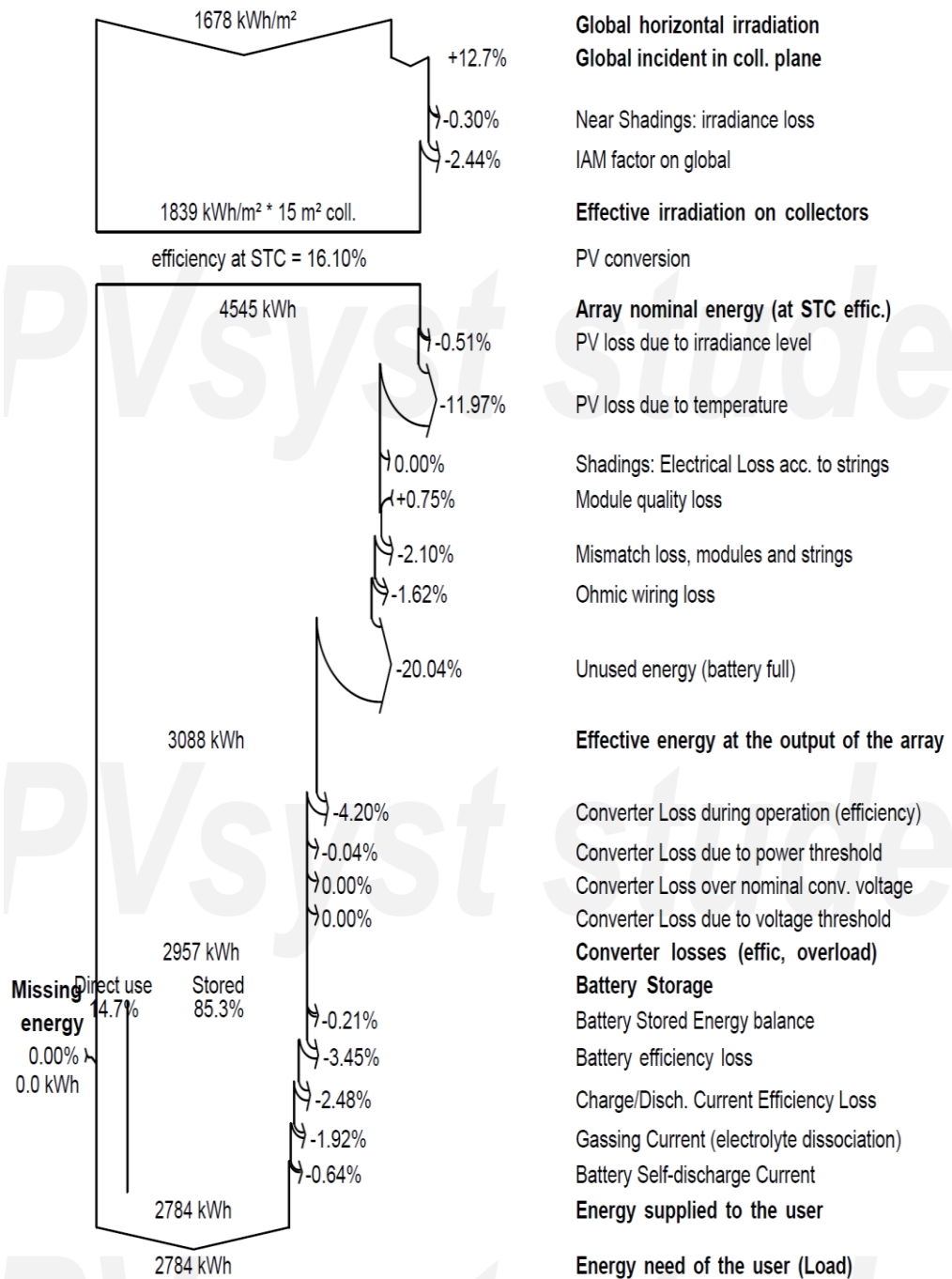


Figure 44: Losses diagram – fixed tilt.

## 4.2 Results of Single-Axis Tracking PV System

### 4.2.1 Balances and Main Simulation Results

Figure 45 shows the balances and main results of the Single-Axis Tracker system for the 205W PV panels. The yearly energy load requirement (E\_Load) and global horizontal irradiation are the same as the fixed-tilt system. The yearly global effective after all optical losses (shadings, IAM, soiling) is 1964.8 kWh/m<sup>2</sup>. The available solar energy is 3978.5kWh per year, the unused energy or full battery is 1018.9kWh, the missing energy is 0kWh, the energy supplied to the user equal to 2784.4kWh, and solar fraction (SolFrac) is 1.000 for a 205W PV panel.

	<b>GlobHor</b> kWh/m <sup>2</sup>	<b>GlobEff</b> kWh/m <sup>2</sup>	<b>E_Avail</b> kWh	<b>EUnused</b> kWh	<b>E_Miss</b> kWh	<b>E_User</b> kWh	<b>E_Load</b> kWh	<b>SolFrac</b> ratio
<b>January</b>	68.4	114.7	249.1	0.0	0.000	236.5	236.5	1.000
<b>February</b>	86.4	118.1	257.2	15.0	0.000	213.6	213.6	1.000
<b>March</b>	125.6	143.5	306.1	56.0	0.000	236.5	236.5	1.000
<b>April</b>	150.5	157.3	332.0	87.9	0.000	228.9	228.9	1.000
<b>May</b>	203.0	206.9	418.6	164.5	0.000	236.5	236.5	1.000
<b>June</b>	211.6	215.6	419.4	170.6	0.000	228.9	228.9	1.000
<b>July</b>	210.5	214.1	408.0	153.9	0.000	236.5	236.5	1.000
<b>August</b>	195.1	202.5	384.2	131.9	0.000	236.5	236.5	1.000
<b>September</b>	157.4	181.0	349.5	105.7	0.000	228.9	228.9	1.000
<b>October</b>	117.2	153.4	308.3	57.6	0.000	236.5	236.5	1.000
<b>November</b>	84.3	138.6	292.8	53.2	0.000	228.9	228.9	1.000
<b>December</b>	67.6	116.3	253.4	22.6	0.000	236.5	236.5	1.000
<b>Year</b>	1677.7	1962.0	3978.5	1018.9	0.000	2784.4	2784.4	1.000

Legends: GlobHor Global horizontal irradiation E\_Miss Missing energy  
 GlobEff Effective Global, corr. for IAM and shadings E\_User Energy supplied to the user  
 E\_Avail Available Solar Energy E\_Load Energy need of the user (Load)  
 EUnused Unused energy (battery full) SolFrac Solar fraction (EUsed / ELoad)

Figure 45: Balances and main result of the photovoltaic system for Single-Axis Tracker

#### 4.2.2 Performance Ratio PR and Solar Fraction SF

The percentage of Solar Fraction was constant (i.e., 100%) as shown in Figure 46. The annual average value of PR (performance ratio  $Y_f / Y_r$ ) is 56.5%, the maximum value for January is 83 %, and the lowest value for June is 45%.

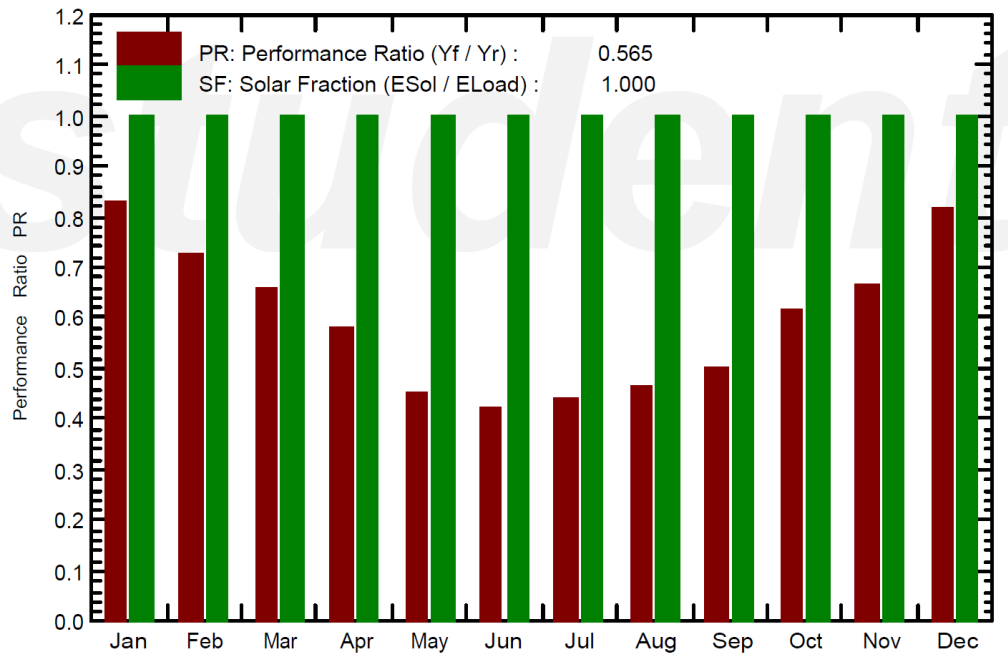


Figure 46: PR 56.5% and solar fraction 100%

#### 4.2.3 Normalized Production

As shown in Figure 47, the annual PV-array losses and system losses are 0.92 kWh/kWp/day and 0.34 kWh/kWp/day, respectively. The unused energy is 1.13 kWh/kWp/day and the energy supplied to the user is 3.1 kWh/kWp/day. In addition, most PV module losses occur in June, July, August, and September. As well, June has the highest unused energy and system losses.

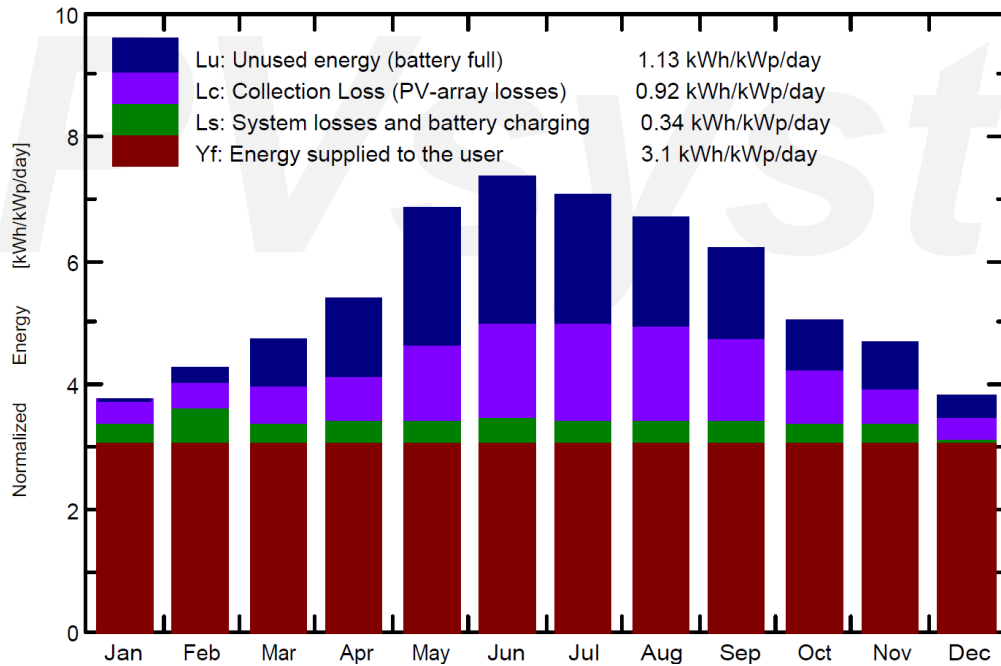


Figure 47: Normalized production for 280W Panel

#### 4.2.4 Shading Diagram

By looking at Figure 48, the shading factor for diffuse is 0.000 and the albedo is 0.00. The iso-shading curves are numbered from 1 to 7. Through the curve, this represents the same quantity of shading, which differ depending on the month. Due to their capability to track the azimuth angle of the sun, the sun is active in the area of the tracking array. In general, the single-axis tracker array has the lowest shading effects compared to the shading impacts on both the fixed tilt and dual-axis tracker arrays. Sunlight is in slight outage in the early morning and after evening hours, mainly in the winter when the sun sank lower on the horizon.

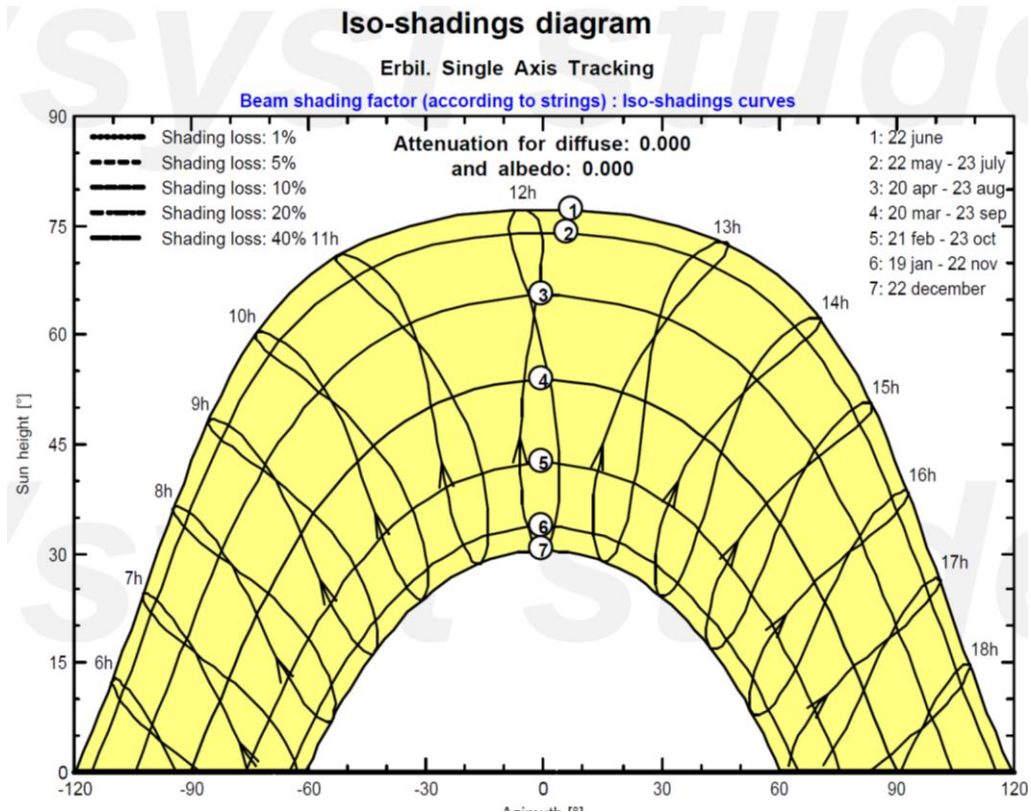


Figure 48: Iso-shading curve- single-axis tracker.

#### 4.2.5 Loss Diagram

Figure 49 represents the system loss diagram for this site. The PV cell converts solar energy to electrical power; the array nominal energy at Standard Test Condition (STC) effc. After PV conversion is 4849 kWh with a 16.10% efficiency at STC. Effective energy at the output of the array is 3088kWh after the battery storage. The diagram below shows that about 40.57% of the losses are accounted for as module losses, 4.15% as converter losses, and 7.88% as battery losses. In addition, after the converter loss, the missing energy is 0% and the direct use of battery storage is 15%, while stored energy accounts for 85%. Similarly, the highest recorded loss is 24.81% that occurs as the unused energy(battery full).

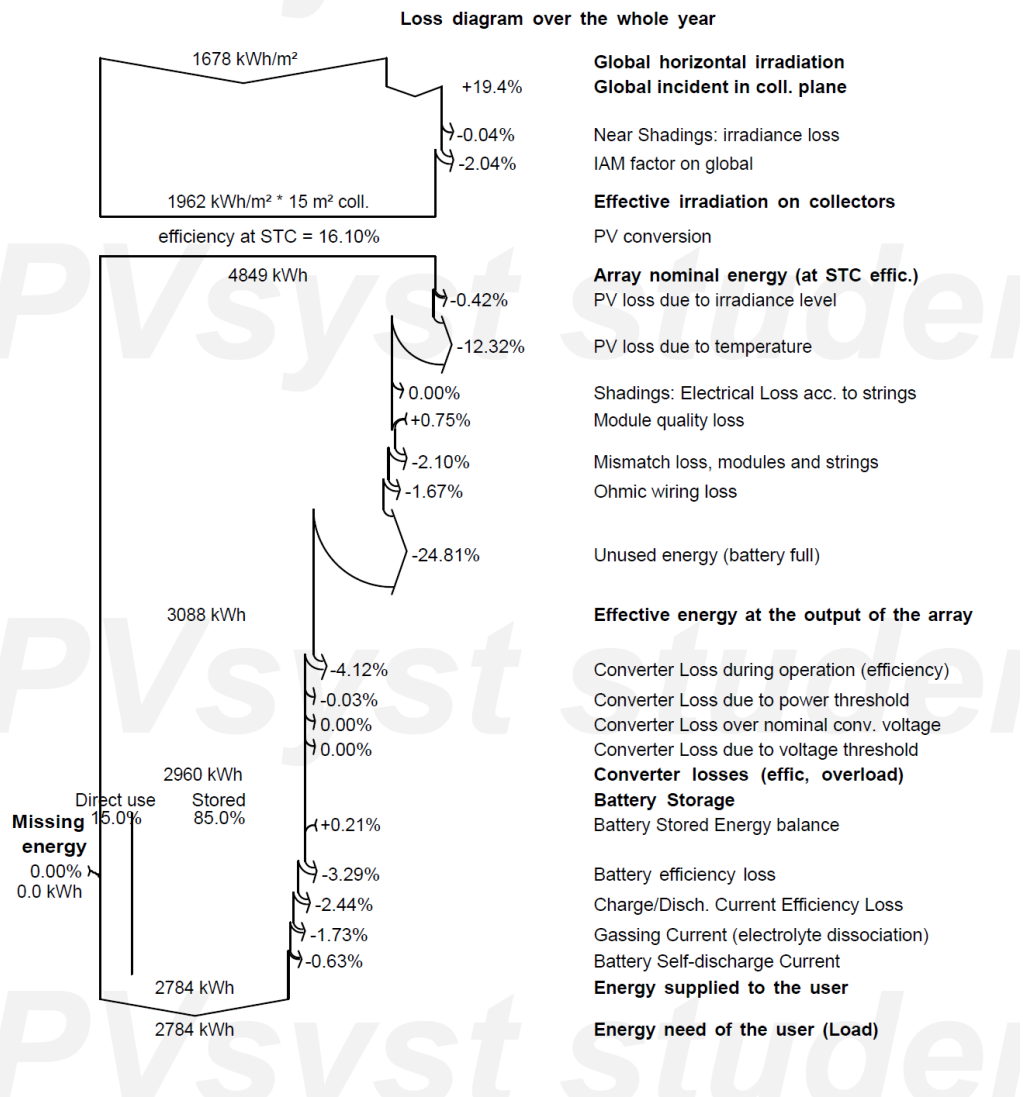


Figure 49: Losses diagram- single-axis tracker

## 4.3 Results of Dual-Axis Tracking PV System

### 4.3.1 Balances and Main Simulation Results

Figure 50 presents the balance and main results for the Dual-Axis Tracker system, which gives the annual global effective, after all optical losses (shadings, IAM, soiling), as 2354.3 kWh/m<sup>2</sup>. The annual E\_Avail is 4556.4 kWh, the full battery is 15634 kWh, the E\_Miss is 0.0 kWh, the E\_User is 2784.4 kWh, the energy need of the load is 2784.4kWh, and the SolFrac is 1.000 for the 205W PV panel.

	GlobHor	GlobEff	E_Avail	EUnused	E_Miss	E_User	E_Load	SolFrac
	kWh/m <sup>2</sup>	kWh/m <sup>2</sup>	kWh	kWh	kWh	kWh	kWh	ratio
January	68.4	132.6	281.8	22.0	0.000	236.5	236.5	1.000
February	86.4	137.4	293.3	52.3	0.000	213.6	213.6	1.000
March	125.6	168.1	348.6	96.5	0.000	236.5	236.5	1.000
April	150.5	185.4	377.8	132.5	0.000	228.9	228.9	1.000
May	203.0	253.5	480.3	226.0	0.000	236.5	236.5	1.000
June	211.6	263.1	476.4	226.9	0.000	228.9	228.9	1.000
July	210.5	262.1	467.1	212.1	0.000	236.5	236.5	1.000
August	195.1	251.5	448.5	196.0	0.000	236.5	236.5	1.000
September	157.4	224.6	412.3	167.3	0.000	228.9	228.9	1.000
October	117.2	182.1	355.2	101.7	0.000	236.5	236.5	1.000
November	84.3	162.9	332.6	88.5	0.000	228.9	228.9	1.000
December	67.6	130.9	282.6	41.6	0.000	236.5	236.5	1.000
Year	1677.7	2354.3	4556.4	1563.4	0.000	2784.4	2784.4	1.000

Legends: GlobHor Global horizontal irradiation E\_Miss Missing energy  
 GlobEff Effective Global, corr. for IAM and shadings E\_User Energy supplied to the user  
 E\_Avail Available Solar Energy E\_Load Energy need of the user (Load)  
 EUnused Unused energy (battery full) SolFrac Solar fraction (EUsed / ELoad)

Figure 50: Balances and main result of the photovoltaic system for Dual-axis tracker.

### 4.3.2 Performance Ratio PR and Solar Fraction SF

There are fluctuations in system output throughout the year, the solar fraction is constant, it was 100%. Performance ratios in the system output in the first six months of the year have been declining and the second six months of the year have had an upward trend. The maximum value for December is 78 % and the lowest value for June is 36%. In Figure 51, the annual performance ratios and solar fraction are 46.6% and 100%, respectively.

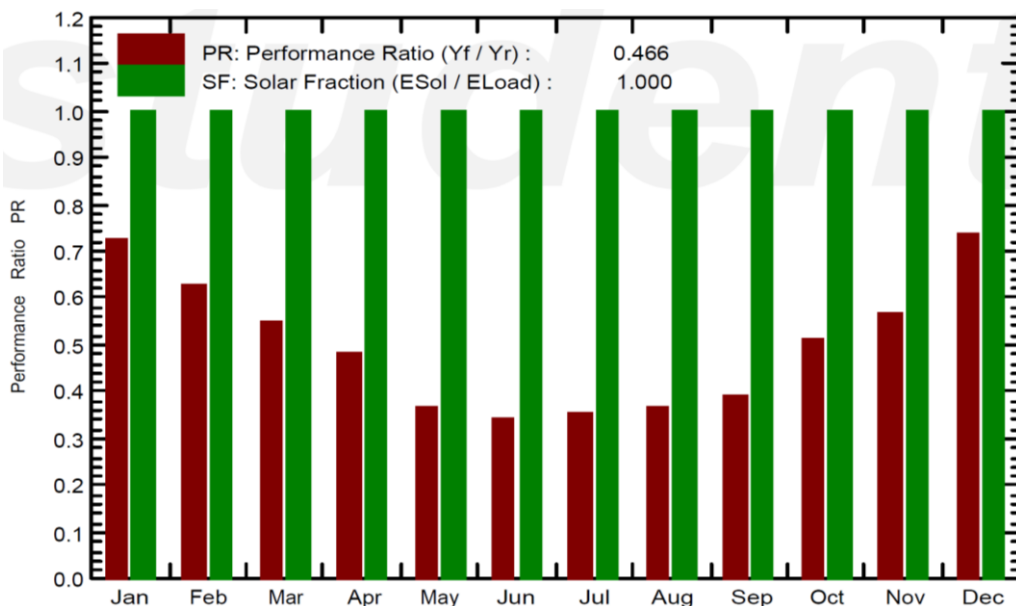


Figure 51: PR 46.6% and solar fraction 100%



### 4.3.3 Normalized Production

Figure 52 gives the normalized annual power production yield. System loss is 0.38 kWh/kWp/day, the energy supplied to the user is 3.1 kWh/kWp/day, unused energy is 1.74 kWh/kWp/day, and collection loss (PV-array losses) is 1.44 kWh/kWp/day.

In addition, most PV module losses and unused energy occur in May, June, July, August, and September. As well, June has the highest system losses and battery charging.

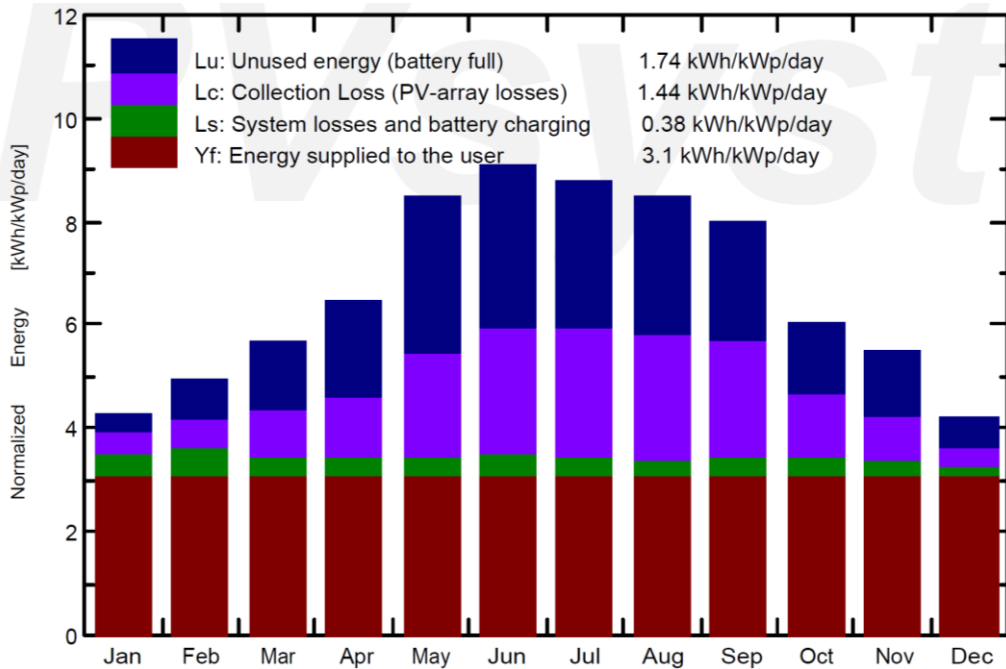


Figure 52: Normalized production for dual-axis tracker.

### 4.3.4 Shading Diagram

Figure 53 shows the sun's position and shading impact on the PV system throughout different times of the days and the seasons during the year. Owing to the location and design of the system, the amount of shading is high on the arrays in winter because the sun is at the lowest angle and the worst impacts are seen. Shading specifications can

be problematic, but the system reduces power consumption on clear days between 9:00 and 16:00 in summer and 9:30 and 15:30 in winter.

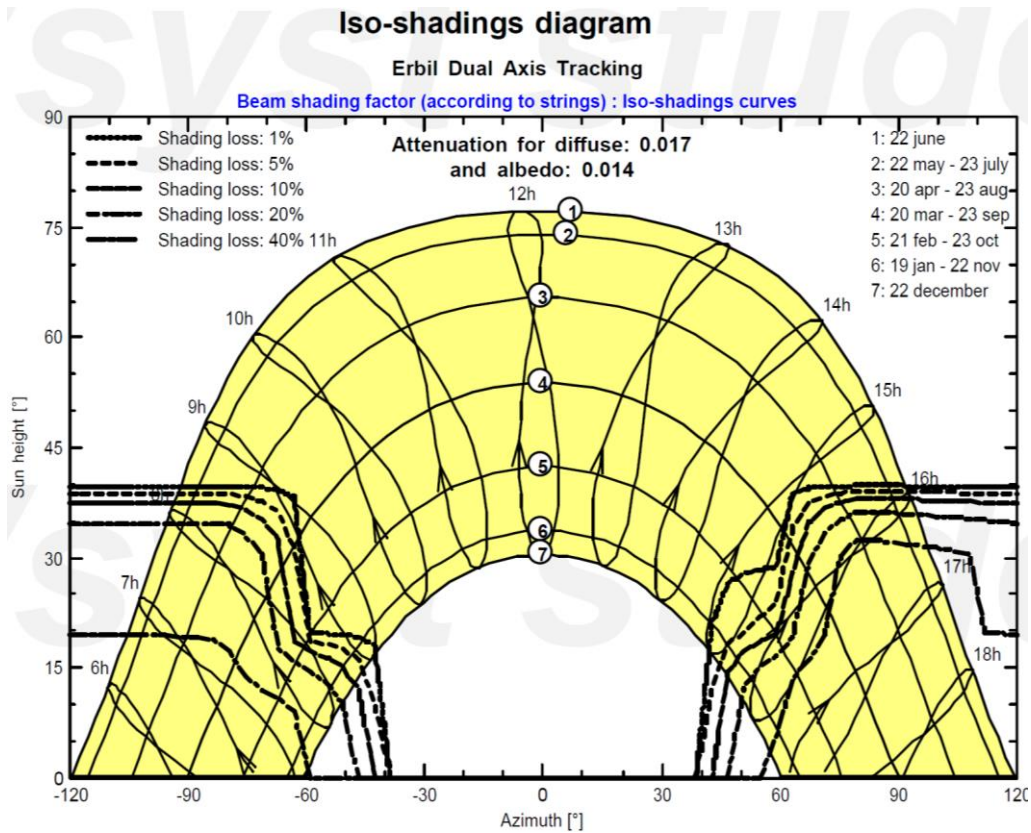


Figure 53: Iso-shading curve for the dual-axis tracking system.

#### 4.3.5 Loss Diagram

There are distinct types of field losses that occur in the standalone photovoltaic frames throughout the year, as shown in Figure 54. The nominal energy of the array for the whole year is 5818 kWh to optical losses, array losses, and system losses. The energy generation of the array is 3122 kWh with efficiency at STC at 16.10%. Also, after the converter loss, the unused energy (battery full) is 33.37%, which is the maximum amount of losses, followed by the PV loss due to temperature with a maximum loss amount of 13.93%. Additionally, the direct use of battery storage is 14.5% while stored energy accounts for 85.5%. According to this, the missing energy is 0.0 %.

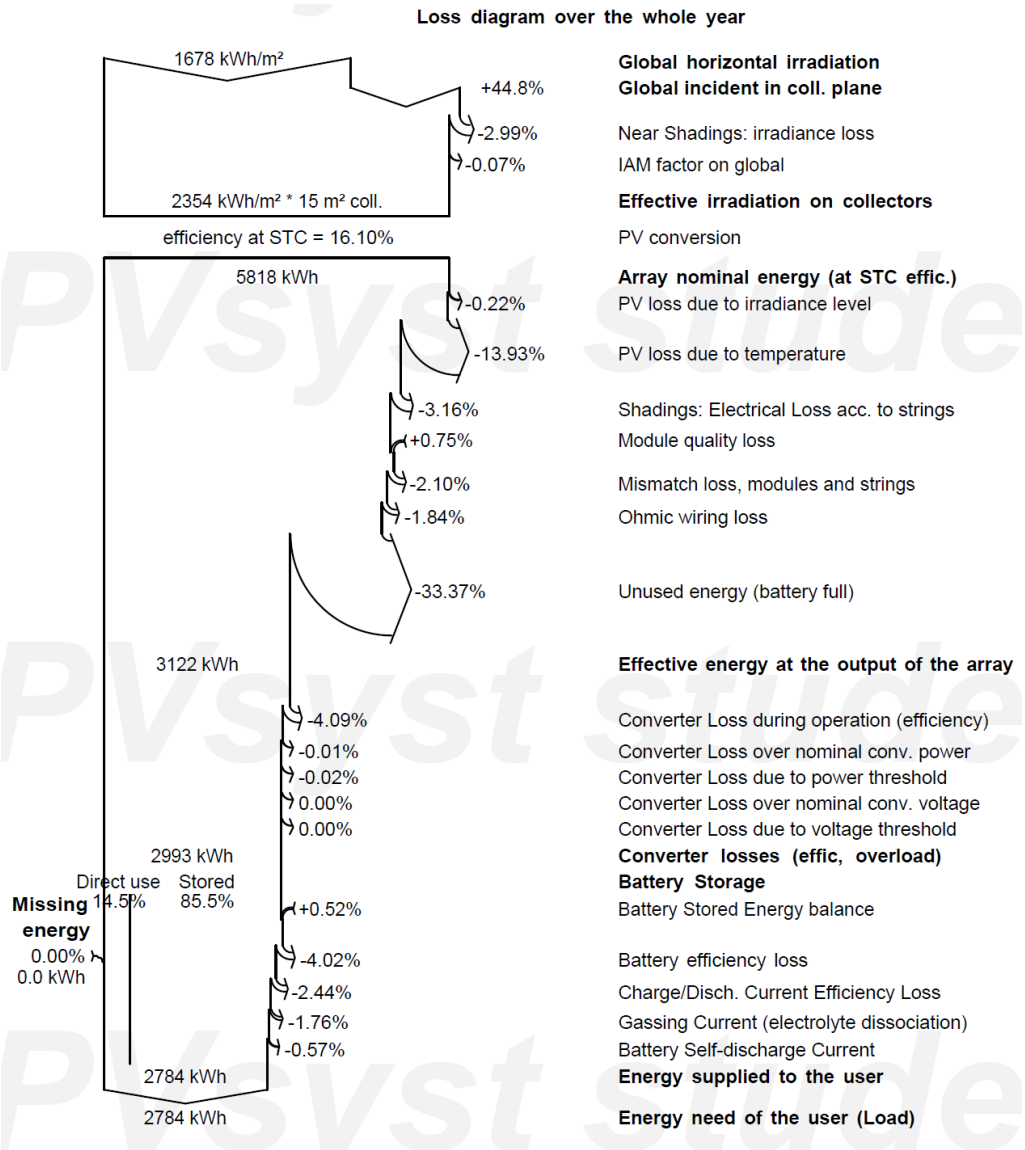


Figure 54: Losses diagram- dual-axis tracker.

#### 4.4 Discussion

This section compares the PV systems examined above and interprets the results of their design applications considering the following factors:

**System Production**, including E Load, E User, E Miss, E Unused, the excess energy injected into the grid, specific production.

**Performance Ratio PR, Solar Fraction SF, Battery storage, System losses,** including PV-array losses, Unused energy (battery full), PV loss due to temperature, and losses due to IAM.

PV systems are originally stand-alone systems. Each PV system is designed using the components of PV modules, charge controller, and battery, having the same types and number, with the same energy demand, same area, and a battery bank for energy storage. From an economic point of view, a stand-alone PV system for small projects is better because the price of the PV system does not increase by the electricity company for 25 years.

Tracking systems increase energy generation, but also incur extra costs to the power plant. The various figures and tables show the simulation results for the fixed-tilt system, the single-axis (EW) tracking system, and two-axis (EW) tracking in the design of the Erbil photovoltaic power plant. Analysis of the systems will reveal the difference in levels of energy production between the systems.

According to the results outlined in Table 4, the yearly energy output of the fixed-tilt system, single-axis tracking system, and dual-axis tracking system are 3731.4 kWh/year, 3978.5 kWh/year, 4556.4 kWh/year; the missing energy levels are 0.00%, and the unused energy 774.1kWh/year, 1018.9kWh/year, and 1563.4kWh/year, respectively.

Finally, after calculating all of the relevant aspects, the energy supplied to the user from the fixed-tilt is 2784 kWh/year, Also from tracking systems are 2784.4 kWh/year, According to these results, dual-axis tracking is the best system.

Comparing the losses in the systems allows some important differences to be appreciated. The differences in the results are majorly caused by differences in the representation of the losses for each system.

The efficiency of the process for the three systems is 16.10%. Losses due to IAM for fixed-tilt is 2.44%, single-axis tracking is 2.04%, and dual-axis tracking is 0.07%. In contrast to the other scenarios, the lowest loss is for the dual-axis tracking system. The PV-array losses of the fixed-tilt system, single-axis tracking system, and dual-axis tracking system are 0.88 kWh/kWp/day, 0.92 kWh/kWp/day, and 1.44 kWh/kWp/day, and the unused energy (battery full) are 20.04%, 24.81%, 33.37%, respectively. The main differences between the results obtained in the systems are the temperature losses, which is 11.97% for the fixed-tilt system, 12.32% for the single-axis system, and 13.93% for the dual-axis system. The lowest value is for the fixed-tilt system, while the highest value is for the dual-axis system.

The PR obtained in the simulations for the single-axis is 56.5%, while the fixed-tilt system had the highest percentage at 59.9% and the dual-axis system the least percentage with 46.6%. SF obtained in the simulations is 100% for three scenarios . The battery loss is 8.7% for the fixed-tilt system, 8.3% for the single-axis system, and 8.27% for the dual-axis system, and the Battery Cycle's SOW "State of Wear" are around 93% and Battery Static SOW "State of Wear" are around 80% for all systems.

Table 4: Discussion summary of the main study findings.

Characteristics	Discussion	Fixed-tilt system	Single-axis tracking system	Dual-axis tracking system
E Load (kWh)	The energy need of the user	2784	2784	2784
Available energy (kWh/year)	The yearly energy output of the system	3731.4	3978.5	4556.4
E User (kWh)	The energy supplied to the user	2784.4	2784.4	2784.4
E Miss	Missing Energy= Eload - Euser	0.0%	0.0%	0.0%
Excess (unused) - (kWh/year)	This energy is the extra energy that cannot be used when the battery is full.	774.1	1018.9	1563.4
Specific prod. (kWh/kWp/year)	It refers to the amount of power (kWh) generated for any (kWp) of module capacity during a normal or actual year.	1517	1617	1852
PV-array losses (kWh/kWp/day)	PV system converts solar radiation on PV cells into electrical energy, which eventually converts into electricity after going through various stages and different sources, thereby resulting in power loss. Main losses include radiation level, array pollution, a decrease of module quality, loss of array mismatch, ohmic losses of AC, DC and, a small number of transformer losses.	0.88	0.92	1.44
Unused energy (battery full)	In fact, at this time, we have less unused energy, while safekeeping the battery charged and using the remains of the production by PV. However, pending the next night, the battery discharge to a less extent than if it is discharged in this part, this means that you will be fully charged the next day and accordingly we have more unused energy.	20.04%	24.81%	33.37%
Performance Ratio PR	The PR is expressed as a percentage and describes the relationship between the real and theoretical energy output of a PV power plant, and is described as a quality factor. The following factors can influence the PR value: Environmental factors • PV module temperature • Solar radiation and power loss • PV module in the shade or dirt Other factors • Recording period • Conduct losses • Performance coefficient of PV modules • Measurement orientation	59.90%	56.6%	46.6%
Solar Fraction SF	Solar fraction depends on many factors, such as the load, collection and storage sizes, operation, and climate.	100%	100%	100%
efficiency at STC	For photovoltaics, voltage and current can be measured and multiplied together to obtain output power, which is subsequently divided by the area of the module and the power of sunlight per square meter to achieve efficiency. STC is the radiation of 1 kW/m <sup>2</sup> , the cell temperature is 25°C, and no wind.	16.10%	16.10%	16.10%
PV loss due to temperature	As mentioned in chapter 2, the PV module's characteristics are determined at an STC of 25 degrees, by considering the temperature factor of the 280 Wp modules chosen, the module efficiency reduces by - 0.40% for any °C increase in cell temperature. The temperature loss of the module is computed by considering the location's temperature profile according to the Meteo database. Since the position is located in Erbil, a high-temperature region, high-temperature losses are obtained.	11.97%	12.32%	13.93%

<b>Characteristics</b>	<b>Discussion</b>	<b>Fixed-tilt system</b>	<b>Single-axis tracking system</b>	<b>Dual-axis tracking system</b>
Battery Cycles SOW "State of Wear"	Dynamic wear due to the No. of cycles. Dynamic aging mode as discharge current function and discharge depth for this hour can be accurately performed. Stored in the SOWCycl variable.	93.3%	93.7%	93.5%
Battery Static SOW "State of Wear"	Static wear due to the age of the battery. The static aging mode decreases as a function of the actual battery temperature defined by the gainer for the simulation. This is stored in the SOWStat simulation variable.	79.80%	79.80%	80%
Battery losses	The range of solar batteries' lifespan is between 5 and 15 years. Tips to extend battery life: <ul style="list-style-type: none"> <li>• correctly configuration with size and number of batteries</li> <li>• Battery Equalization</li> <li>• Rotate the batteries</li> <li>• Use large interconnection cables for battery</li> <li>• Keep cooling</li> <li>• Shorten the charging period and charge properly</li> <li>• Check the condition of the solar battery regularly and keep battery power</li> </ul>	8.7%	8.3%	8.27%
losses due to IAM	IAM (Incidence Angle Modifier) is related to the reduction of radiation reaching the PV cell due to the refraction of the sun's rays while passing through the anti-reflection coating of the PV module and glass. The higher the angle of the incident (depending on the position of the sun), the greater the losses.	2.44%	2.04%	0.07%

## **Chapter 5**

### **CONCLUSION AND RECOMMENDATION**

#### **5.1 Conclusion of the Study**

The study explored the potential utility of solar photovoltaic technology, widely accepted as the most significant source of renewable. One of the biggest challenges of the next century is determining how best to reduce our reliance on power generated from the burning of fossil fuels. Relative to other sources of renewable energy, the use of photovoltaic panels to convert solar energy into electric energy is accepted as the foremost source of alternative energy production. However, constant changes in the angle relative to the Earth's surface can affect the consistency in the number of watts generated by solar panels. As such, the efficiency of photovoltaic panels can be improved with the addition of a solar tracking system, which effectively adjusts the payload towards the sun as it changes position during the day.

Unfortunately, however, conventional solar photovoltaic systems suffer from a few, though significant, disadvantages, such as their inefficiency, intermittency, and higher costs relative to fossil fuel energy sources. The use of photovoltaic systems to capture the maximum amount of energy from the sun is not an easy task and can be impacted by several factors, such as the orientation of the solar panel, angle of sun incidence, ambient temperature and weather, the geographical location of solar irradiances, and even the type of photovoltaic material in use. The present study attempts to evaluate the mechanisms and principles underlying photovoltaic systems, including fixed-tilt



and tracking systems, to determine which is more suitable. It categorizes the solar tracking systems based on their technologies, taking a comparative look at the performance, efficiency, tracking techniques, advantages, and disadvantages of each system.

This thesis compares both the photovoltaic properties and the amount of energy generated by three installed systems in Erbil, Iraq: one with a fixed tilt angle, and the other fitted with solar trackers. While each system could potentially improve the amount of electrical energy produced, the literature does not contain any example of an innovative system containing the properties of all three systems.

It also reviews and compares the advantages and disadvantages of the different types of tracking systems in detail. Despite the greater popularity and lower cost of conventional fixed systems, the results of this review show that the dual-axis tracking system is more efficient than other systems, although the single-axis tracking system offers a somewhat more economical and flexible alternative.

Outlined below are the most important findings and contributions of this study:

- Following a comparative analysis of three scenarios of stand-alone solar PV systems, the study demonstrated the optimal design for a utility size stand-alone solar PV system from the study location (Erbil). It concluded that the single-axis and dual-axis tracking designs, as well as a fixed-tilt design, are viable for the solar PV stand-alone system. The Pvsyst simulation tool was used to assess the performances of the different methods, which were subsequently discussed.

- Based on a comparative analysis of the various system's daily power generation capacity, it was found that all of the systems considered were able to meet the annual power output requirements. However, the study found that the single-axis tracking and fixed-tilt systems produced less power than the dual-axis tracking system. Furthermore, the study also found that the amount of power generated was not significantly impacted by the time-based adjustments to the tilt angles of any of the schemes (fixed-tilt, single-axis tracking, and dual-axis tracking).
- Dual-axis tracking produced 30% more excess power than the fixed-tilt system, while single-axis tracking produced 21% more than the fixed-tilt system.
- The tracking systems are more costly in terms of installation, operation, and maintenance costs, relative to the fixed system. (Al Garni, et al., 2018).
- The conclusions drawn from the evaluation of the tracking systems and system design proposed in this study are applicable to any location for the improvement of stand-alone solar PV system performances. However, the results of the simulation depend to a large extent on the meteorological conditions of the site, load profile, and the costs of the components used at the particular location.
- The PVsyst software is an incredibly useful tool for evaluating various PV design applications by considering factors most likely to affect the performance of the PV system, including component costs, resource availability, and the load profile.

To sum up, this study contributes to the existing literature on the technical performance, economic aspects, and feasibility of solar PV with different systems and

time adjustments. It is important, however, to take into consideration a number of possible limitations. For one, the economic viability of renewable energy sources can be affected by the renewable energy feed-in tariff and such be analyzed further to determine its impact on a system's energy performance. Also requiring further investigation are the effects of different temperature coefficients and solar PV models on the cost of energy, net present cost, and power generation.

## **5.2 Recommendation for Future Studies**

Future research should include comparative analyses of the performance of grid-connected and off-grid designs for various locations under different climatic conditions, as well as that of hybrid systems like solar-wind-biomass, in order to determine the optimal design parameters.

This study places significant emphasis on the simulation of a 7.6 kWp solar-based PV power plant, explaining the design process in selecting the PV module, size/capacity of the battery and charge controller, location, the arrangement of the strings, among others. As such, it provides a useful reference tool for investigations into the installation of off-grid systems. It is also a useful guide for solar practitioners and beginners alike with an interest in installing solar PV systems by providing direction on how to accurately estimate potential losses using the PVSYST software as the software can be used in generating a complete installation report and examining the losses and power output of a potential or existing plant.

## REFERENCES

- Abdullah, H. K., & Alibaba, H. Z. (2017). Retrofits for energy efficient office buildings: integration of optimized photovoltaics in the form of responsive shading devices. *Sustainability*, 9(11), 2096.
- Abdullah, H. K., & Alibaba, H. Z. (2018). Towards Nearly Zero-Energy Buildings : the Potential of Photovoltaic-Integrated Shading Devices To Achieve Autonomous Solar Electricity and Acceptable Thermal Comfort in Naturally-Ventilated Office Spaces. In *16th International Conference on Clean Energy* (pp. 1–11). Famagusta, North Cyprus: Eastern Mediterranean University.
- Al-Douri, Y., & Abed, F. M. (2016). Solar energy status in Iraq: Abundant or not— Steps forward. *Journal of Renewable and Sustainable Energy*, 8(2), 025905.
- Alfadhli, M. M., Alghoussein, S., & Alarifi, F. (2019). The use of parallel Istisna Sukuk in financing solar energy project in Kuwait. *International Academic Journal of Economics and Finance*, 3(4), 204-217.
- Ali, W., Farooq, H., Rehman, A. U., Awais, Q., Jamil, M., & Noman, A. (2018, November). Design considerations of stand-alone solar photovoltaic systems. In *2018 International Conference on Computing, Electronic and Electrical Engineering (ICE Cube)* (pp. 1-6). IEEE.

- Al-Kayiem, H. H., & Mohammad, S. T. (2019). Potential of renewable energy resources with an emphasis on solar power in Iraq: An outlook. *Resources*, 8(1), 42.
- AlShemmary, E. N. A., Kadhom, L. M., & Al-Fahham, W. J. (2013). Information technology and stand-alone solar systems in tertiary institutions. *Energy Procedia*, 36, 369-379.
- Awasthi, A., Shukla, A. K., SR, M. M., Dondariya, C., Shukla, K. N., Porwal, D., & Richhariya, G. (2020). Review on sun tracking technology in solar PV system. *Energy Reports*, 6, 392-405
- Bagher, A. M., Vahid, M. M. A., & Mohsen, M. (2015). Types of solar cells and application. *American Journal of optics and Photonics*, 3(5), 94-113.
- Bailek, N., Bouchouicha, K., Aoun, N., Mohamed, E. S., Jamil, B., & Mostafaeipour, A. (2018). Optimized fixed tilt for incident solar energy maximization on flat surfaces located in the Algerian Big South. *Sustainable Energy Technologies and Assessments*, 28, 96-102.
- Banerjee, R. (2015). Solar tracking system. *International Journal of Scientific and Research Publications*, 5(3), 1-7.
- Burnham, L., Riley, D., Walker, B., & Pearce, J. M. (2019, June). Performance of bifacial photovoltaic modules on a dual-axis tracker in a high-latitude, high-

albedo environment. In *2019 IEEE 46<sup>th</sup> Photovoltaic Specialists Conference (PVSC)* (pp. 1320-1327). IEEE.

Copt, R. P., Thomas, R., & Mermoud, A. (1999). Corneal thickness in ocular hypertension, primary open-angle glaucoma, and normal-tension glaucoma. *Archives of ophthalmology*, 117(1), 14-16.

Dunlop, J. (2015), System Sizing. Sizing Principles, *Interactive vs. Stand-alone Systems*, Calculations and Software Tools. Chapter 9. Jim Dunlop Solar.

Fouad, M. M., Shihata, L. A., & Morgan, E. I. (2017). An integrated review of factors influencing the performance of photovoltaic panels. *Renewable and Sustainable Energy Reviews*, 80, 1499-1511.

Goodrich, A., James, T., & Woodhouse, M. (2012). Residential, commercial, and utility-scale photovoltaic (PV) system prices in the United States: current drivers and cost-reduction opportunities (No. NREL/TP-6A20-53347). National Renewable Energy Lab. (NREL), Golden, CO (United States).

Guda, H. A., & Aliyu, U. O. (2015). Design of a stand-alone photovoltaic system for a residence in Bauchi. *International Journal of Engineering and Technology*, 5(1), 34-44.

Hafez, A. Z., Yousef, A. M., & Harag, N. M. (2018). Solar tracking systems: Technologies and trackers drive types—A review. *Renewable and Sustainable Energy Reviews*, 91, 754-782.

- Huynh, D. C., Nguyen, T. M., Dunnigan, M. W., & Mueller, M. A. (2013, November). Comparison between open-and closed-loop trackers of a solar photovoltaic system. In *2013 IEEE Conference on Clean Energy and Technology (CEAT)* (pp. 128-133). IEEE.
- Ismail, M. M., Anis, W. R., & Ghoneim, R. (2016). Journal homepage: <http://www.journalijar.com> INTERNATIONAL JOURNAL OF ADVANCED RESEARCH. *International Journal*, 4(3), 2001-2017.
- Jones, G. G., & Bouamane, L. (2012). " Power from Sunshine": A Business History of Solar Energy. *Harvard Business School Working Paper Series*.
- Karafil, A., Ozbay, H., Kesler, M., & Parmaksiz, H. (2015, November). Calculation of optimum fixed tilt angle of PV panels depending on solar angles and comparison of the results with experimental study conducted in summer in Bilecik, Turkey. In *2015 9th International Conference on Electrical and Electronics Engineering (ELECO)* (pp. 971-976). IEEE.
- Koussa, M., Cheknane, A., Hadji, S., Haddadi, M., & Nouredine, S. (2011). Measured and modelled improvement in solar energy yield from flat plate photovoltaic systems utilizing different tracking systems and under a range of environmental conditions. *Applied Energy*, 88(5), 1756-1771.
- Kumar, N. M., Chopra, S. S., de Oliveira, A. K. V., Ahmed, H., Vaezi, S., Madukanya, U. E., & Castañón, J. M. (2020). Solar PV module technologies. In *Photovoltaic Solar Energy Conversion* (pp. 51-78). Academic Press.

Kurdistan Region of Iraq, Erbil Governorate. (2018). Sustainable Energy Action Plan (SEAP). Erbil, Iraq: The European Union.

Li, G., Tang, R., & Zhong, H. (2012). Optical performance of horizontal single-axis tracked solar panels. *Energy Procedia*, 16, 1744-1752.

Mahmoud, M. (2012). Design and Simulation of a Photovoltaic System with Maximum Power Control to Supply a Load with Alternating Current (Doctoral dissertation). An-Najah National University, Nablus, Palestine.

Mohanty, P., Sharma, K. R., Gujar, M., Kolhe, M., & Azmi, A. N. (2016). PV system design for off-grid applications. *In Solar Photovoltaic System Applications* (pp. 49-83). Springer, Cham.

Mohanty, P., Muneer, T., Gago, E. J., & Kotak, Y. (2016). Solar radiation fundamentals and PV system components. *In Solar Photovoltaic System Applications* (pp. 7-47). Springer, Cham.

Mundaca, L., & Richter, J. L. (2015). Assessing 'green energy economy' stimulus packages: Evidence from the US programs targeting renewable energy. *Renewable and Sustainable Energy Reviews*, 42, 1174-1186.

Nadia, A. R., Isa, N. A. M., & Desa, M. K. M. (2018). Advances in solar photovoltaic tracking systems: A review. *Renewable and sustainable energy reviews*, 82, 2548-2569.



- Pal, A. M., Das, S., & Raju, N. B. (2015). Designing of a standalone photovoltaic system for a residential building in Gurgaon, India. *Sustainable Energy*, 3(1), 14-24.
- Pal, M., & Subbra Das, A. (2015). Analytical Model for Determining the Sun's Position at All-Time Zones. *International Journal of Energy Engineering*, 5(3), 58-65.
- Perraki, V., & Megas, L. (2014). Single axis tracker versus fixed tilt PV: experimental and simulated results. In *Proceedings of the 29 th European Photovoltaic Solar Energy Conference*, Amsterdam (The Netherlands) (pp. 2711-2714).
- Qadir, K. W., & Saeed, M. A. (2011). Study and analysis of global and extraterrestrial solar radiation over Kurdistan Region-Iraq. In *3rd International Scientific Conference of Salahaddin University-Erbil*. Quesada, G., Guillon, L., Rouse, D. R., Mehrtash, M.,
- Dutil, Y., & Paradis, P. L. (2015). Tracking strategy for photovoltaic solar systems in high latitudes. *Energy Conversion and Management*, 103, 147-156.
- Racharla, S., & Rajan, K. (2017). Solar tracking system—a review. *International Journal of Sustainable Engineering*, 10(2), 72-81.
- Rida, K. S., Al-Waeli, A. A., & Al-Asadi, K. A. (2016). The impact of air mass on photovoltaic panel performance. *Eng. Sci. Rep*, 1(1), 1-9.

- Seme, S., Štumberger, B., Hadžiselimović, M., & Sredenšek, K. (2020). Solar Photovoltaic Tracking Systems for Electricity Generation: A Review. *Energies*, 13(16), 4224.
- Shaikh, M. R. S. (2017). A review paper on electricity generation from solar energy.
- Sidek, M. H. M., Azis, N., Hasan, W. Z. W., Ab Kadir, M. Z. A., Shafie, S., & Radzi, M. A. M. (2017). Automated positioning dual-axis solar tracking system with precision elevation and azimuth angle control. *Energy*, 124, 160-170.
- Singh, O., & Rajput, S. K. (2016, May). Mathematical modeling and simulation of solar photovoltaic array system. In *2016 International Conference on Research Advances in Integrated Navigation Systems (RAINS)* (pp. 1-5). IEEE.
- Sobamowo, M. G., Yinusa, A. A., & Waheed, M. A. (2020). Coupled Effects of Surface Inclination and Magnetic Field on Free Convection Heat Transfer of Nanofluid over a Flat Plate in a Porous Medium in the Presence of Thermal Radiation. *International Journal of Mathematical Sciences and Optimization: Theory and Applications*, 2020(1), 780-799.
- Sobhani, M., Zakeri, S., & Taghizadeh, M. M. (2014). Review on renewable energy, sustainable energy, and clean energies. *Technical Journal of Engineering and Applied Sciences*, 4(3), 120-123.

Sumathi, V., Jayapragash, R., Bakshi, A., & Akella, P. K. (2017). Solar tracking methods to maximize PV system output—A review of the methods adopted in recent decade. *Renewable and Sustainable Energy Reviews*, 74, 130-138.

Yadav, A. K., & Chandel, S. S. (2013). Tilt angle optimization to maximize incident solar radiation: A review. *Renewable and Sustainable Energy Reviews*, 23, 503-513.

## **APPENDICES**

## Appendix A: Results of Fixed Tilt Installation PV System

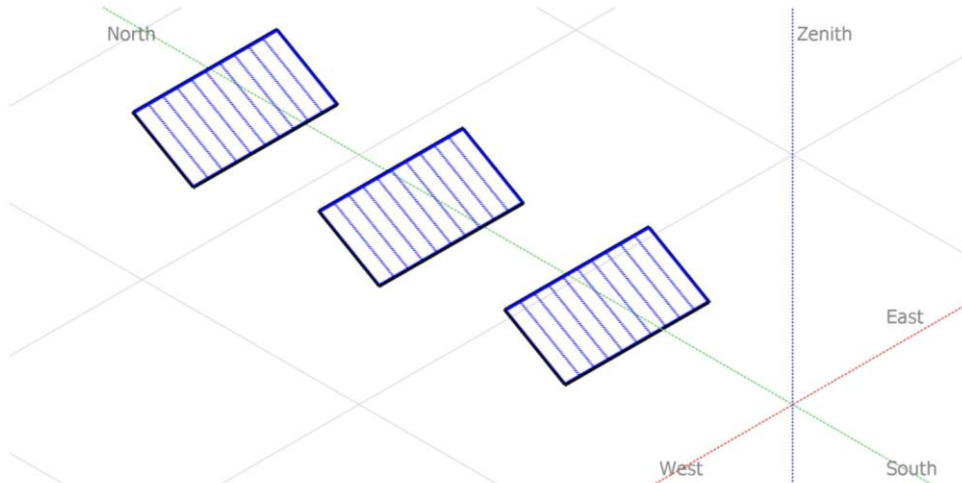
PVSYST 7.0.17	Parinaz Muhammed Abdulkarim (Cyprus)	18/02/21	Page 1/6
<b>Stand alone system: Simulation parameters</b>			
<b>Project :</b> Erbil - Fixed Tilt			
<b>Geographical Site</b>		<b>Erbil</b>	<b>Country Iraq</b>
<b>Situation</b>	Latitude	36.18° N	Longitude 44.01° E
Time defined as	Legal Time	Time zone UT+3	Altitude 392 m
	Albedo	0.20	
<b>Meteo data:</b>	<b>Erbil</b>	Meteonorm 7.3 (1985-2000), Sat=100% - Synthetic	
<b>Simulation variant : New simulation variant</b>			
	Simulation date	18/02/21 02h18	
<b>Simulation parameters</b>		System type	<b>Stand alone system with batteries</b>
<b>Collector Plane Orientation</b>		Tilt	30°
		Azimuth	0°
<b>Models used</b>		Transposition	Perez
		Diffuse	Perez, Meteonorm separate
		Circumsolar	separate
<b>Near Shadings</b>		According to module strings	Electrical effect 100 %
<b>User's needs :</b>		Daily household consumers average	Constant over the year 7.6 kWh/Day
<b>PV Array Characteristics</b>			
<b>PV module</b>		Si-mono	Model <b>TSM-205 D80</b>
Original PVsyst database	Manufacturer	Generic	
Number of PV modules	In series	4 modules	In parallel 3 strings
Total number of PV modules	nb. modules	12	Unit Nom. Power 205 Wp
Array global power	Nominal (STC)	<b>2460 Wp</b>	At operating cond. 2192 Wp (50°C)
Array operating characteristics (50°C)	U mpp	134 V	I mpp 16 A
Total area	Module area	<b>15.3 m²</b>	
<b>System Parameter</b>		System type	<b>Stand alone system</b>
<b>Battery</b>		Model	<b>MK 8G8D Gel</b>
	Manufacturer	MK Battery	
<b>Battery Pack Characteristics</b>		Nb. of units	4 in series x 7 in parallel
	Voltage	48 V	Nominal Capacity 1309 Ah
	Discharging min. SOC	20.0%	Stored energy 50.3 kWh
	Temperature	Average between fixed (20°C) and External	
<b>Controller</b>		Model	Universal controller with MPPT converter
	Technology	MPPT converter	Temp coeff. -5.0 mV/°C/Elem.
Converter	Maxi and EURO efficiencies	97.0 / 95.0%	
<b>Battery Management control</b>		Threshold commands as	SOC calculation
	Charging	SOC = 0.92 / 0.75	approx. 53.0 / 49.5 V
	Discharging	SOC = 0.20 / 0.45	approx. 46.6 / 48.3 V
<b>PV Array loss factors</b>			
Thermal Loss factor	Uc (const)	20.0 W/m²K	Uv (wind) 0.0 W/m²K / m/s
Wiring Ohmic Loss	Global array res.	140 mΩ	Loss Fraction 1.5 % at STC
Series Diode Loss	Voltage drop	0.7 V	Loss Fraction 0.5 % at STC
Module Quality Loss			Loss Fraction -0.8 %
Module mismatch losses			Loss Fraction 2.0 % at MPP
Strings Mismatch loss			Loss Fraction 0.10 %
Incidence effect, ASHRAE parametrization	IAM =	1 - bo (1/cos i - 1)	bo Param. 0.05

### Stand alone system: Near shading definition

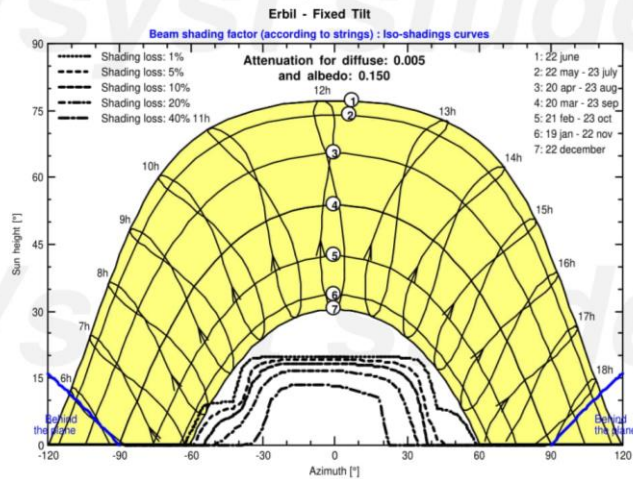
**Project :** Erbil - Fixed Tilt  
**Simulation variant :** New simulation variant

Main system parameters	System type	Stand alone system with batteries	
<b>Near Shadings</b>	According to module strings	Electrical effect	100 %
PV Field Orientation	tilt 30°	azimuth	0°
PV modules	Model TSM-205 D80	Pnom	205 Wp
PV Array	Nb. of modules 12	Pnom total	<b>2460 Wp</b>
Battery	Model MK 8G8D Gel	Technology	Lead-acid, sealed, AGM
Battery pack	Nb. of units 28	Voltage / Capacity	<b>48 V / 1309 Ah</b>
User's needs	Daily household consumers	Constant over the year	Global 2784 kWh/year

#### Perspective of the PV-field and surrounding shading scene



#### Iso-shadings diagram



**Stand alone system: Detailed User's needs**

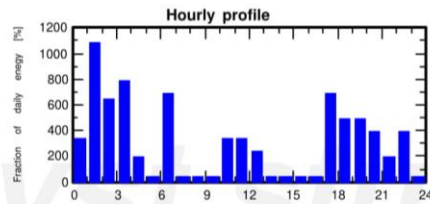
**Project :** Erbil - Fixed Tilt  
**Simulation variant :** New simulation variant

Main system parameters	System type	Stand alone system with batteries	
<b>Near Shadings</b>	According to module strings	Electrical effect	100 %
PV Field Orientation	tilt 30°	azimuth	0°
PV modules	Model TSM-205 D80	Pnom	205 Wp
PV Array	Nb. of modules 12	Pnom total	<b>2460 Wp</b>
Battery	Model MK 8G8D Gel	Technology	Lead-acid, sealed, AGM
Battery pack	Nb. of units 28	Voltage / Capacity	<b>48 V / 1309 Ah</b>
User's needs	Daily household consumers	Constant over the year	Global 2784 kWh/year

**Daily household consumers, Constant over the year, average = 7.6 kWh/day**

**Annual values**

	Number	Power	Use	Energy
Lamps (LED or fluo)	10	15W/lamp	6H/day	900Wh/day
TV / PC / Mobile	3	100W/app	4H/day	1200Wh/day
Domestic appliances	4	50W/app	5H/day	1000Wh/day
Fridge / Deep-freeze	1		24Wh/day	900Wh/day
Dish- and Cloth-washer	1		2Wh/day	4Wh/day
Other uses	3	150W tot	4H/day	1800Wh/day
Other uses	1	600W tot	3H/day	1800Wh/day
Stand-by consumers			24H/day	24Wh/day
<b>Total daily energy</b>				<b>7628Wh/day</b>



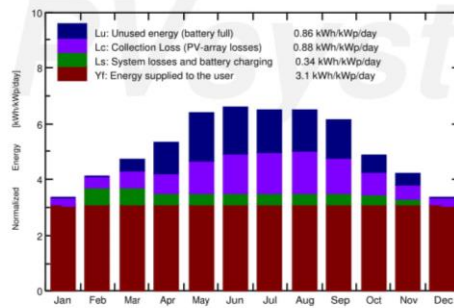
Stand alone system: Main results

Project : Erbil - Fixed Tilt  
 Simulation variant : New simulation variant

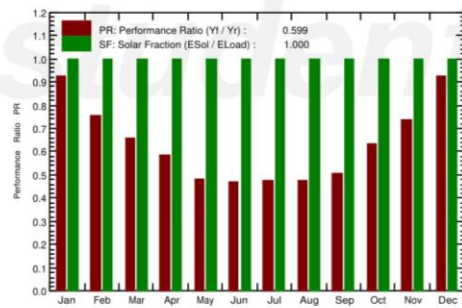
Main system parameters		System type	Stand alone system with batteries	
Near Shadings	According to module strings		Electrical effect	100 %
PV Field Orientation	tilt	30°	azimuth	0°
PV modules	Model	TSM-205 D80	Pnom	205 Wp
PV Array	Nb. of modules	12	Pnom total	<b>2460 Wp</b>
Battery	Model	MK 8G8D Gel	Technology	Lead-acid, sealed, AGM
Battery pack	Nb. of units	28	Voltage / Capacity	<b>48 V / 1309 Ah</b>
User's needs	Daily household consumers	Constant over the year	Global	2784 kWh/year

Main simulation results		Available Energy		Specific prod.	
System Production		<b>3731 kWh/year</b>		1517 kWh/kWp/year	
	Used Energy	2784 kWh/year	Excess (unused)	774 kWh/year	
	Performance Ratio PR	59.87 %	Solar Fraction SF	100.00 %	
Loss of Load	Time Fraction	0.0 %	Missing Energy	0 kWh/year	
Battery aging (State of Wear)	Cycles SOW	93.3%	Static SOW	79.8%	
	Battery lifetime	4.9 years			

Normalized productions (per installed kWp): Nominal power 2460 Wp



Performance Ratio PR and Solar Fraction SF



New simulation variant  
Balances and main results

	GlobHor kWh/m²	GlobEff kWh/m²	E_Avail kWh	EUnused kWh	E_Miss kWh	E_User kWh	E_Load kWh	SolFrac ratio
January	68.4	101.1	222.9	0.0	0.000	236.5	236.5	1.000
February	86.4	111.8	244.6	0.0	0.000	213.6	213.6	1.000
March	125.6	142.3	303.2	30.7	0.000	236.5	236.5	1.000
April	150.5	154.9	326.3	79.2	0.000	228.9	228.9	1.000
May	203.0	192.8	388.5	132.9	0.000	236.5	236.5	1.000
June	211.6	192.3	372.1	123.8	0.000	228.9	228.9	1.000
July	210.5	195.4	370.4	114.7	0.000	236.5	236.5	1.000
August	195.1	196.3	370.9	115.2	0.000	236.5	236.5	1.000
September	157.4	179.2	346.4	99.5	0.000	228.9	228.9	1.000
October	117.2	147.6	298.1	46.5	0.000	236.5	236.5	1.000
November	84.3	123.5	263.9	29.9	0.000	228.9	228.9	1.000
December	67.6	101.5	224.1	1.7	0.000	236.5	236.5	1.000
Year	1677.7	1838.8	3731.4	774.1	0.000	2784.4	2784.4	1.000

Legends: GlobHor Global horizontal irradiation E\_Miss Missing energy  
 GlobEff Effective Global, corr. for IAM and shadings E\_User Energy supplied to the user  
 E\_Avail Available Solar Energy E\_Load Energy need of the user (Load)  
 EUnused Unused energy (battery full) SolFrac Solar fraction (EUsed / ELoad)

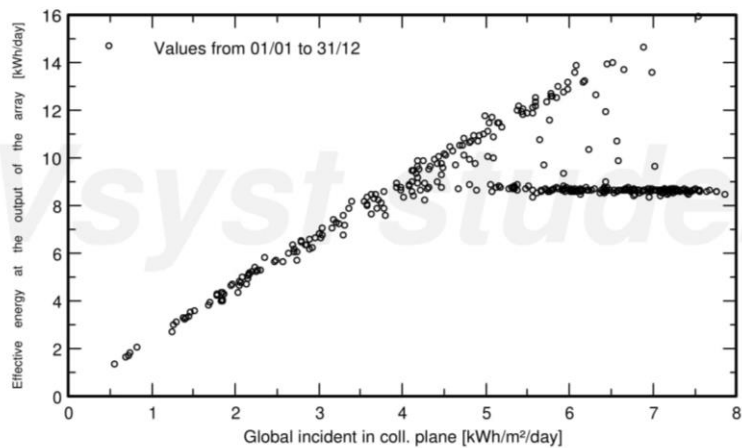


### Stand alone system: Special graphs

**Project :** Erbil - Fixed Tilt  
**Simulation variant :** New simulation variant

Main system parameters		System type	Stand alone system with batteries	
<b>Near Shadings</b>	According to module strings		Electrical effect	100 %
PV Field Orientation	tilt	30°	azimuth	0°
PV modules	Model	TSM-205 D80	Pnom	205 Wp
PV Array	Nb. of modules	12	Pnom total	<b>2460 Wp</b>
Battery	Model	MK 8G8D Gel	Technology	Lead-acid, sealed, AGM
Battery pack	Nb. of units	28	Voltage / Capacity	<b>48 V / 1309 Ah</b>
User's needs	Daily household consumers	Constant over the year	Global	2784 kWh/year

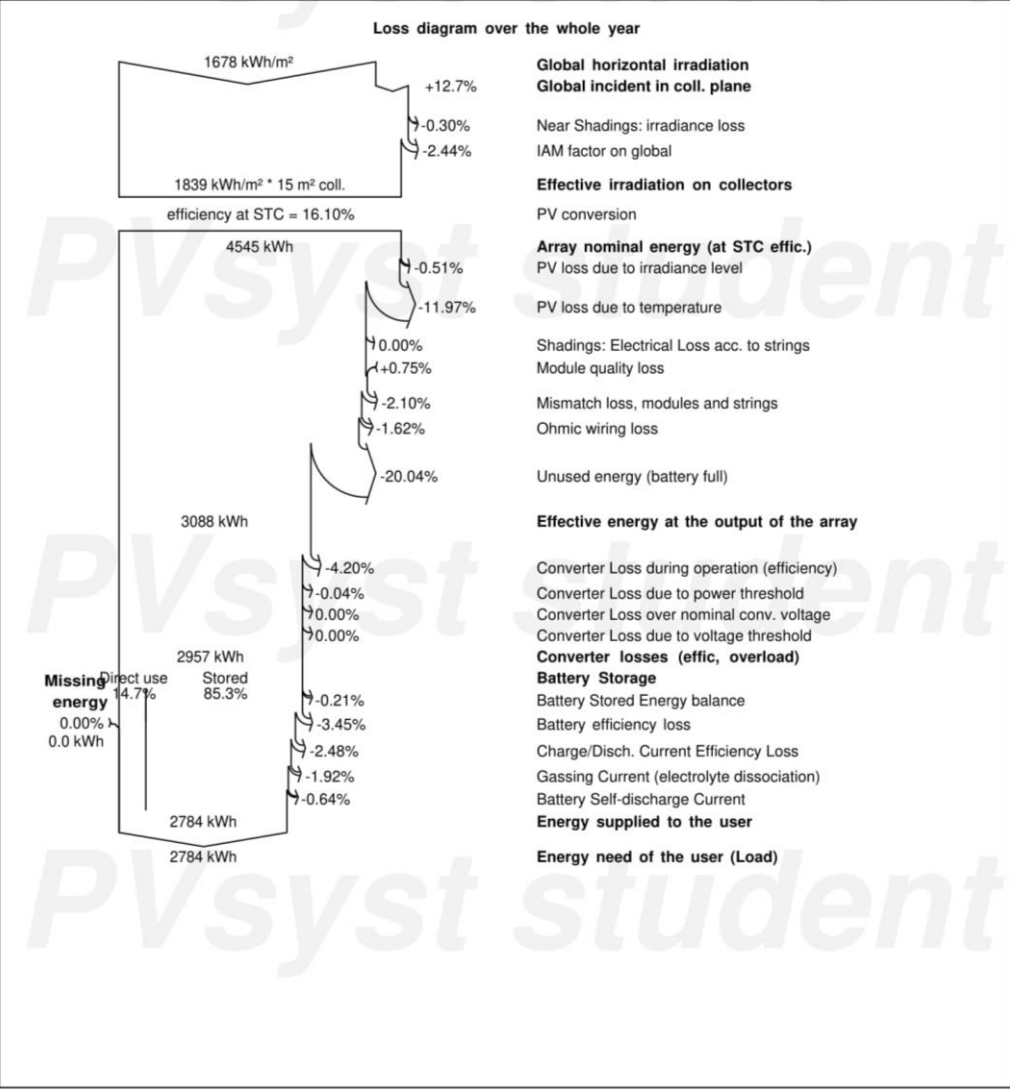
**Daily Input/Output diagram**



### Stand alone system: Loss diagram

**Project :** Erbil - Fixed Tilt  
**Simulation variant :** New simulation variant

Main system parameters	System type	Stand alone system with batteries
<b>Near Shadings</b>	According to module strings	Electrical effect 100 %
PV Field Orientation	tilt 30°	azimuth 0°
PV modules	Model TSM-205 D80	Pnom 205 Wp
PV Array	Nb. of modules 12	Pnom total <b>2460 Wp</b>
Battery	Model MK 8G8D Gel	Technology Lead-acid, sealed, AGM
Battery pack	Nb. of units 28	Voltage / Capacity <b>48 V / 1309 Ah</b>
User's needs	Daily household consumers	Global 2784 kWh/year



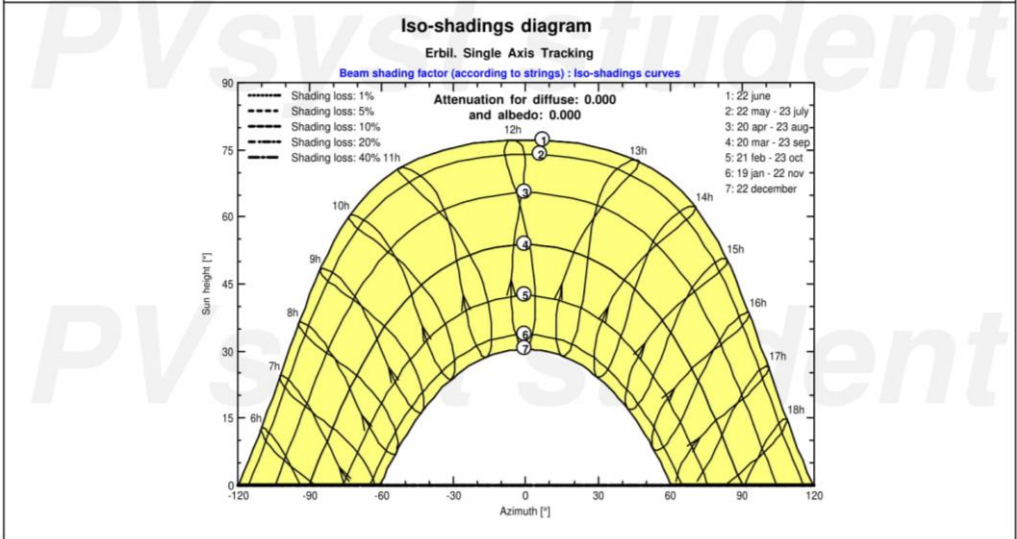
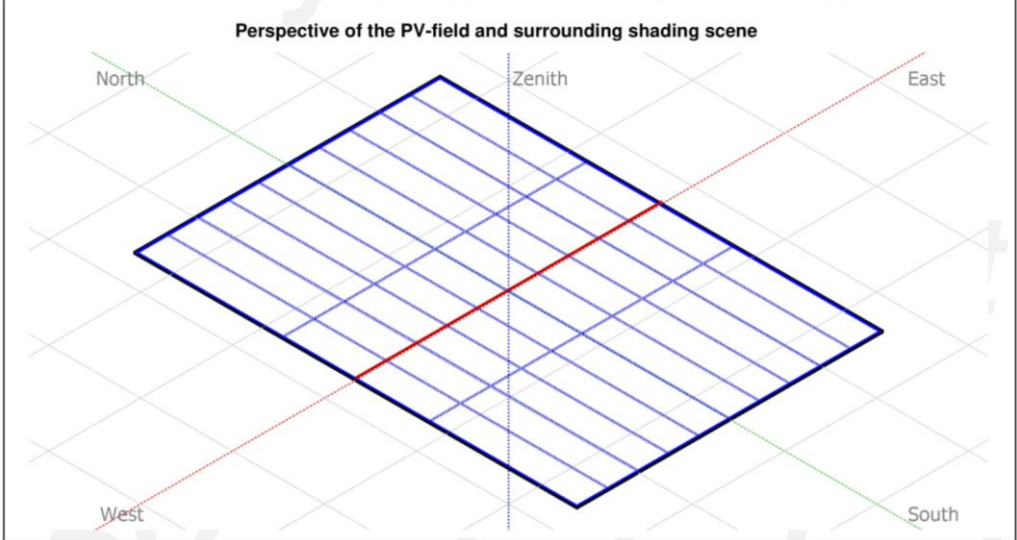
## Appendix B: Results of Single Axis Tracking Installation PV System

PVSYST 7.0.17	Parinaz Muhammed Abdulkarim (Cyprus)	18/02/21	Page 1/6
<b>Stand alone system: Simulation parameters</b>			
<b>Project :</b> <b>Erbil. Single Axis Tracking</b>			
<b>Geographical Site</b>		<b>Erbil</b>	<b>Country</b> <b>Iraq</b>
<b>Situation</b>		Latitude 36.18° N	Longitude 44.01° E
Time defined as		Legal Time Time zone UT+3	Altitude 392 m
<b>Meteo data:</b>		<b>Erbil</b>	Meteonorm 7.3 (1985-2000), Sat=100% - Synthetic
<b>Simulation variant : New simulation variant</b>			
		Simulation date	18/02/21 17h30
<b>Simulation parameters</b>		System type	<b>Stand alone system with batteries</b>
<b>Tracking plane, horizontal E-W axis</b>		Normal azimuth to axis	0°
Rotation Limitations		Minimum Tilt -90°	Maximum Tilt 90°
<b>Models used</b>		Transposition Perez	Diffuse Perez, Meteonorm separate
<b>Near Shadings</b>		According to module strings	Electrical effect 100 %
<b>User's needs :</b>		Daily household consumers average	Constant over the year 7.6 kWh/Day
<b>PV Array Characteristics</b>			
<b>PV module</b>		Si-mono Model	<b>TSM-205 D80</b>
Original PVSyst database		Manufacturer	Generic
Number of PV modules		In series	4 modules
Total number of PV modules		nb. modules	12
Array global power		Nominal (STC)	<b>2460 Wp</b>
Array operating characteristics (50°C)		U mpp	134 V
Total area		Module area	<b>15.3 m<sup>2</sup></b>
<b>System Parameter</b>		System type	<b>Stand alone system</b>
<b>Battery</b>		Model	<b>MK 8G8D Gel</b>
Battery Pack Characteristics		Manufacturer	MK Battery
		Nb. of units	4 in series x 7 in parallel
		Voltage	48 V
		Discharging min. SOC	20.0%
		Temperature	Average between fixed (20°C) and External
<b>Controller</b>		Model	Universal controller with MPPT converter
Converter		Technology	MPPT converter
		Maxi and EURO efficiencies	97.0 / 95.0%
Battery Management control		Threshold commands as	SOC calculation
		Charging	SOC = 0.90 / 0.75
		Discharging	SOC = 0.20 / 0.45
			approx. 52.1 / 49.5 V
			approx. 46.6 / 48.3 V
<b>PV Array loss factors</b>			
Thermal Loss factor		Uc (const)	20.0 W/m <sup>2</sup> K
		Uv (wind)	0.0 W/m <sup>2</sup> K / m/s
Wiring Ohmic Loss		Global array res.	140 mΩ
Serie Diode Loss		Voltage drop	0.7 V
Module Quality Loss			Loss Fraction 1.5 % at STC
Module mismatch losses			Loss Fraction 0.5 % at STC
Strings Mismatch loss			Loss Fraction -0.8 %
Incidence effect, ASHRAE parametrization		IAM = 1 - bo (1/cos i - 1)	Loss Fraction 2.0 % at MPP
			Loss Fraction 0.10 %
			bo Param. 0.05

**Stand alone system: Near shading definition**

**Project :** Erbil. Single Axis Tracking  
**Simulation variant :** New simulation variant

Main system parameters	System type	Stand alone system with batteries		
<b>Near Shadings</b>	According to module strings	Electrical effect	100 %	
PV Field Orientation	Tracking, horizontal axis E-W	Normal azimuth to axis	0°	
PV modules	Model	TSM-205 D80	Pnom	205 Wp
PV Array	Nb. of modules	12	Pnom total	<b>2460 Wp</b>
Battery	Model	MK 8G8D Gel	Technology	Lead-acid, sealed, AGM
Battery pack	Nb. of units	28	Voltage / Capacity	<b>48 V / 1309 Ah</b>
User's needs	Daily household consumers	Constant over the year	Global	2784 kWh/year



**Stand alone system: Detailed User's needs**

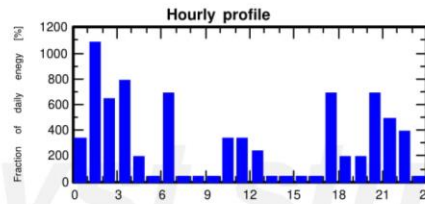
**Project :** Erbil. Single Axis Tracking  
**Simulation variant :** New simulation variant

<b>Main system parameters</b>	System type	<b>Stand alone system with batteries</b>		
<b>Near Shadings</b>	According to module strings	Electrical effect	100 %	
PV Field Orientation	Tracking, horizontal axis E-W	Normal azimuth to axis	0°	
PV modules	Model	TSM-205 D80	Pnom	205 Wp
PV Array	Nb. of modules	12	Pnom total	<b>2460 Wp</b>
Battery	Model	MK 8G8D Gel	Technology	Lead-acid, sealed, AGM
Battery pack	Nb. of units	28	Voltage / Capacity	<b>48 V / 1309 Ah</b>
User's needs	Daily household consumers	Constant over the year	Global	2784 kWh/year

**Daily household consumers, Constant over the year, average = 7.6 kWh/day**

**Annual values**

	Number	Power	Use	Energy
Lamps (LED or fluo)	10	15W/lamp	6H/day	900Wh/day
TV / PC / Mobile	3	100W/app	4H/day	1200Wh/day
Domestic appliances	4	50W/app	5H/day	1000Wh/day
Fridge / Deep-freeze	1		24Wh/day	900Wh/day
Dish- and Cloth-washer	1		2Wh/day	4Wh/day
Other uses	3	150W tot	4H/day	1800Wh/day
Other uses	1	600W tot	3H/day	1800Wh/day
Stand-by consumers			24H/day	24Wh/day
<b>Total daily energy</b>				<b>7628Wh/day</b>



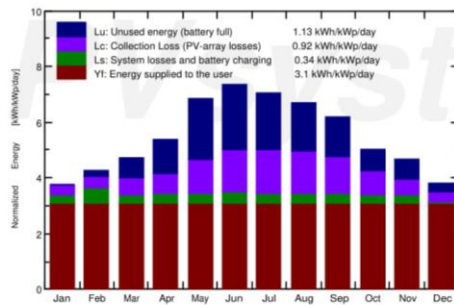
Stand alone system: Main results

**Project :** Erbil. Single Axis Tracking  
**Simulation variant :** New simulation variant

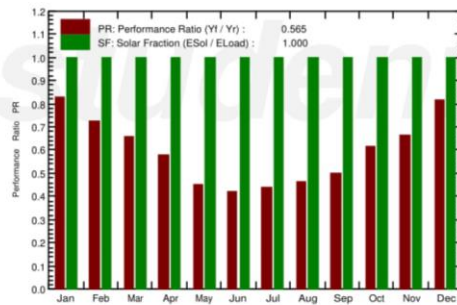
Main system parameters		System type	Stand alone system with batteries	
<b>Near Shadings</b>	According to module strings		Electrical effect	100 %
PV Field Orientation	Tracking, horizontal axis E-W		Normal azimuth to axis	0°
PV modules	Model	TSM-205 D80	Pnom	205 Wp
PV Array	Nb. of modules	12	Pnom total	<b>2460 Wp</b>
Battery	Model	MK 8G8D Gel	Technology	Lead-acid, sealed, AGM
Battery pack	Nb. of units	28	Voltage / Capacity	<b>48 V / 1309 Ah</b>
User's needs	Daily household consumers	Constant over the year	Global	2784 kWh/year

Main simulation results		Available Energy	3978 kWh/year	Specific prod.	1617 kWh/kWp/year
System Production	Used Energy	2784 kWh/year		Excess (unused)	1019 kWh/year
Loss of Load	Performance Ratio PR	56.49 %		Solar Fraction SF	100.00 %
Battery aging (State of Wear)	Time Fraction	0.0 %		Missing Energy	0 kWh/year
	Cycles SOW	93.7%		Static SOW	79.8%

Normalized productions (per installed kWp): Nominal power 2460 Wp



Performance Ratio PR and Solar Fraction SF



**New simulation variant**  
Balances and main results

	GlobHor kWh/m <sup>2</sup>	GlobEff kWh/m <sup>2</sup>	E_Avail kWh	EUnused kWh	E_Miss kWh	E_User kWh	E_Load kWh	SolFrac ratio
January	68.4	114.7	249.1	0.0	0.000	236.5	236.5	1.000
February	86.4	118.1	257.2	15.0	0.000	213.6	213.6	1.000
March	125.6	143.5	306.1	56.0	0.000	236.5	236.5	1.000
April	150.5	157.3	332.0	87.9	0.000	228.9	228.9	1.000
May	203.0	206.9	418.6	164.5	0.000	236.5	236.5	1.000
June	211.6	215.6	419.4	170.6	0.000	228.9	228.9	1.000
July	210.5	214.1	408.0	153.9	0.000	236.5	236.5	1.000
August	195.1	202.5	384.2	131.9	0.000	236.5	236.5	1.000
September	157.4	181.0	349.5	105.7	0.000	228.9	228.9	1.000
October	117.2	153.4	308.3	57.6	0.000	236.5	236.5	1.000
November	84.3	138.6	292.8	53.2	0.000	228.9	228.9	1.000
December	67.6	116.3	253.4	22.6	0.000	236.5	236.5	1.000
Year	1677.7	1962.0	3978.5	1018.9	0.000	2784.4	2784.4	1.000

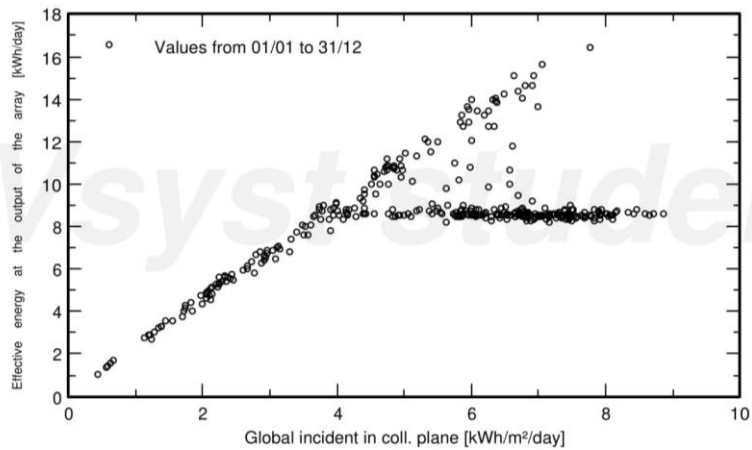
Legends: GlobHor Global horizontal irradiation E\_Miss Missing energy  
 GlobEff Effective Global, corr. for IAM and shadings E\_User Energy supplied to the user  
 E\_Avail Available Solar Energy E\_Load Energy need of the user (Load)  
 EUnused Unused energy (battery full) SolFrac Solar fraction (EUser / ELoad)

**Stand alone system: Special graphs**

**Project :** Erbil. Single Axis Tracking  
**Simulation variant :** New simulation variant

Main system parameters	System type	Stand alone system with batteries	
<b>Near Shadings</b>	According to module strings	Electrical effect	100 %
PV Field Orientation	Tracking, horizontal axis E-W	Normal azimuth to axis	0°
PV modules	Model TSM-205 D80	Pnom	205 Wp
PV Array	Nb. of modules 12	Pnom total	<b>2460 Wp</b>
Battery	Model MK 8G8D Gel	Technology	Lead-acid, sealed, AGM
Battery pack	Nb. of units 28	Voltage / Capacity	<b>48 V / 1309 Ah</b>
User's needs	Daily household consumers	Constant over the year	Global 2784 kWh/year

**Daily Input/Output diagram**

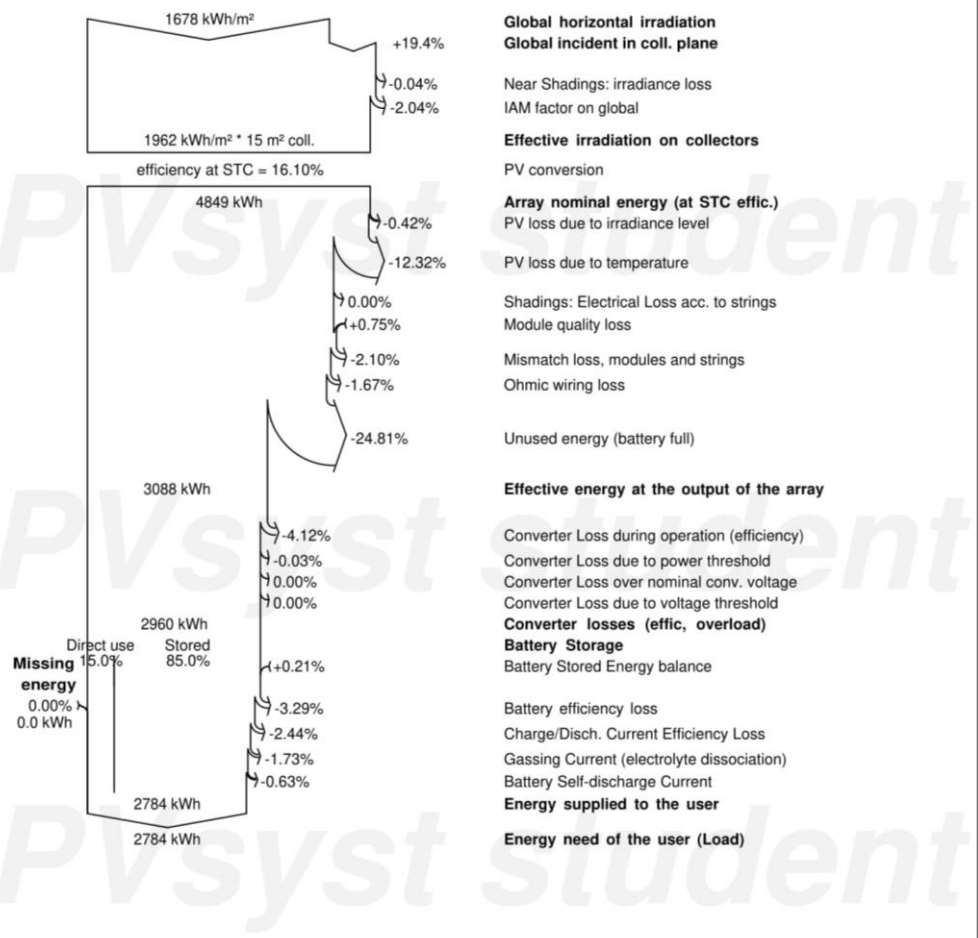


### Stand alone system: Loss diagram

**Project :** Erbil. Single Axis Tracking  
**Simulation variant :** New simulation variant

Main system parameters	System type	Stand alone system with batteries
<b>Near Shadings</b>	According to module strings	Electrical effect 100 %
PV Field Orientation	Tracking, horizontal axis E-W	Normal azimuth to axis 0°
PV modules	Model	TSM-205 D80 Pnom 205 Wp
PV Array	Nb. of modules	12 Pnom total <b>2460 Wp</b>
Battery	Model	MK 8G8D Gel Technology Lead-acid, sealed, AGM
Battery pack	Nb. of units	28 Voltage / Capacity <b>48 V / 1309 Ah</b>
User's needs	Daily household consumers	Constant over the year Global 2784 kWh/year

Loss diagram over the whole year





## Appendix C: Results of Dual Axis Tracking Installation PV System

PVSYST 7.0.17	Parinaz Muhammed Abdulkarim (Cyprus)	18/02/21	Page 1/7
<b>Stand alone system: Simulation parameters</b>			
<b>Project : Erbil Dual Axis Tracking</b>			
<b>Geographical Site</b>	<b>Erbil</b>	<b>Country</b>	<b>Iraq</b>
<b>Situation</b>	Latitude 36.18° N	<b>Longitude</b>	44.01° E
Time defined as	Legal Time Time zone UT+3	<b>Altitude</b>	392 m
	Albedo 0.20		
<b>Meteo data:</b>	<b>Erbil</b>	Meteonorm 7.3 (1985-2000), Sat=100% - Synthetic	
<b>Simulation variant : New simulation variant</b>			
	Simulation date	18/02/21 22h10	
<b>Simulation parameters</b>			
	System type	<b>Stand alone system with batteries</b>	
<b>Tracking two axis, frame E-W</b>	Frame axis azimuth	0°	
Frame Rotation Limitations	Minimum Tilt	10°	Maximum Tilt 80°
Tracker's tilt on frame	Minimum Phi	-45°	Maximum Phi 45°
<b>Models used</b>	Transposition	Perez	Diffuse Perez, Meteonorm separate
			Circumsolar
<b>Near Shadings</b>	According to module strings	Electrical effect	100 %
<b>User's needs :</b>	Daily household consumers average	Constant over the year	7.6 kWh/Day
<b>PV Array Characteristics</b>			
<b>PV module</b>	Si-mono	Model	<b>TSM-205 D80</b>
Original PVsyst database		Manufacturer	Generic
Number of PV modules		In series	4 modules
Total number of PV modules		nb. modules	12
Array global power		Nominal (STC)	<b>2460 Wp</b>
Array operating characteristics (50°C)		U mpp	134 V
Total area		Module area	<b>15.3 m²</b>
			In parallel 3 strings
			Unit Nom. Power 205 Wp
			At operating cond. 2192 Wp (50°C)
			I mpp 16 A
<b>System Parameter</b>			
	System type	<b>Stand alone system</b>	
<b>Battery</b>	Model	<b>MK 8G8D Gel</b>	
	Manufacturer	MK Battery	
Battery Pack Characteristics	Nb. of units	4 in series x 7 in parallel	
	Voltage	48 V	Nominal Capacity 1309 Ah
	Discharging min. SOC	20.0%	Stored energy 50.3 kWh
	Temperature	Fixed (20°C)	
<b>Controller</b>	Model	Universal controller with MPPT converter	
	Technology	MPPT converter	Temp coeff. -5.0 mV/°C/Elem.
Converter	Maxi and EURO efficiencies	97.0 / 95.0%	
Battery Management control	Threshold commands as	SOC calculation	
	Charging	SOC = 0.90 / 0.75	approx. 52.1 / 49.5 V
	Discharging	SOC = 0.20 / 0.45	approx. 46.6 / 48.3 V
<b>PV Array loss factors</b>			
Thermal Loss factor	Uc (const)	20.0 W/m²K	Uv (wind) 0.0 W/m²K / m/s
Wiring Ohmic Loss	Global array res.	140 mΩ	Loss Fraction 1.5 % at STC
Serie Diode Loss	Voltage drop	0.7 V	Loss Fraction 0.5 % at STC
Module Quality Loss			Loss Fraction -0.8 %
Module mismatch losses			Loss Fraction 2.0 % at MPP
Strings Mismatch loss			Loss Fraction 0.10 %

### Stand alone system: Simulation parameters

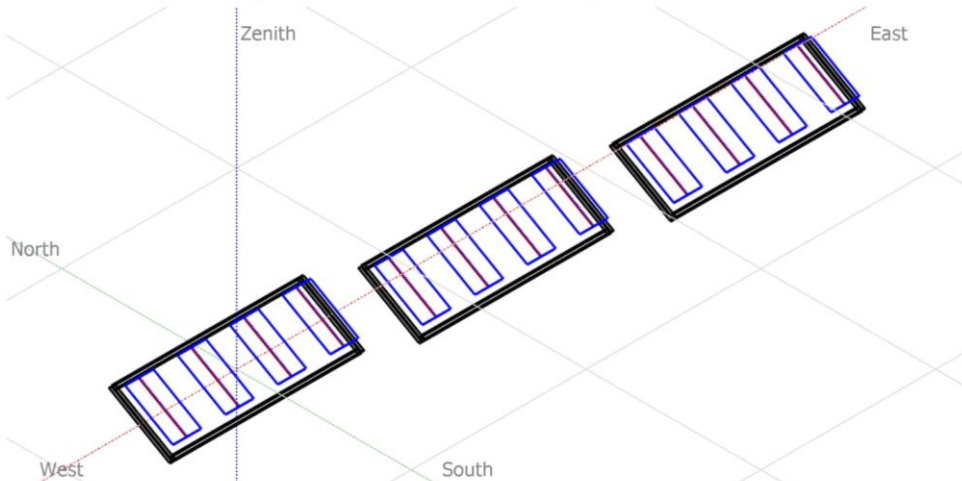
Incidence effect, ASHRAE parametrization      IAM =  $1 - b_o (1/\cos i - 1)$        $b_o$  Param. 0.05

### Stand alone system: Near shading definition

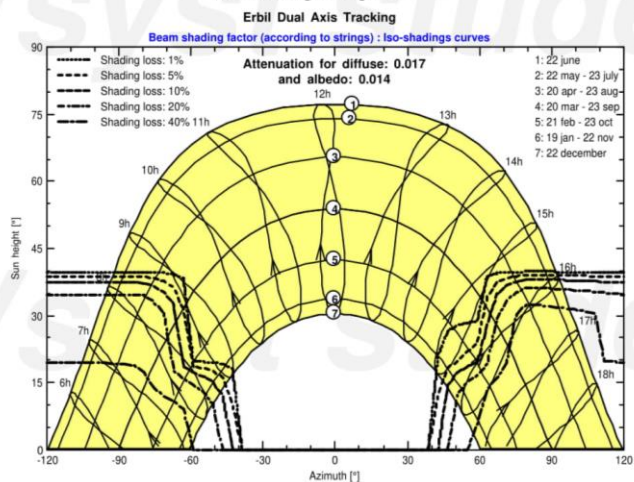
**Project :** Erbil Dual Axis Tracking  
**Simulation variant :** New simulation variant

Main system parameters	System type	Stand alone system with batteries	
<b>Near Shadings</b>	According to module strings	Electrical effect	100 %
PV Field Orientation	tilt		
PV modules	Model	TSM-205 D80	Pnom 205 Wp
PV Array	Nb. of modules	12	Pnom total <b>2460 Wp</b>
Battery	Model	MK 8G8D Gel	Technology Lead-acid, sealed, AGM
Battery pack	Nb. of units	28	Voltage / Capacity <b>48 V / 1309 Ah</b>
User's needs	Daily household consumers	Constant over the year	Global 2784 kWh/year

Perspective of the PV-field and surrounding shading scene



Iso-shadings diagram



**Stand alone system: Detailed User's needs**

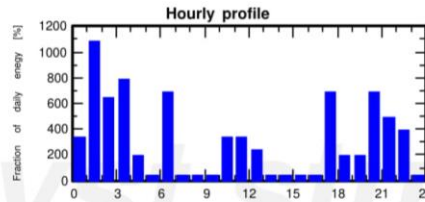
**Project :** Erbil Dual Axis Tracking  
**Simulation variant :** New simulation variant

<b>Main system parameters</b>	System type	<b>Stand alone system with batteries</b>	
<b>Near Shadings</b>	According to module strings	Electrical effect	100 %
PV Field Orientation	tilt		
PV modules	Model	TSM-205 D80	Pnom 205 Wp
PV Array	Nb. of modules	12	Pnom total <b>2460 Wp</b>
Battery	Model	MK 8G8D Gel	Technology Lead-acid, sealed, AGM
Battery pack	Nb. of units	28	Voltage / Capacity <b>48 V / 1309 Ah</b>
User's needs	Daily household consumers	Constant over the year	Global 2784 kWh/year

**Daily household consumers, Constant over the year, average = 7.6 kWh/day**

**Annual values**

	Number	Power	Use	Energy
Lamps (LED or fluo)	10	15W/lamp	6H/day	900Wh/day
TV / PC / Mobile	3	100W/app	4H/day	1200Wh/day
Domestic appliances	4	50W/app	5H/day	1000Wh/day
Fridge / Deep-freeze	1		24Wh/day	900Wh/day
Dish- and Cloth-washer	1		2Wh/day	4Wh/day
Other uses	3	150W tot	4H/day	1800Wh/day
Other uses	1	600W tot	3H/day	1800Wh/day
Stand-by consumers			24H/day	24Wh/day
<b>Total daily energy</b>				<b>7628Wh/day</b>



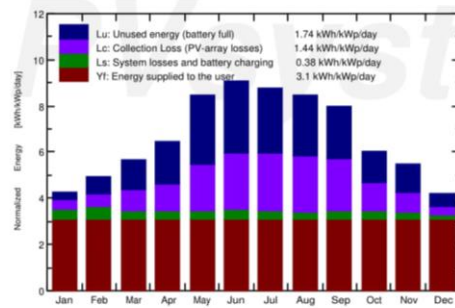
### Stand alone system: Main results

**Project :** Erbil Dual Axis Tracking  
**Simulation variant :** New simulation variant

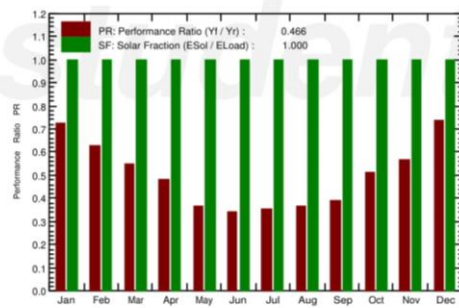
<b>Main system parameters</b>		System type	<b>Stand alone system with batteries</b>	
<b>Near Shadings</b>	According to module strings		Electrical effect	100 %
PV Field Orientation	tilt			
PV modules	Model	TSM-205 D80	Pnom	205 Wp
PV Array	Nb. of modules	12	Pnom total	<b>2460 Wp</b>
Battery	Model	MK 8G8D Gel	Technology	Lead-acid, sealed, AGM
Battery pack	Nb. of units	28	Voltage / Capacity	<b>48 V / 1309 Ah</b>
User's needs	Daily household consumers	Constant over the year	Global	2784 kWh/year

<b>Main simulation results</b>				
System Production	<b>Available Energy</b>	<b>4556 kWh/year</b>	Specific prod.	1852 kWh/kWp/year
	Used Energy	2784 kWh/year	Excess (unused)	1563 kWh/year
	Performance Ratio PR	46.60 %	Solar Fraction SF	100.00 %
Loss of Load	Time Fraction	0.0 %	Missing Energy	0 kWh/year
Battery aging (State of Wear)	Cycles SOW	93.5%	Static SOW	80.0%
	Battery lifetime	5.0 years		

**Normalized productions (per installed kWp): Nominal power 2460 Wp**



**Performance Ratio PR and Solar Fraction SF**



#### New simulation variant Balances and main results

	GlobHor kWh/m <sup>2</sup>	GlobEff kWh/m <sup>2</sup>	E_Avail kWh	EUnused kWh	E_Miss kWh	E_User kWh	E_Load kWh	SolFrac ratio
<b>January</b>	68.4	132.6	281.8	22.0	0.000	236.5	236.5	1.000
<b>February</b>	86.4	137.4	293.3	52.3	0.000	213.6	213.6	1.000
<b>March</b>	125.6	168.1	348.6	96.5	0.000	236.5	236.5	1.000
<b>April</b>	150.5	185.4	377.8	132.5	0.000	228.9	228.9	1.000
<b>May</b>	203.0	253.5	480.3	226.0	0.000	236.5	236.5	1.000
<b>June</b>	211.6	263.1	476.4	226.9	0.000	228.9	228.9	1.000
<b>July</b>	210.5	262.1	467.1	212.1	0.000	236.5	236.5	1.000
<b>August</b>	195.1	251.5	448.5	196.0	0.000	236.5	236.5	1.000
<b>September</b>	157.4	224.6	412.3	167.3	0.000	228.9	228.9	1.000
<b>October</b>	117.2	182.1	355.2	101.7	0.000	236.5	236.5	1.000
<b>November</b>	84.3	162.9	332.6	88.5	0.000	228.9	228.9	1.000
<b>December</b>	67.6	130.9	282.6	41.6	0.000	236.5	236.5	1.000
<b>Year</b>	1677.7	2354.3	4556.4	1563.4	0.000	2784.4	2784.4	1.000

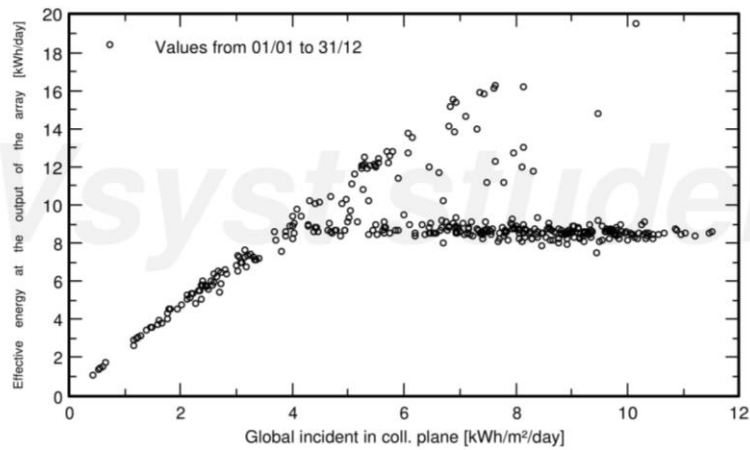
Legends: GlobHor Global horizontal irradiation      E\_Miss Missing energy  
 GlobEff Effective Global, corr. for IAM and shadings      E\_User Energy supplied to the user  
 E\_Avail Available Solar Energy      E\_Load Energy need of the user (Load)  
 EUnused Unused energy (battery full)      SolFrac Solar fraction (EUsed / ELoad)

**Stand alone system: Special graphs**

**Project :** Erbil Dual Axis Tracking  
**Simulation variant :** New simulation variant

Main system parameters	System type	Stand alone system with batteries	
<b>Near Shadings</b>	According to module strings	Electrical effect	100 %
PV Field Orientation	tilt		
PV modules	Model	TSM-205 D80	Pnom 205 Wp
PV Array	Nb. of modules	12	Pnom total <b>2460 Wp</b>
Battery	Model	MK 8G8D Gel	Technology Lead-acid, sealed, AGM
Battery pack	Nb. of units	28	Voltage / Capacity <b>48 V / 1309 Ah</b>
User's needs	Daily household consumers	Constant over the year	Global 2784 kWh/year

**Daily Input/Output diagram**



### Stand alone system: Loss diagram

**Project :** Erbil Dual Axis Tracking  
**Simulation variant :** New simulation variant

Main system parameters	System type	Stand alone system with batteries	
<b>Near Shadings</b>	According to module strings	Electrical effect	100 %
PV Field Orientation	tilt		
PV modules	Model	TSM-205 D80	Pnom 205 Wp
PV Array	Nb. of modules	12	Pnom total <b>2460 Wp</b>
Battery	Model	MK 8G8D Gel	Technology Lead-acid, sealed, AGM
Battery pack	Nb. of units	28	Voltage / Capacity <b>48 V / 1309 Ah</b>
User's needs	Daily household consumers	Constant over the year	Global 2784 kWh/year

**Loss diagram over the whole year**

